博士論文

Functional analysis of transcriptional regulators for secondary metabolites production in *Actinomycetes*

放線菌における二次代謝産物生産を調節する転写因子の機能解析

見﨑 裕也

広島大学大学院統合生命科学研究科

2022 年 2 月

目次

1．主論文

Functional analysis of transcriptional regulators for secondary metabolites production in *Actinomycetes*
（放線菌における二次代謝産物生産を調節する転写因子の機能解析）
見﨑 裕也

2．参考論文

(1) SrrB, a pseudo-receptor protein, acts as a negative regulator for lankacidin and lankamycin production in *Streptomyces rochei*
Yuya Misaki, Shouji Yamamoto, Toshihiro Suzuki, Miyuki Iwakuni, Hiroaki Sasaki, Yuzuru Takahashi, Kuninobu Inada, Haruyasu Kinashi, and Kenji Arakawa.
Front. Microbiol., **11**, 1089 (2020).

(2) Overexpression of SRO_3163, a homolog of *Streptomyces* antibiotic regulatory protein, induces the production of novel cyclohexene-containing enamide in *Streptomyces rochei*
Yuya Misaki, Yosi Nindita, Kota Fujita, Amirudin Akhmad Fauzi, and Kenji Arakawa.
Biosci. Biotechnol. Biochem., **86**(2), 177-184 (2022)

主論文

Contents

Chapter 1. General Introduction

The World Health Organization warned us a serious increase in antibiotic resistance mutants and shortages of new antibiotic candidates, leading to a global health crisis in the 21st century [**1**]. This report emphasizes the importance of discovering new types of antibiotics. From the 1940's to the present, numerous antibiotics have been isolated from natural biological resources (plants, animals, and microorganisms), and in some cases, their original structures were modified through semi-synthesis and/or chemoenzymatic synthesis to improve their pharmacological activity (**Figure 1.1**). Streptomycin is a first-discovered antibiotic that was isolated from *Actinomycetes* (**Figure 1.1** upper left).

From the first discovery of streptomycin in the 1940's, many new bioactive compounds have been obtained from nature (**Figure 1.1**). Most of the useful antibiotics have been discovered around 1940-1980s. However, new classes of antibiotics have not been approved as pharmaceutical drugs since the 1990s [**2**].

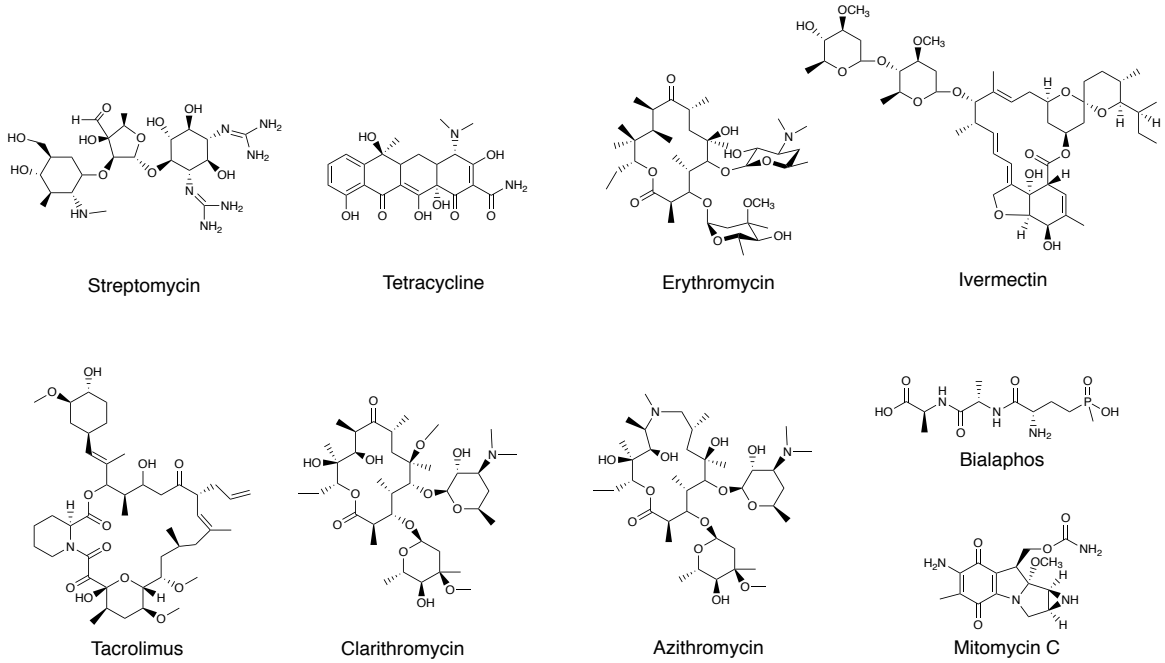

Figure 1.1 Beneficial compounds originated from the metabolites of *Actinomycetes*.

Streptomyces is well known as the largest genus of *Actinobacteria* and produces a wide variety of secondary metabolites including antibiotics, antifungal agents, immunosuppressants, herbicides, and anticancer agents (**Figure 1.1**). Their production is strictly controlled by signaling molecules and their specific receptors in *Streptomyces* [**3**][**4**][**5**][**6**].

The low-molecular-weight signaling molecules induce secondary metabolite production at nano-molar concentrations in *Streptomyces*. As shown in **Figure 1.2**, the signaling molecules hitherto discovered are classified into three groups; (1) γ-butyrolactone-type, (2) furan-type, and (3) butenolide-type.

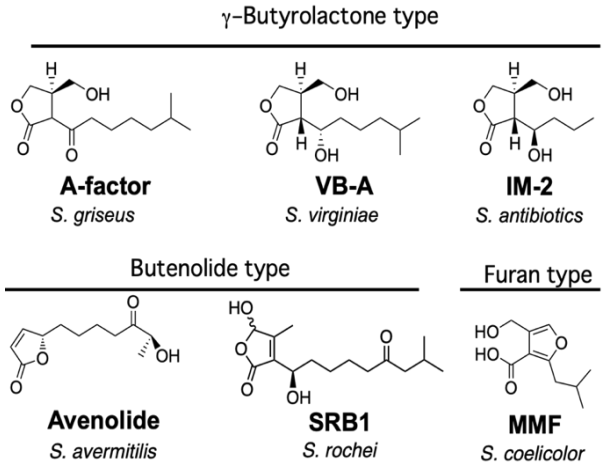

Figure 1.2 Signaling molecules identified from *Streptomyces* sp. A-factor in *S. griseus* [7][8], virginia butanolides (VB) in *S. virginiae* [9] and IM-2 in *S. lavendulae* [10], Avenolide. in *S. avermitilis* [11], SRBs in *S. rocehi* [12] and methylenomycin furan (MMF) in *S. coelicolor* [13].

The most well-known signaling molecule/receptor system is A-factor/ArpA cascade in *Streptomyces griseus* for streptomycin and grixazone production [**14**][**15**] (**Figure 1.3**). In the absence of A-factor, ArpA protein specifically binds to the promoter region of the target activator gene *adpA* and represses its transcription. When A-factor reaches a critical concentration, A-factor/ArpA complex dissociates from the promoter region of *adpA*, and transcription of *adpA* is initiated. Then, the AdpA binds to its targets (AdpA-regulons) to activate streptomycin and grixazone production and morphological differentiation [**14**][**15**]. Gene sets involved in the signaling-molecule regulatory cascade for secondary metabolite production are listed in **Table 1.1**. TetR-type transcriptional regulators (include signaling molecule receptors) and SARP (*Streptomyces* Antibiotics

Regulatory Protein)-type transcriptional regulators could constitute the complex regulatory cascade in various *Streptomyces*.

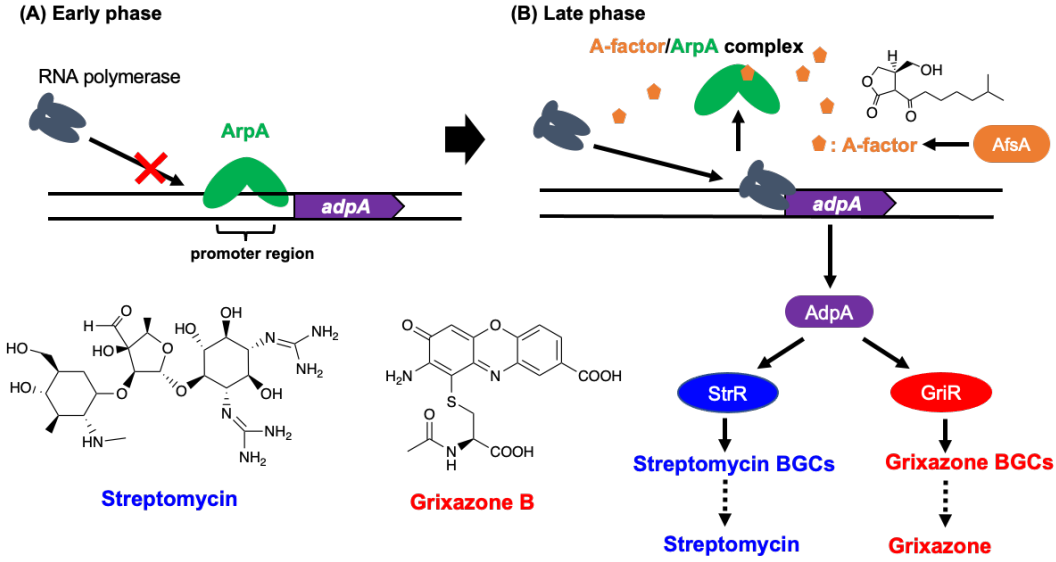

Figure 1.3 Regulatory cascade for Streptomycin and Grixazones in *Streptomyces griseus*
(A) Early phase of culture
(B) Late phase of culture

Table 1.1. Components of regulatory cascade for secondary metabolite production

	Signaling molecule synthesis gene	Signaling molecule(s)	Receptor gene	**Pseudo-receptor gene (pI of gene product)**	Direct target gene	Secondary metabolite(s)
S. griseus	*afsA*	A-factor	*arpA*		*adpA*	Streptomycin, grixazone
S. rochei	***srrX***	**SRB1, SRB2**	***srrA***	***srrB* (11.2)**	***srrY***	**Lankacidin, lankamycin**
S. fradiae	N.D.	N.D.	*tylP*	***tylQ* (6.4)**	*tylS*	Tylosin
S. coelicolor	*scbA*	SCB1-3	*scbR*	***scbR2* (5.8)**	*KasO*	Coelimycin P-1, actinorhodin, undecylprodigiosin
S. coelicolor	*mmfL*	MMFs	*mmfR*			Methylenomycin
S. virginiae	*barX*	Virginia butanolides	*barA*	***barB* (10.2)**		Virginiamycin
S. venezuelae	*jadW1*	SVB1	*jadR3*	***jadR2* (7.8)**	*jadR1*	Jadomycin
S. lavendulae	*farA*	IM-2	*farR*	***farR2* (9.7)**		Showdomycin
S. ambofaciens	N.D.	N.D.	*alpZ*	***alpW* (11.6)**	*alpV*	Kinamycins
S. avermitilis	*aco*	Avenolide	*avaR1*	***avaR2* (9.6)**		Avermectins

N.D. ; Not determined

([**16**][**17**]); e.g., streptomycin and grixazone production in *S. griseus* [**8**][**14**][**15**][**18**], lankamycin and lankacidin (Figure 1.6) in *S. rochei* [**12**][**19**][**20**][**21**] , tylosin in *S. fradiae* [**22**][**23**][**24**], coelimycin P-1 in *S. coelicolor* [**25**][**26**][**27**][**28**][**29**], actinorhodin and undecylprodigiosin in *S. coelicolor* [**30**][**31**], virginiamycin in *S. virginiae* [**9**][**31**][**32**], jadomycin in *S. venezuelae* [**33**][**34**][**35**][**10**][**36**], kinamycin in *S. ambofaciens* [**37**][**38**][**39**], and avermectin in *S. avermitilis* [**11**][**40**][**41**].

TetR-type receptors have a conserved DNA-binding helix-turn-helix motif at the N-terminus and a ligand-binding residue at the C-terminus [**42**]. Their phylogenetic trees were shown in Figure 1.5. In general, the signaling molecule receptor genes (*arpA* in *S. griseus*, *srrA* in *S. rochei*, etc.) locate adjacent to the signaling molecule synthase genes (*afsA* in *S. griseus*, *srrX* in *S. rochei*, etc.) [**43**], hence, I can predict the presence of the signaling-molecule/receptor systems in *Streptomyces* species [**44**]. Many signaling molecule receptor genes were characterized by their mutational analysis, however, the comprehensive analysis of the signaling-molecules/receptor system was quite limited due to the difficulty for isolation of signaling molecules (extremely low concentration around 10^{-9} M in culture). A few examples are the followings; A-factor/ArpA system in *S. griseus* [**14**][**15**], SCBs/ScbR in *S. coelicolor* [**25**], SVBs/JadR3 in *S. venezuelae* [**36**], virginia butanolides/BarA in *S. virginiae* [**31**][**45**], IM-2/FarA in *S. lavendulae* [**46**], avenolide/AvaR1 in *S. avermitilis* [**11**], SRBs/SrrA in *S. rochei* [**20**], and MMFs/MmfR [**47**] **(Table 1.1**).

Another major class of TetR-type repressors in *Streptomyces* are termed as "pseudo-receptors" (**Figure 1.4**). Generally they act as negative regulators for secondary metabolite production in *Streptomyces* (details will be described in Chapter 2).

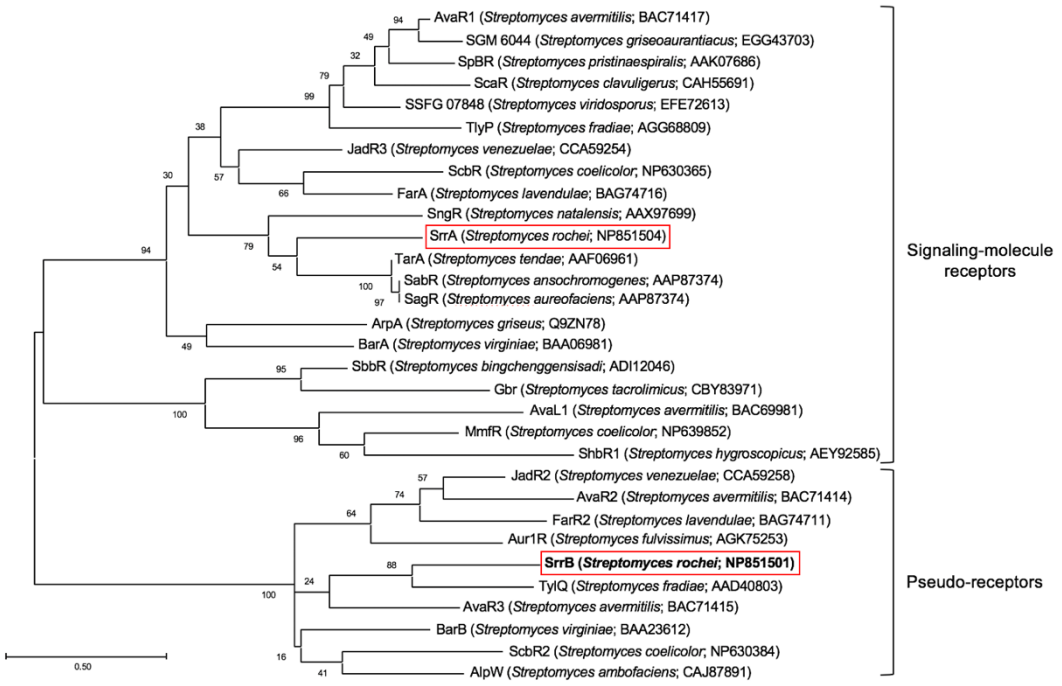

Figure 1.4 Phylogenetic analysis of the signaling molecule receptors and the pseudo-receptors. Phylogenetic tree was constructed by the neighbor-joining algorithm of MEGA X version 10.1.5 software [**48**]. Bootstrap values, expressed as a percentage of 1000 replications, are given at branching points.

SARP-type regulator genes are widely distributed among Actinobacteria such as *Streptomyces*, *Micromonospora*, *Nocardia*, and *Amycolatopsis* [**50**]. They are main targets of the signaling molecule receptors, and act as pathway-specific activators for antibiotic production in *Streptomyces* [**4**]. This family proteins are characterized by a winged helix-turn-helix (HTH) DNA-binding domain at their N-terminus and a bacterial transcriptional activator domain (BTAD) at their C-terminus [**49**][**51**]. The well characterized SARPs in *Streptomyces* are followings; ActII-ORF4 for actinorhodin production in *S. coelicolor* [**52**][**53**], RedD for undecylprodigiosin in *S. coelicolor* [**52**], DnrI for daunorubicin in *S. puceticus* [**54**][**55**], FdmR1 for fredericamycin in *S. griseus* ATTCC 49344 [**56**], TylS for tylosin in *S. fradiae* [**23**][**57**], and SrrY and SrrZ for lankamycin and lankacidin in *S. rochei*[**21**]. Phylogenetic tree of SARP-type activators is shown in **Figure. 1.5.**

SARPs specifically bind to a heptameric "direct repeat (DR)" sequence (5′-TCGAGXX-3′) at the promoter region of their targets, among which a 4-bp spacers are located [**51**][**53**][**58**]. Molecular studies of AfsR protein in *S. coelicolor* revealed that 8

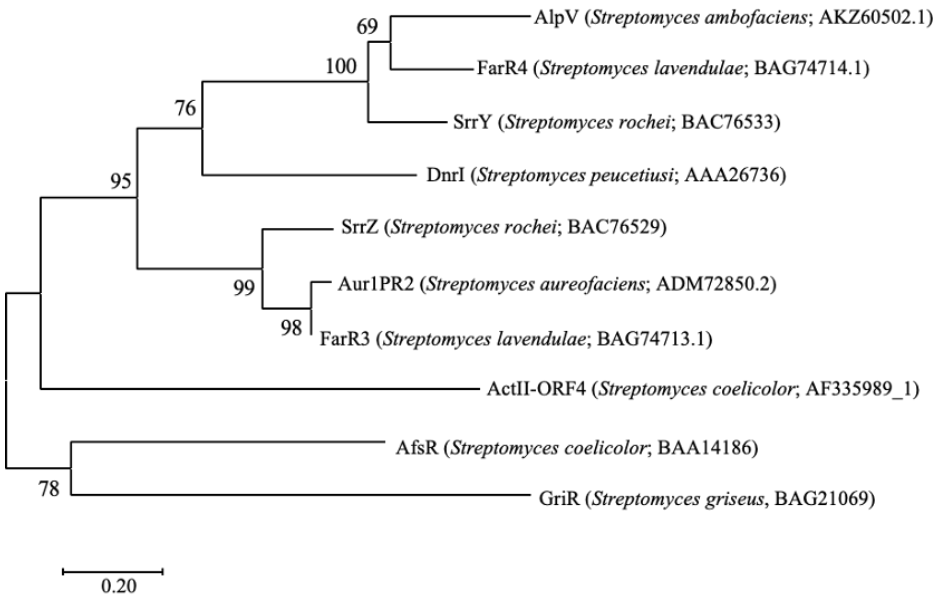

Figure 1.5 Phylogenetic analysis of the SARP-type activator.
Phylogenetic analysis of the signaling molecule receptors and the pseudo-receptors. Phylogenetic tree was constructed by the neighbor-joining algorithm of MEGA X version 10.1.5 software [**48**]. Bootstrap values, expressed as a percentage of 1000 replications, are given at branching points.

bp distance from the −10 region of the promoter [**59**] is important for construction of tripartite complex, the *afsS* promoter (a target of SARP)/AfsR (SARP)/RNA polymerase. The DNA-binding sequences including heptameric DRs and 4-bp spacers at the promoter of target DNA(s) has been determined in several *Streptomyces* species [**21**][**60**] (**Figure 1.6**). The DR sequences for secondary metabolites production hitherto identified are the followings; SrrY-binding at upstream of *srrZ* for lankamycin production in *S. rochei* [**21**], ActII-ORF4-binding at upstream of both *actI-ORF1* and *actI-ORFA* for actinorhodin in *S. coelicolor* [**53**], DnrI-binding at upstream of *dnrG* and *dspE* for daunorubicin in *S. peucetius* [**61**], FdmR1-binding at upstream of *fdmR1*, *fdmD*, and *fdmV* for fredericamycin in *S. griseus* ATCC 49344 [**56**], Aur1PR4-binding at upstream of *sa13* for auricin in *S. aureofaciens* [**62**], GriR-binding at upstream of *griJ* and *griC* for grixazone in *S. griseus* [**63**], and PapR2-binding at upstream of *papR1* for pristinamycin in *S. pristinaespiralis* [**64**].

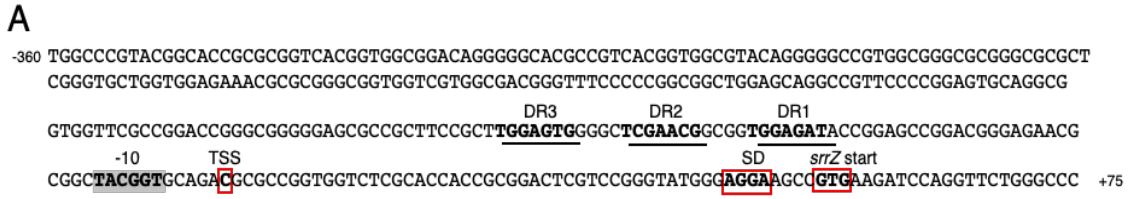

Figure 1.6 (**A**) SARP (SrrY)-binding sequences at the upstream region of *srrZ*. Underlines indicate heptameric direct repeat sequences (DR1,DR2, and DR3). The -10 sequence in indicated by gray shading, and the TSS, the SD sequence, and the *srrZ* start codon are boxed [**21**][**60**].
(B) Alignment of the promoter region containing SARP-binding heptameric direct repeat and 4-bp spacers sequences determined in several *Streptomyces* species. The possible -10 regions are shaded in grey. The boldfaces indicate the transcription start sites (TSS), and the underlines indicate the heptameric direct repeat sequences. TSS of *papR1* is unknown.

Streptomyces rochei 7434AN4 produces two structurally unrelated polyketide antibiotics, lankamycin (**1**) and lankacidins (**2**-**6**) (**Figure 1.7**) and carries three linear plasmids pSLA2-L, -M, and -S [**65**].Together with the biosynthetic genes for lankamycin and lankacidins (**Figure1.7**), many regulatory genes including a biosynthetic gene for signaling molecules SRBs (**7**,**8**) (**Figure1.7**) (*srrX*), six *tetR*-type repressor genes (*srrA, srrB, srrC, srrD, srrE*, and *srrF*), and three SARP family activator genes (*srrY, srrZ*, and *srrW*) are located on a giant linear plasmid pSLA2-L (210,614 bp) [**66**] (**Figure 1.8**).

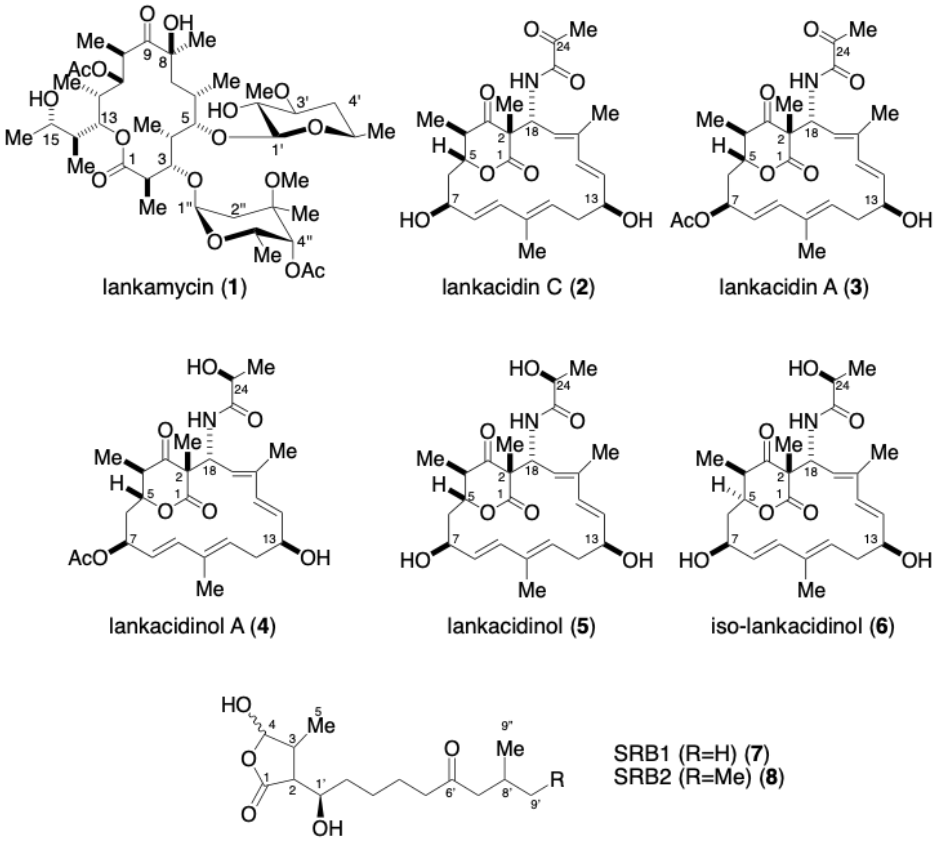

Figure 1.7 Chemical structures of antibiotics and signaling molecules produces in *S. rochei*
Me, methyl; Ac, acetyl.

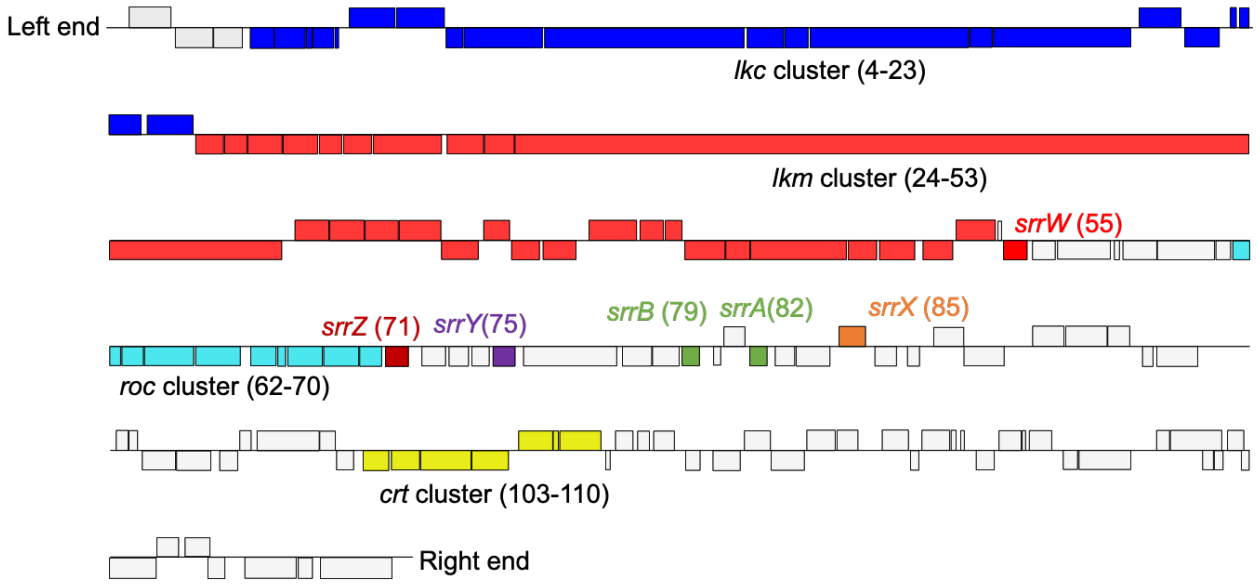

Figure 1.8 DNA map of pSLA2-L
Regulatory genes involved in this paper are highlighted. The number in parentheses indicates the ORF number.

Our group revealed that SRBs/SrrA complex dissociates from the promoter region of *srrY*, leading to the activation of lankacidin production [**20**], whereas the gene product of *srrY* further activates a second activator gene *srrZ* to produce lankamycin [**21**] (Details including schematic model are described in Chapter 2). In addition, our group also determined the complete nucleotide sequence of the *S. rochei* 7434AN4 chromosome [**67**]. The assembled sequence has revealed an 8,364,802-bp linear chromosome with 7,568 protein-coding ORFs together with 35 secondary metabolite BGCs. Furthermore, the chromosome contains 110 *tetR*-type repressor genes and 12 SARP-type activator genes, which may constitute the complex regulatory network for secondary metabolism coded on the chromosome.

Recent advances in next-generation nucleotide sequencing technology implied that *Streptomyces* species harbors more than 30 secondary metabolite biosynthetic gene clusters (BGCs) in the genome. However, many of them are weakly expressed or not at all under ordinary laboratory culture conditions. These clusters are termed "silent" or "cryptic" BGCs. To activate these "silent" or "cryptic" BGCs, various genome mining approaches were performed; for example, heterologous expression of entire BGCs, control of regulatory networks, and comparative metabolite analysis [**16**][**68**][**69**].

Genetic manipulation of transcriptional regulatory genes is one of the main approaches for activation of silent BGCs. The most characterized transcriptional regulator in *Streptomyces* is a TetR-type repressor [**50**][**70**]. Inactivation of the *tetR*-type repressor genes sometimes causes the activation of cryptic secondary metabolite BGCs; for example, deletion of *alpW* resulted in accumulation of kinamycin in *Streptomyces ambofaciens* [**39**], and *scbR* mutation led to activate coelimycin P1 in *Streptomyces coelicolor* [**28**][**29**]. On the other hand, overexpression of the transcriptional activator genes could also lead to the production of cryptic secondary metabolites; overexpression of an LuxR-family transcriptional activator gene led to accumulate a 51-membered macrolide stambomycin in *Streptomyces ambofaciens* [**71**], overexpression of the LuxR-family regulator activated the biosynthesis of 6-*epi*-alteramides in *Streptomyces albus* J1074 [**72**], and forced expression of the SARP-type activator led to accumulate a novel amide-containing polyene ishigamide in *Streptomyces* sp. MSC090213JE08 [**73**]. Thus, extensive genetic manipulation of the regulators causes the activation of silent BGCs. Further understanding of the regulatory system in *Streptomyces* may lead to a natural

product discovery with notable biological activities. In this thesis, I focused on the transcriptional regulators, TetR-type repressor and SARP-type activators, both of them are responsible for secondary metabolite production in *Streptomyces*. The followings are schematic summary in my PhD thesis (**Figures 1.9 and 1.10**).

In **Chapter 2**, I performed a functional analysis of a pseudo-receptor like gene, *srrB*, which is located in the vicinity of the SRB receptor gene *srrA*. I revealed that *srrB* acts as a negative regulator by binding to the promoter region of the target gene *srrY* to repress antibiotic production in *S. rochei* (**Figure 1.9**) [Misaki, Y., Yamamoto, S., Suzuki, T., Iwakuni, M., Sasaki, H., Takahashi, Y., Inada, K., Kinashi, H. and Arakawa, k."SrrB, a pseudo-receptor protein, acts as a negative regulator for lankacidin and lankamycin production in *Streptomyces rochei*" *Front. Microbiol.*, **11**, 1089 (2020).]

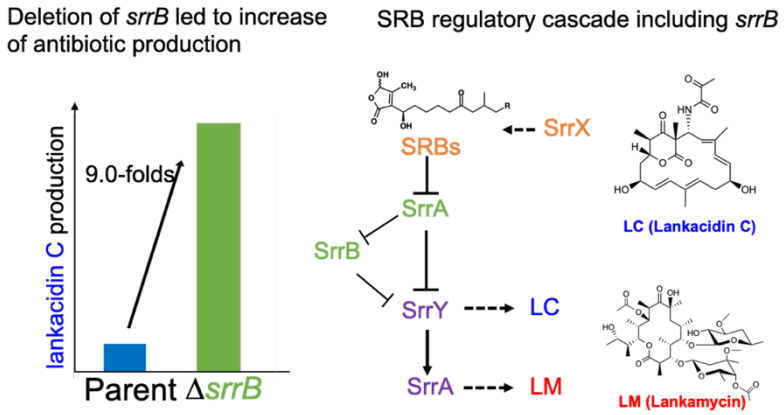

Figure 1.9 Graphical abstract of Chapter 2.

In **Chapter 3**, I attempted activation of cryptic BGCs by overexpression of SARP-type activators. The recombinant of overexpression of SARP (SRO_3163) accumulated UV-active compound YM3163-A. I carried out purified and elucidated the structure of YM3163-A. As a result, YM3163-A is novel compound, 2-(cyclohex-2-en-1-ylidene)acetamide, ant its confirmed by chemical synthesis (**Figure 1.10**). [Misaki, Y., Nindita, Y., Fujita, K., Fauzi, A.A. and Arakawa, K., "Overexpression of SRO_3163, a homolog of *Streptomyces* antibiotic regulatory protein, induces the production of novel cyclohexene-containing enamide in *Streptomyces rochei*" *Biosci. Biotechnol. Biochem.*, **86,** 177-184 (2021).]

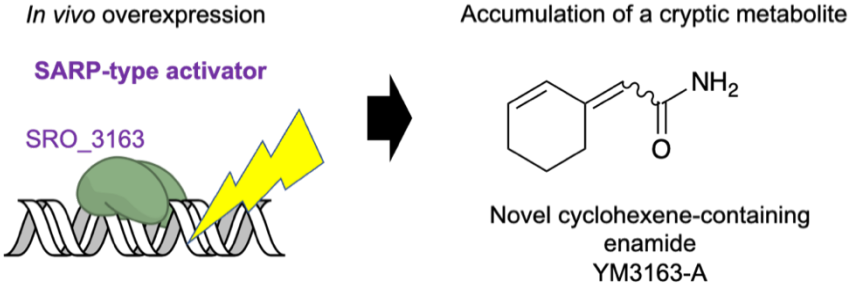

Figure 1.10 Graphical abstract of Chapter 3.

Chapter 2

Functional analysis of pseudo-receptor like gene *srrB* in *Streptomyces rochei*

2.1 Introduction

Our laboratory revealed that SRBs/SrrA complex dissociates from the promoter region of *srrY*, leading to activate lankacidin production [**20**]. Then, the gene product of *srrY* further activates a second activator gene *srrZ* to produce lankamycin (Suzuki et al. 2010) (**Figure 2.1.1**).

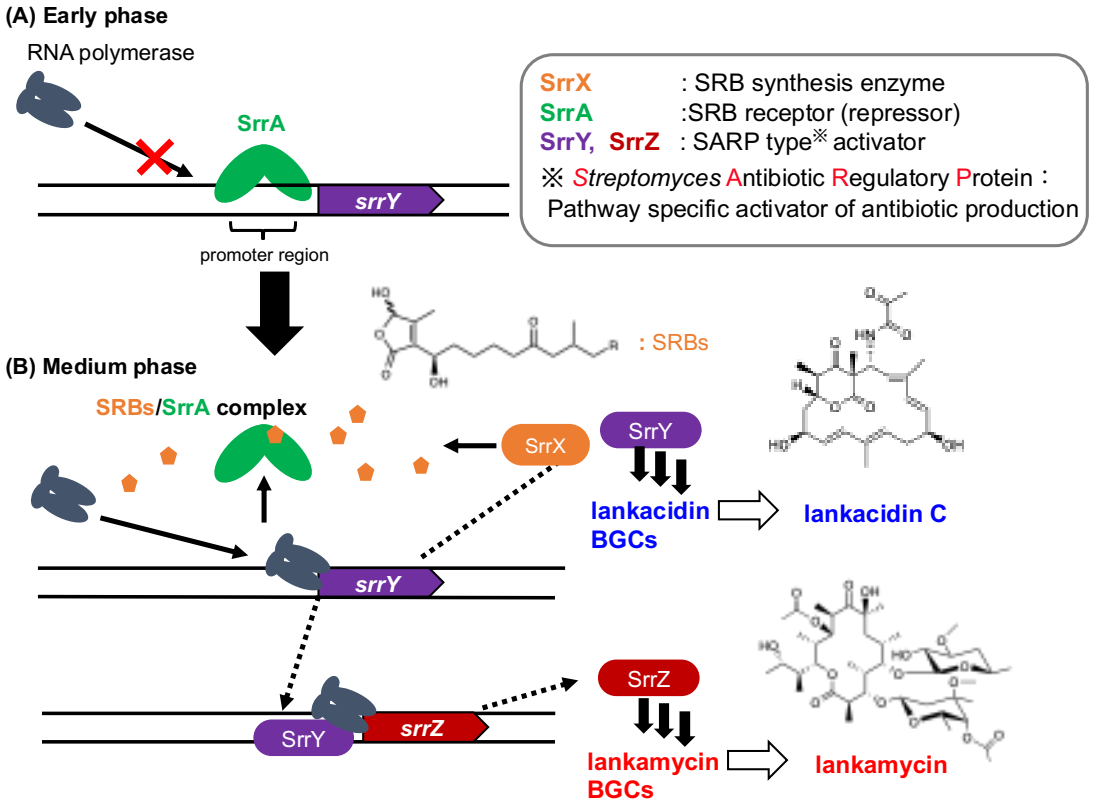

Figure 2.1.1 Regulatory cascade for lankacindin and lankamycin
(**A**) Early phase of culture; SRBs are absent.
(**B**) Medium phase of culture; SRBs are accumulated.

In addition, mutation of an additional signaling-molecules receptor gene *srrB* led to increase the production of both lankacidin and lankamycin [**19**]. Based on *in silico* analysis, SrrB belongs to a major class of TetR-type transcriptional regulators. Its phylogenetic analysis (**Figure 1.5**) indicated that SrrB is classified into pseudo-receptor

family protein. Amino acid alignments of pseudo-receptor family proteins are shown in **Figure 2.1.2**, in which they have a conserved helix-turn-helix motif and a possible ligand-binding residue Trp.

The pseudo-receptors are widely found in *Streptomyces* species, and they act as negative regulators for secondary metabolite production. Our preceding result [**19**] suggested that *srrB* negatively regulates lankacidin and lankamycin production, however, its functional role has not been clarified.

In this chapter, I extensively investigated the function of *srrB* by analyzing antibiotic production and transcription, the results of which indicated that SrrB acts as a negative regulator by binding to the promoter region of the activator gene *srrY* to control lankacidin and lankamycin production at the later stage of fermentation in *S. rochei*.

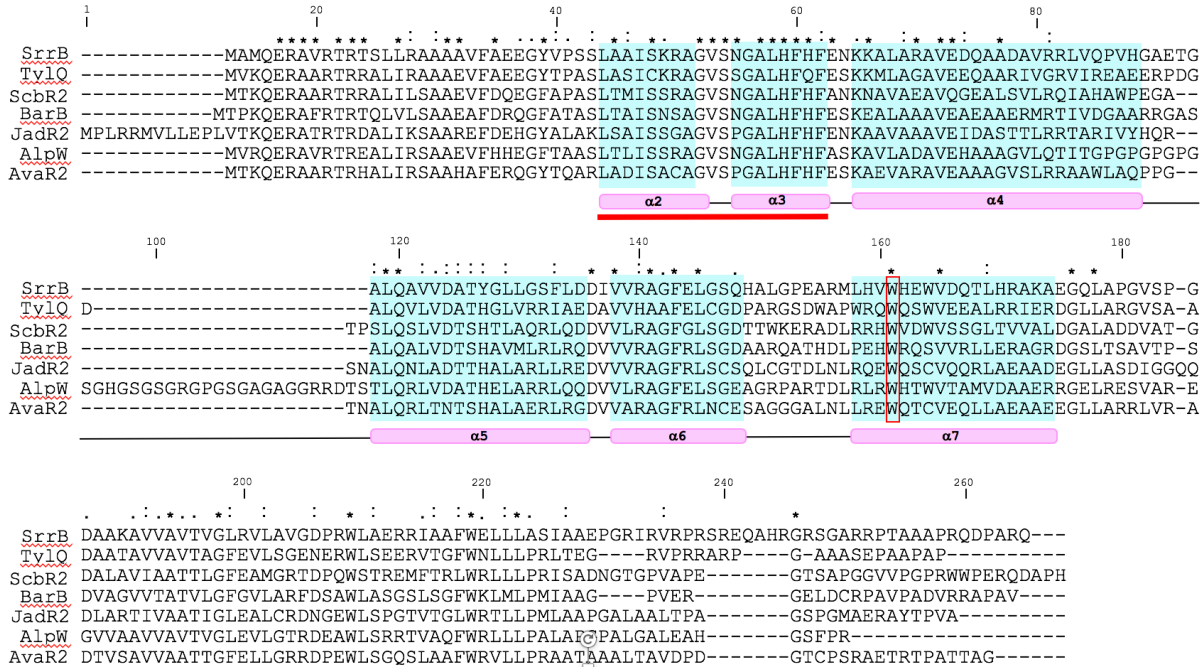

Figure 2.1.2 Alignment of Amino acid sequences of the pseudo-receptors including SrrB was performed by BioEdit version 7.2.5 software (https://bioedit.software.informer.com/) [**74**](Hall, 1999). Conserved α-helix structures are shaded light blue. Helix-turn-helix motif at the N-terminal is marked as a red underline. Red box indicates an important residue for ligand binding. Highly conserved amino acid residues are marked below the alignment as identical (asterisk), well conserved (colon), or partially conserved (period). The GenBank accession numbers are shown as follows: *S. rochei*, SrrB (NP851501); S. *fradiae*, TylQ (AAD40803); *S. coelicolor* A3(2), ScbR2 *(*NP630384); *S. virginiae*, BarB (BAA23612); *S. venezuelae*, JadR2 *(*CCA59258); *S. ambofaciens*, AlpW *(*CAJ87891); *S. avermitilis*, AvaR2 *(*BAC71414).

2.2 Material and Methods

2.2.1 Plasmid isolation from *E. coli*

Plasmid DNA isolation was performed using alkaline-lysis method described by Sambrook *et al*. [**75**]. The cell pellet from 1.5 ml of overnight culture was resuspended with 100 µl of solution I (25 mM Tris-HCl, 10mM EDTA, 50 mM D-glucose, pH 8.0) . The suspension was treated with 200 µl of solution II (0.2 M NaOH, 1% SDS) and the resultant was neutralized with 150 µl of solution III (60 mL 5 M Potassium acetate, 11.5 mL Glacial acetic acid, 28.5 mL H_2O). The mixture was mixed with 450 µl of phenol:chloroform=1:1 (v/v) and centrifuged. The aqueous upper layer was transferred to a new tube. Nucleic acids were precipitated from the supernatant by adding 2.5 volumes of ice-cold 99% ethanol, mixed by gentle inversion. The mixture was stored in −80°C for 30 minutes, and centrifuged. The supernatant was removed, and the resulting pellet was washed with 300 µl of ice-cold 70% ethanol. The dried pellet was dissolved in 30 µl of TE buffer (100 mM Tris-HCl (pH 8.0), 10 mM EDTA (pH 8.0)) and stored in −20°C.

2.2.2 Total DNA preparation for *Streptomyces*

Total DNA was prepared by a neutral method according to the protocol [**76**] with slight modifications. The pellet from 5 mL culture was suspendered in 13 mL of 10.3% sucrose. To the suspension was added 1 mL of 0.5 M EDTA (pH 8.0) and 4 mL of lysozyme (5 mg/mL in Tris-sucrose-EDTA (0.3 mM Sucrose, 25 mM Tris-base, 30 mM EDTA), Wako Chemical, Gunma, Japan) was added and incubated at 37℃ for 1 h. Two milliliters of Actinase E (5 mg/mL in Tris-saline-EDTA (50 mM NaCl, 30 mM Tris-base, 5 mM EDTA), Kaken Seiyaku, Tokyo, Japan) was added, and the mixture was incubated at 37℃ for 1 h. Then the mixture treated with 0.25 mL of 10% SDS was then shaken for an additional 30 min at 37℃. The mixture was then mixed with 0.5 mL of 5 M NaCl, and incubated at 37℃ for another 30 min and left at 4℃ overnight. The mixture was centrifuged at 12,000 rpm for 20 min, and the supernatant fluid was precipitated with equal volume of 2-propanol. To purify the DNA, the precipitate was dissolved in TE buffer and extracted with phenol-chloroform (1:1, v/v). The aqueous layer was

precipitated with 3-times volume of 99% ice-cold ethanol, and the resulting pellets were dissolved in TE buffer, and stored in −20℃.

2.2.3 Southern hybridization

Southern hybridization was carried out using DIG labeling kit (Roche) according to the manufacture's protocol. A 15 μL of DNA solution was boiled for 10 minutes and placed on ice immediately. To the denatured DNA, 2 μl of hexanucleotide mixture solution and 2 μL of dNTP labeling mixtures solution were added. After adding 1 μL of Klenow enzyme, the mixture was incubated at 37°C for more than 12 hours. The labeling was stopped by the addition of 2 μL of 0.5 M EDTA, 2.5 μL of 4 M LiCl, and 75 μL of 99% ethanol. The mixture was placed at -80°C for 30 minutes. After centrifugation, the pellet was washed with 70% ethanol, and dissolved with 30 μL of distilled water.

After the gel electrophoresis image stained by Ethidium Bromide (EtBr) was taken, the agarose gel was rinsed with 0.25 M HCl for 10 min, and then continued to soak in alkaline transfer buffer (0.5 M NaOH, 1.5 M NaCl) for 15 min twice and neutralization buffer (1 M Tris base, 1.5 M NaCl, pH 8.0) for 20 min. The DNA was transferred onto the nitrocellulose membrane by upward capillary transfer method for 8-24 h. The membrane was washed with 2×SSC (0.3 M NaCl, 30 mM Sodium citrate dihydrate) briefly, and irradiated by UV light to fix the single-stranded DNA. The membrane was then placed in Hybri-bag Hard (Cosmo Bio, Tokyo, Japan) filled with hybridization buffer (250 mL 20 × SSC, 5 g skim milk, 1mL 10% SDS, 10 mL 10% N-lauroylsarcosine, fill up to 1,000mL) and was incubated at 70°C. After one hour, the denatured probe was added to the Hybri-bag, and the membrane was further incubated overnight at 70°C. The incubated membrane was rinsed with 2×SSC-0.1% (w/v) SDS for 5 min at room temperature twice and with 0.1×SSC-0.1% (w/v) SDS at 70℃ for 15 min twice. The membrane was rinsed in buffer I (1 M Tris base, 1.5 M NaCl, pH 7.5) and soaked in buffer II (0.5% (w/v) skim milk in buffer I) for 30 min at room temperature with gentle agitation. After washing with buffer I, the membrane was incubated in buffer I containing anti- digoxygenin-AP Fab fragment (Roche Diagnostics, Rotkreuz, Switzerland) (2 μL in 10 mL) for 1 h. The membrane was washed with buffer I for 15 min twice, and then soaked in buffer III (1 M Tris base, 1.5 M NaCl, 50 mM $MgCl \cdot 6H_2O$). The DIG-labeled

DNA was detected using colorimetric detection substrates, NBT/BCIP solution [45 μL NBT solution (75 mg nitrobluetetrazolium salt, 1mL 70% (v/v) dimethylformamide) and 35 μL X-phosphate solution (50 mg 5-bromo-4-chloro-3-indolylphosphate toluinidium salt, 1 mL 100% dimethylformamide) in 10 mL buffer III].

2.2.4 Strains, plasmids, and oligonucleotides, and culture conditions

All the strains and plasmids used in this study were listed in **Table 2.1.1**. *S. rochei* strain 51252 carrying only the linear plasmid pSLA2-L was used as the parent strain [**65**]. All strains, plasmids, and oligonucleotides used in this study are listed in **Table 2.1**. *Streptomyces* strains were grown in YM medium (0.4% yeast extract, 1.0% malt extract, 0.4% D-glucose, pH 7.3) for antibiotic production and RNA isolation. *Escherichia coli* strains were grown in Luria-Bertani (LB) medium supplemented with ampicillin (100 μg/ml), apramycin (50 μg/ml), and/or chloramphenicol (25 μg/ml) when necessary. For protoplasts preparation, *Streptomyces* strains were grown in YEME medium [**77**]. Protoplasts were regenerated on R1M plates [**78**]. PCR amplification was done on a 2720 Thermal Cycler (Thermo Fisher Scientific, Waltham, MA, USA) with KOD-Plus- DNA polymerase (Toyobo, Osaka, Japan).

Table 2.1.1 Bacterial strains, plasmids, and oligonucleotides used in this chapter.

Strains/plasmids/oligonucleotides	Description	Source/Refe
Bacterial strains		
Streptomyces rochei 7434AN4	Wild type (pSLA2-L, M, S)	[65]
Streptomyces rochei 51252	Ultraviolet irradiation of 7434AN4 (pSLA2-L)	[65]
Streptomyces rochei KA07	*in frame* deletion of *srrB* in 51252 (*ΔsrrB*)	[19]
Streptomyces rochei KA12	*in frame* deletion of *srrA* in 51252 (*ΔsrrA*)	[19]
Streptomyces rochei TS03	*in frame* deletion of *srrA* in KA07 (*ΔsrrAB*)	This study
Streptomyces rochei KA61	*in frame* deletion of *srrY* in 51252 (*ΔsrrY*)	[20]
Streptomyces rochei KA64	*in frame* deletion of *srrY* in KA07 (*ΔsrrBY*)	This study
Streptomyces rochei KA20	*kan*::*srrX* in KA07 (*ΔsrrXB*)	[12]
Escherichia coli XL1-Blue	*recA1 endA1 gyrA96 thi-1 hsdR17 supE44 relA1 lac* [F' *proAB lacIqZΔ*(*M15* Tn10 (Tet^r))	Stratagene
Escherichia coli BL21(DE3)pLysS	F' *ompT hsdS*$_B$ (r$_B^-$ m$_B^-$) *gal dcm* (DE3) pLysS(Cam^r)	Novagen
Plasmids		
Cosmid A8	38.9-kb pSLA2-L DNA (nt 106,868-145,771) cloned into SuperCos-1 at *Bam*HI site	[6]
pKAR3004	4.3 kb *Pst*I-*Eco*47III fragment containing *srrB* in pUC19	[19]
pKAR3014	3.0 kb *Nco*I-*Sac*I fragment deleted 207-bp *Bsp*EI fragment from *srrA*	[19]
pKAR3055	1.5 kb EcoRI-PstI fragment deleted 267-bp *Pvu*II fragment from *srrY*	[20]
pKAR3036	0.68 kb *Nde*I-*Eco*RI fragment containing *srrB* in pET32b(+)	This study
pKAR4002	9.2 kb *Pst*I fragment containing *srrY* in pUC19	[20]
pUC19	Cloning vector; *amp*	Takara
pET32b(+)	T7 expression vector for histidine-tagging, *amp*	Novagen
pIJ8600	Integrative *E. coli-Streptomyces* shuttle vector, inducible *tipA* promoter, *apr*, *tsr*	79
pKAR3065	0.68 kb *Nde*I-*Xba*I PCR fragment containing srrB in pIJ8600	This study
Oligonucleotides (5' - 3')		
KAR7901OE	CGCAGATCTCATATGGCCATGCAGGAACGT	This study
KAR7902OE	CTAGAATTCGTACAGCTCGGCCACCATGGC	This study
SRRBf3	ACCCGCACGGCCCGTACATC	This study
SRRBr3	GTACCCCTCTTCCGCGAACA	This study
SRRYf2	GGCGTCGTCTGCCTGCTGCC	[20]
SRRYr2	ATATCCGCCGGGGGCGGTGG	[20]
SRRYf4	CTCCCCTTGTCGTCGTCGAG	This study
SRRYr4	GCGCCCGCGGCGTCACCGAGA	[20]
RT75-F	CAGGTTCTCGTGCGTGCGGTA	This study
RT75-R	GTGCGACGTACAAGCGGGACC	This study
KA82010E	CTAGGATCCGCATATGGCACAGCAGGAAC	This study
SRRAr2B	GGGGGATCCCACCAGCACCGAGGGCACCGC	This study
SRRBf1E	GGGGAATTCGAGCGGTGGAGGACCAGGCCG	This study
SRRBr4	AGGAGCAGTTCCCAGAACGC	This study
16S-357F	CCTACGGGAGGCAGCAG	[80]
16S-907R	CCCCGTCAATTCCTTTGAGTT	[81]
KA-RT079S1	GCGAGACACCGGGAGCCAACTG	This study
KA-RT079AS1	TCGCGGAAGAGGGGTACGTGCC	This study
srrB-8600f1	GAACATATGGCCATGCAGGAA	This study
srrB-8600r1	TGAAGATCTCACTGTCGGGCTG	This study
srrB-GSP1	GCTGCGAACCCAGCTCGAAAC	This study
srrB-GSP2	GTCCGTAGGTCGCGTCGACG	This study
RT79-R2	CGCCTTCTTGTTCTCGAAGTG	This study

2.2.5 Construction of *srrA* and *srrB* double mutant

The target plasmid pKAR3014 that carries in-frame deletion of *srrA* in *E. coli-Streptomyces* shuttle vector pRES18 [**82**] was constructed as described previously [**19**]. Targeted mutagenesis was performed as follows. Plasmid pKAR3014 was transformed into protoplasts of *S. rochei* strain KA07 (*srrB* mutant), and thiostrepton-resistant strains were obtained. Among these transformants, single-crossover strains were selected by Southern hybridization. Some single-crossover colonies were continuously grown in YEME liquid medium to facilitate a second crossover. Finally, thiostrepton sensitive strains were selected as double crossover strains, to obtain a strain TS03 (*srrAB* mutant). Gene disruption was checked by Southern hybridization analysis using DIG DNA Labeling and Detection Kit (Roche Diagnostics GmbH, Mannheim, Germany) (**Figure 2.2.1**).

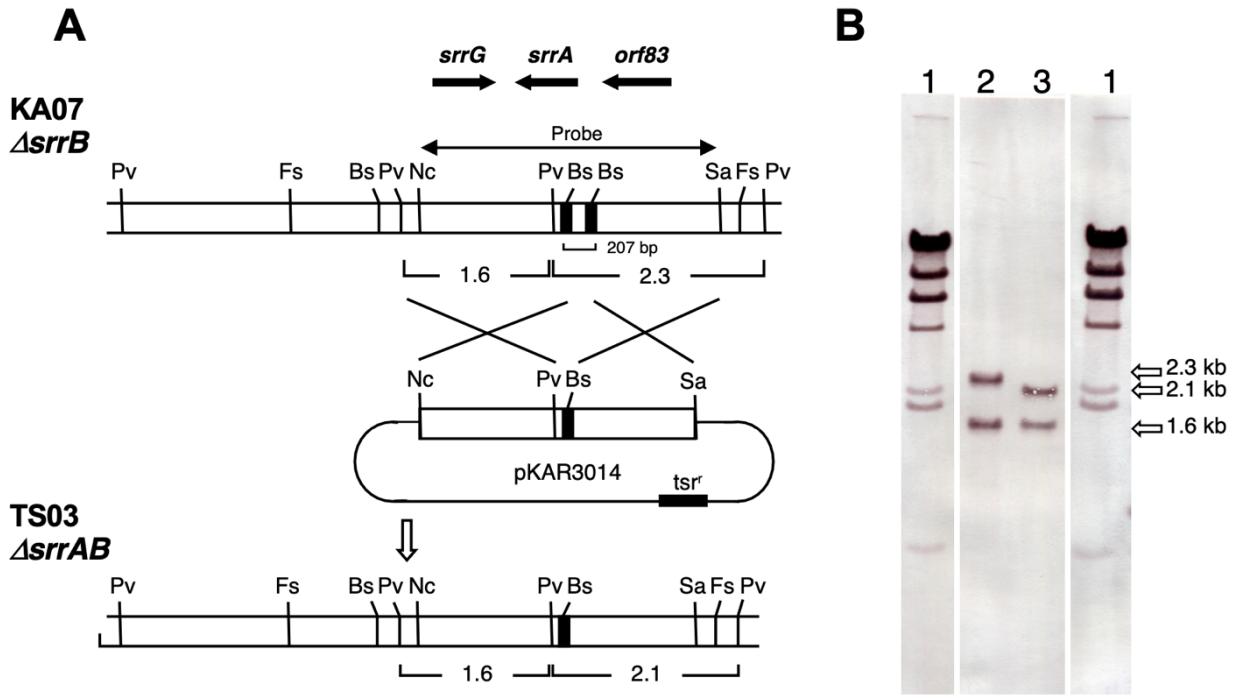

Figure 2.2.1 (**A**) Construction of the Δ*srrAB* mutant TS03. Pv, *Pvu*II; Fs, *Fsp*I; Bs, *Bsp*EI; Nc, *Nco*I; Sa, *Sac*I. (**B**) Southern blot analysis. Lane 1, I/*Hin*dIII; lane 2, strain 51252 (parent)/ *Pvu*II; lane 3, strain TS03 (Δ*srrAB*)/ *Pvu*II.

2.2.6 Construction of *srrY* and *srrB* double mutant

The target plasmid pKAR3055 that carries in-frame deletion of *srrY* in pRES18 was constructed as described previously [**20**]. This plasmid was transformed into protoplasts of *S. rochei* strain KA07, and an *srrB-srrY* double mutant KA64 was constructed in a similar manipulation as above mentioned (**Figure 2.2.2**).

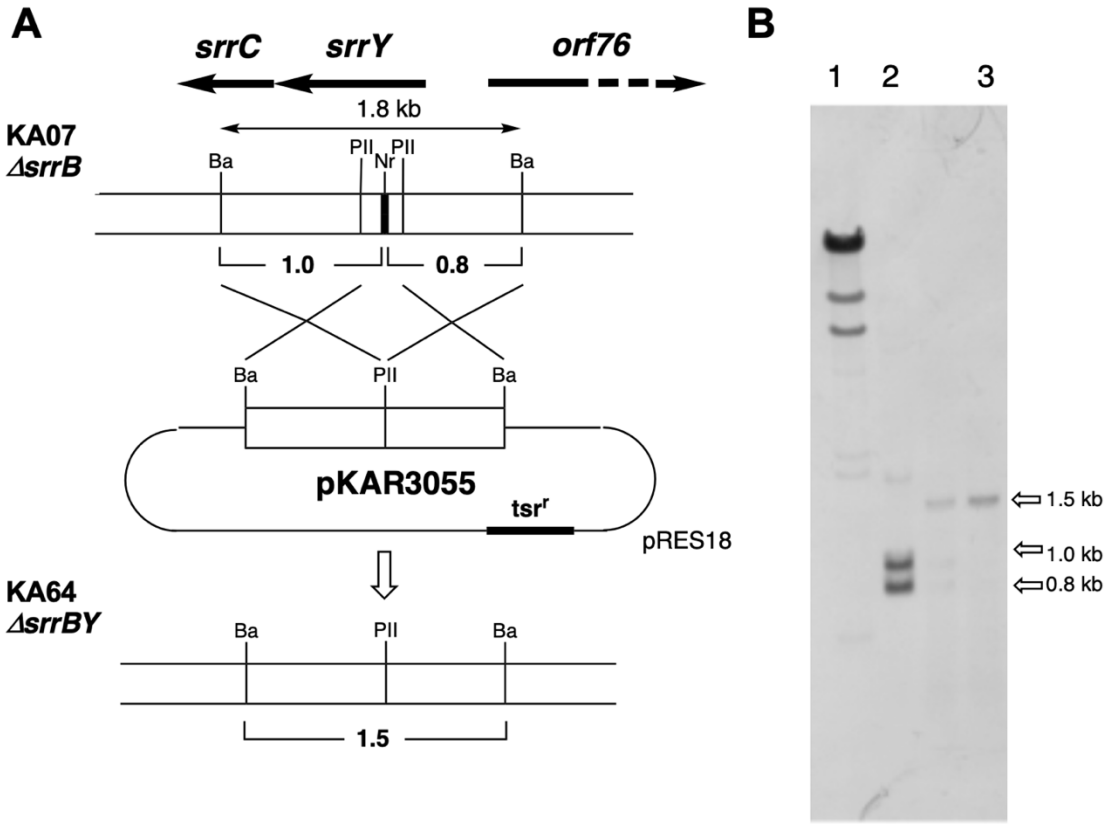

Figure 2.2.2 (**A**) Construction of the Δ*srrBY* mutant KA64. Ba, *Bam*HI; Nr, *Nru*I; PII, *Pvu*II.
(**B**) Southern blot analysis. Lane 1, I/*Hin*dIII; lane 2, strain KA07 (parent)/ *Bam*HI & *Nru*I; lane 3, strain KA64 (Δ*srrBY*)/ *Bam*HI & *Nru*I.

2.2.7 Construction of *in vivo srrB* expression plasmid

The *srrB* gene was amplified using cosmid A8 [**66**] and primers, srrB-8600f1 and srrB-8600r1. The resulting PCR product was digested with *Nde*I and *Xba*I and cloned into pIJ8600, an *E. coli-Streptomyces* shuttle vector carrying a *tipA* promoter [**79**], to obtain pKAR3065.This plasmid was introduced into strain 51252, and transformants were cultured for 24 h at 28°C in YM liquid medium with 10 μg/ml apramycin. Thiostrepton (10 μg/ml as final concentration) was added at 24 h to induce *srrB* expression. After cultivation for additional 24 h, the broth filtrate was extracted twice with equal volume of ethyl acetate. The combined organic phase was dried with Na_2SO_4, and concentrated *in vacuo* to obtain crude extracts.

2.2.8 Construction of *srrB* overexpression plasmid in *E. coli*

The *srrB*-coding sequence was PCR amplified using the template cosmid A8 [**66**] and primers, KAR7903OE and KAR7902OE. The amplified fragment was digested with *Bgl*II and *Eco*RI and cloned into pET32b(+), a $(His)_6$-tagged expression vector, to obtain pKAR3036.

2.2.9 Isolation and analysis of metabolites

The 48-h cultures of *S. rochei* strains were harvested, and the supernatant was extracted twice with equal volume of ethyl acetate. The crude extracts were purified by Sephadex LH-20 chromatography (1 × 40 cm, GE Healthcare, Chicago, IL, USA) with methanol. Then the fractions containing antibiotics were purified by silica gel chromatography with chloroform-methanol (80:1–10:1, v/v). NMR spectra were recorded on an ECA-500 spectrometer (JEOL, Tokyo, Japan) equipped with a field gradient accessory. Chloroform-*d* ($CDCl_3$) and methanol-d_4 (CD_3OD) were used as solvents. Chemical shifts were recorded in δ value based on the solvent signals (δ_C = 77.0 in $CDCl_3$, δ_C = 49.0 in CD_3OD, and δ_H = 3.30 in residual CH_3OH) or an internal standard tetramethylsilane (δ_H = 0). High resolution ESI-MS spectra were measured by a LTQ Orbitrap XL mass spectrometer (Thermo Fisher Scientific). The ^1H- and ^{13}C-NMR assignments for lankamycin (**1**), lankacidin C (**2**), lankacidin A (**3**), lankacidinol A (**4**), iso-lankacidinol (**5**), and lankacidinol (**6**) (**Figure 1.7**) have already been reported[**21**][**83**][**84**].

2.2.10 SRB assay

Two strains KA61 (Δ*srrY*) and KA64 (Δ*srrY*Δ*srrB*) were cultured at 28°C for 30 h, and the supernatant (60 ml) was acidified to pH 3 and extracted with equal volume of ethyl acetate twice. The combined organic phase was concentrated in vacuo. Appropriately diluted culture extract (100 µl) was added to the fresh culture (5 ml) of strain KA20, an *srrX*-deficient strain, and cultured at 28°C for 36 h to restore lankamycin and lankacidin production.

2.2.11 Time-course analysis

S. rochei strains were grown in YM liquid medium and harvested at various time periods at 12-36 h. Cells were used for measurement of dry cell weight (DCW) and isolation of total RNA, while the culture supernatant was for measurement of antibiotic production.

2.2.12 Measurement of DCW

Cultures were collected at various time periods and centrifuged at 5,000 rpm for 10 min. The resulting pellet was washed twice with 10.3% sucrose, and then placed in a 60°C dry oven until the weight reaches to a constant value.

2.2.13 RNA preparation and reverse transcription-PCR (RT-PCR)

S. rochei strains were cultured at 28°C in YM liquid medium for various time periods. Total RNAs was extracted from cells with a TRI reagent (Invitrogen, Carlsbad, CA) according to the manufacturer's instructions. Trace amounts of DNA were removed with RNase-free DNase I (Takara, Kyoto, Japan). The concentration of purified RNA was determined by UV absorbance at 260 nm using Ultrospec 3300 pro spectrometer (GE Healthcare). The cDNAs were synthesized using Transcriptor Reverse Transcriptase (Roche Diagnostics). Each reaction mixture contained 1 µg of total RNA and 0.08 A_{260} units random primer. Each mixture was sequentially treated at 85°C for 5 min, at 25°C for 10 min, and 55°C for 45 min for the cDNA synthesis. The 16S rRNA was used as an internal standard [**80**][**81**].

2.2.14 5′ Rapid amplification of cDNA ends (5′ RACE)

Transcriptional start site (TSS) of *srrB* was determined using 5′RACE System, Version 2.0 (Invitrogen, Carlsbad, CA, USA). Total RNA was prepared from a 24-h culture sample of parent strain. One microgram of total RNA was converted to the cDNA using specific primer srrB-GSP1, and the resultant was treated with ribonuclease and purified through spin column to afford cDNA. A homopolymeric tail was then added to the 3'-end of cDNA using terminal deoxynucleotidyl transferase and dCTP. PCR was performed with poly C tailed cDNA as a template using abridged anchor primer and inner specific primer RT79-R2. TSS was determined from nucleotide sequence of amplified PCR product using ABI PRISM 310 Genetic Analyzer (Life Technologies, Carlsbad, CA, USA).

2.2.15 Overexpression and purification of SrrB protein

E. coli BL21(DE3)pLysS was used as hosts for plasmid pKAR3036. Cells were grown in LB liquid medium supplemented with 100 μg/ml ampicillin and 25 μg/ml chloramphenicol at 37°C to OD_{600} = 0.6 and then were induced with 1 mM isopropyl β-thiogalactopyranoside (IPTG). Cultivation was continued for 12 h at 16°C, and then cells were harvested and disrupted by SONIFER 250 ultrasonic homogenizer (Branson Ultrasonics Corporation, Danbury, CT, USA). The $(His)_6$-fusion protein was purified by Ni^{2+}-nitrotriacetic acid agarose (Qiagen GmbH, Hilden, Germany) according to the manufacture's protocol. After dialysis with PBS buffer (137 mM NaCl, 8.1mM $Na_2HPO_4 \cdot 12H_2O$, 2.68 mM KCl, 1.47 mM KH_2PO_4), the $(His)_6$-tagged SrrB protein was treated with enterokinase (Novagen, Madison, WI, USA), and the $(His)_6$-tag peptide upstream of the N-terminal SrrB was removed by Enterokinase Cleavage Capture Kit (Novagen) according to the manufacture's protocol. The protein was analyzed by SDS-PAGE with 15% polyacrylamide gel. The protein concentration was determined according to the methods of Bradford using Bio-Rad protein assay (Bio-Rad, Hercules, CA, USA) with bovine serum albumin as a standard.

2.2.16 Preparation of DNA probes and gel shift assay

The *srrB* probes for gel shift assay were prepared as follows. For preparation of probe B1, a 564-bp DNA fragment containing the upstream region of *srrB* was amplified

using pKAR3004 as a template and primers SRRBf3 and SRRBr3 (positions −81 to +483 from TSS of *srrB*; nt 140,677-141,240 of pSLA2-L). For preparation of probe B2, a 386-bp DNA fragment containing the internal region of *srrB* was amplified using pKAR3004 as a template and primers SRRBf1E and SRRBr4 (positions +574 to +959 from TSS of *srrB*; nt 140,201-140,586 of pSLA2-L).

Probe B1 was then 3′-end labeled with [γ-^{32}P]ATP (GE Healthcare) and T4 polynucleotide kinase (Toyobo). The reaction mixture contained the binding buffer (20 mM Tris-HCl [pH 8.0], 100 mM NaCl, 1 mM dithiothreitol, 0.1 mg of bovine serum albumin and 5% glycerol), 0.5 nM labeled DNA and 2 μM SrrA protein. SrrA protein was prepared as reported previously[20]. When necessary, synthetic SRB1 [(1-′*R*)-isomer; **Figure 1.7**] [**12**]was added to the reaction mixture. For competition experiment, unlabeled probes B1 and B2 were used at a final concentration of 200 nM. The reaction mixture was incubated at 26°C for 30 min, and subjected to electrophoresis at room temperature on a native 4.5% polyacrylamide gel in 0.5 × TBE buffer (46 mM Tris base, 46 mM boric acid, 1 mM EDTA). The ^{32}P-labeled DNAs were detected by autoradiography.

Preparation of *srrY* probes for gel shift assay was described previously[**20**]. To analyze the effect of SRB on the binding of SrrA and SrrB, various concentration of synthetic SRB1 [(1′*R*)-isomer; **Figure 1.7**] [**12**] was added to the reaction mixture. In order to evaluate the effect of endogenous metabolites in *S. rochei* and other antibiotics on the binding of SrrB, the following compounds (1 mM) were separately added to the reaction mixture; lankamycin, lankacidin, chlorotetracycline, kanamycin, and ampicillin.

2.2.17 DNase I Footprinting

The method used for DNase I footprinting analysis for the upstream region of *srrY* was described previously [**20**]. For the upstream region of *srrB*, the primer SRRBf3 was 5′-end labeled using [γ-^{32}P]ATP (GE Healthcare) and T4 polynucleotide kinase (Toyobo), and then PCR reaction was performed with unlabeled primer SRRBr3 and pKAR3004 as a template to afford a 564-bp product containing the upstream region of *srrB* (positions −81 to +483 from TSS of *srrB*; nt 140,677-141,240 of pSLA2-L). Binding reaction mixture (50 μl) contained 10 nM labeled DNA, 20 mM Tris-HCl (pH8.0), 1 mM $MgCl_2$, 100 mM NaCl, 1 mM dithiothreitol, 0.1 mg/ml BSA, 5% glycerol, and various concentrations of SrrA. The binding reaction mixture was incubated for 30 min at 25°C, and then a mixture was treated with DNase I (Roche Diagnostics) solution [1 ng in 50 μl of 5 mM $MgCl_2$ and 5 mM $CaCl_2$] for 2 minutes at room temperature. The reaction was terminated by 100 μl of phenol-chloroform. The aqueous fraction containing DNAs was precipitated by ethanol and separated on a 5% polyacrylamide gel containing 6 M urea. The labeled DNAs were detected by autoradiography. Sequencing ladders were generated by Maxam-Gilbert sequencing of the labeled DNA used for binding reaction.

2.3 Results

2.3.1 SrrB acts as a negative regulator for antibiotics production

To evaluate the effect of *srrB*-mutation on the metabolic titer, I performed comparative metabolite analysis of the *srrB* mutant and its parent strain 51252. The *srrB* mutant KA07 accumulated larger amount of compounds **1**-**6** compared with the parent strain 51252. Namely, KA07 produced 6-folds of lankamycin (**1**) (**Figure 2.3.1 (A)**) and

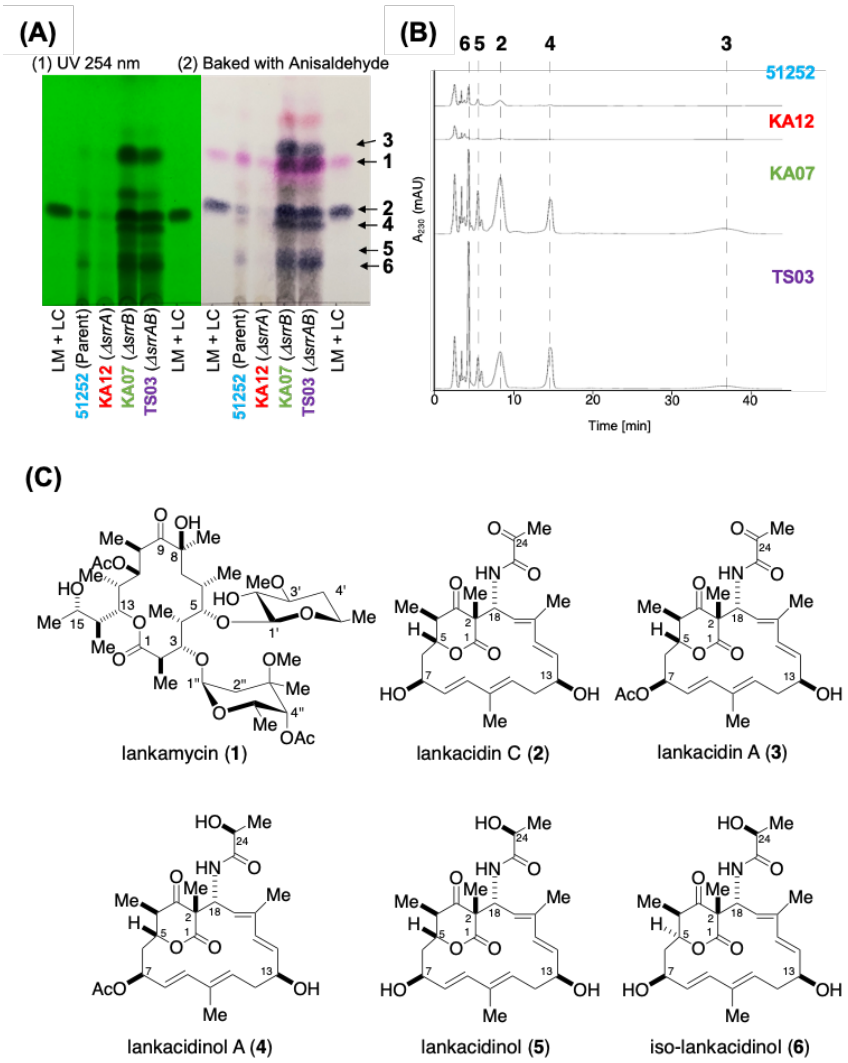

Figure 2.3.1 Metabolite profiles and cell growth of four *S. rochei* strains; 51252 (parent), KA12 (Δ*srrA*), KA07 (Δ*srrB*), and TS03 (Δ*srrA-srrB*). (**A**) TLC analysis of the crude extract of *S. rochei* strains. All strains were grown at 28°C for 48 h. The left panel represents the TLC plate under ultraviolet irradiation (254 nm). The right panel represents the TLC plate after baking with anisaldehyde-H_2SO_4. TLC plates were developed with chloroform-methanol = 15:1 (v/v). (**B**) HPLC analysis of metabolites produced by *S. rochei* strains. The crude extracts were applied on a COSMOSIL Cholester column (4.6 × 250 mm, Nacalai Tesque) and eluted with a mixture of acetonitrile-10 mM sodium phosphate buffer (pH 8.2) (3:7, v/v) at a flow rate of 1.0 ml/min. (**C**) Chemical structures of antibiotics produced in *S. rochei*. Antibiotics lankamycin (**1**), lankacidin C (**2**), lankacidin A (**3**), lankacidinol A (**4**), iso-lankacidinol (**5**), and lankacidinol (**6**). Me, methyl; Ac, acetyl.

9.9, 25, 4.2, and 5.7-folds of lankacidin C (**2**), lankacidinol A (**4**), iso-lankacidinol (**5**), and lankacidinol (**6**), respectively (**Figure 2.3.1 (B)**).

In order to investigate the effect of SrrA on antibiotic production, I further analyzed two mutants, a *srrA* mutant KA12 and an *srrA-srrB* double mutant TS03. KA12 produced about 40% of metabolites when compared with the parent, while TS03 overproduced metabolites **1**-**6** at the same level with the *srrB* mutant KA07. These results confirmed the following two aspects; *srrA* mutation causes a slight decrease of the metabolic titer, whereas SrrB acts as a negative regulator for lankacidin and lankamycin production in *S. rochei*. To determine the role of *srrB* in the regulation of lankacidin and lankamycin production, I further performed time-course analysis of metabolite profile, growth curve, and transcription in the parent and three mutants (KA07, KA12, and TS03) at various time periods. As shown in **Figure 2.3.2**, all strains grew in a similar proportion up to 60 h periods, indicating that overproduction in KA07 and TS03 was due to *srrB* mutation but not to cell growth difference.

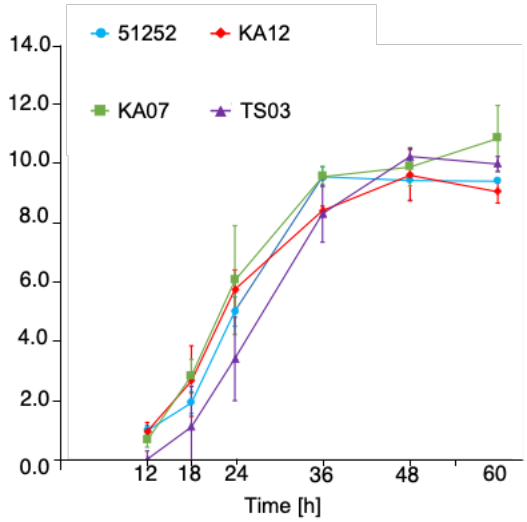

Figure 2.3.2 Time-course growth of *S. rochei* strains. Symbols represent each dry cell weight (DCW; g/l); strain 51252, blue circles and line; strain KA12, red diamonds and line; strain KA07, green squares and line; TS03, purple triangles and line. Results are representative of at least three independent experiments.

The time-course of antibiotic production was analyzed by the titer of lankacidin C (**2**), a major product among lankacidin derivatives (**2**-**6**; Figure 2.3.1(**C**)). As shown in **Figure 2.3.3**, compound **2** was detected after 18 h, and its titer at 48-h growth in the *srrB* deficient strains, KA07 and TS03, were 9.0- and 7.2-times of 51252, respectively, which agrees with the overproduction profiles in KA07 and TS03.

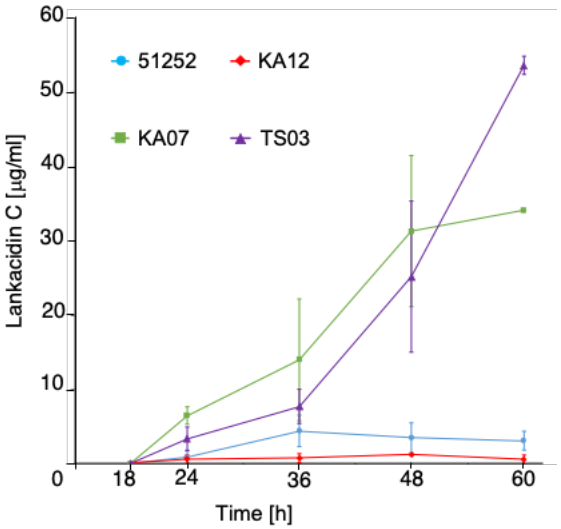

Figure 2.3.3 Time-course production of **2** in *S. rochei* strains. Symbols represent each production yield of **2** (μg/ml); strain 51252, blue circles and line; strain KA12, red diamonds and line; strain KA07, green squares and line; TS03, purple triangles and line. Results are representative of at least three independent experiments.

To confirm the negative regulatory property of SrrB *in vivo*, overexpression of SrrB in *S. rochei* was carried out. The intact *srrB* gene was introduced into plasmid pIJ8600, an *E. coli-Streptomyces* shuttle plasmid with a thiostrepton-inducible *tipA* promoter, to give pKAR3065. I tested antibiotic production in the *S. rochei* 51252 recombinants containing either the empty vector pIJ8600 or the *srrB* overexpression plasmid (pKAR3065). Compared with the control recombinant *S. rochei* 51252/pIJ8600, the *S. rochei* 51252/pKAR3065 recombinant significantly reduced antibiotic production (**Figure 2.3.4**). These results clearly indicated that SrrB acts as a negative regulator for antibiotic production in *S. rochei*.

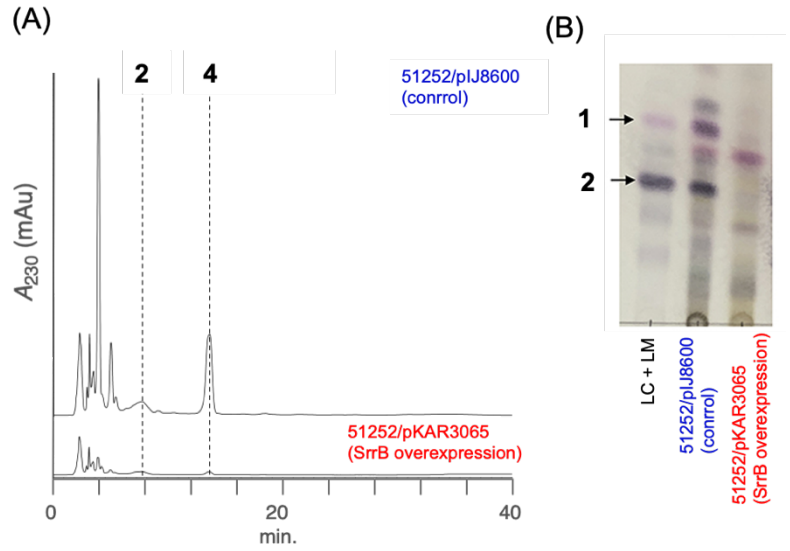

Figure 2.3.4 Effect of *srrB* overexpression on antibiotic production.
Thiostrepton (10 μg/ml) was added to the 24-h culture of *S. rochei* 51252 recombinants harboring either pIJ8600 (control) or pKAR3065 (intact *srrB*), and then the cultures were further incubated at 28° C for 24 h. (**A**) HPLC analysis of crude extracts. The crude extracts were applied on a COSMOSIL Cholester column (4.6 x 250 mm, Nacalai Tesque) and eluted with a mixture of acetonitrile-10 mM sodium phosphate buffer (pH 8.2) (3:7, v/v) at a flow rate of 1.0 ml/min. (**B**) TLC analysis of crude extracts. Crude extracts were separated by TLC [eluent; chloroform-methanol = 15:1 (v/v)] and detected by baking with anisaldehyde-H_2SO_4. Lane 1, LM and LC standard; lane 2, recombinant harboring pIJ8600 (control); lane 3, recombinant harboring pKAR3065 (intact *srrB*).

In preliminary experiment, gel shift assay indicated that SrrA and SrrB could bind to the upstream region of *srrX*, a gene responsible for SRB biosynthesis. This finding suggested that the signaling molecule receptor/pseudo-repressor repress the transcription of *srrX*. Two strains were used to evaluate the comparative yield of SRB; an *srrY* single mutant KA61 and an *srrY-srrB* double mutant KA64, both of which are unable to produce LC or LM due to a mutation on the major activator *srrY*. The yields of SRBs were evaluated by a help of bioassay using an *srrX*-deficient mutant as described previously [**12**] (**Figure 2.3.5**). One-eighth of the crude extract of KA64 contained an equivalent amount of SRBs to that of KA61 (**Figure 2.3.6**), suggesting that *srrB* negatively controls the titer of SRBs.

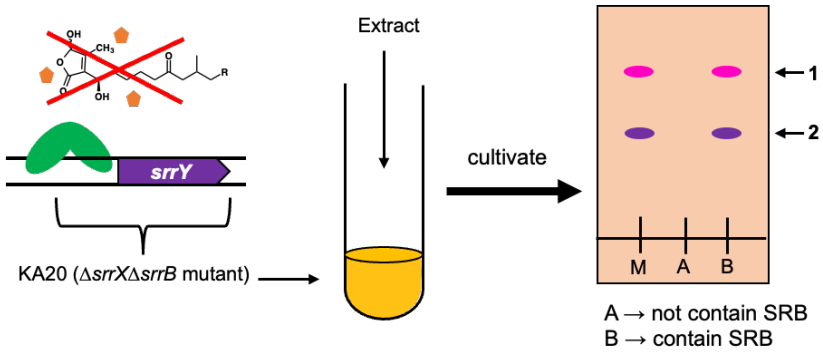

Figure 2.3.5 SRB detection assay.
SRB assay was carried out using strain KA20, a mutant of SRB biosynthesis gene *srrX*, as a test strain. This strain restores antibiotic production in the presence of SRB fraction.

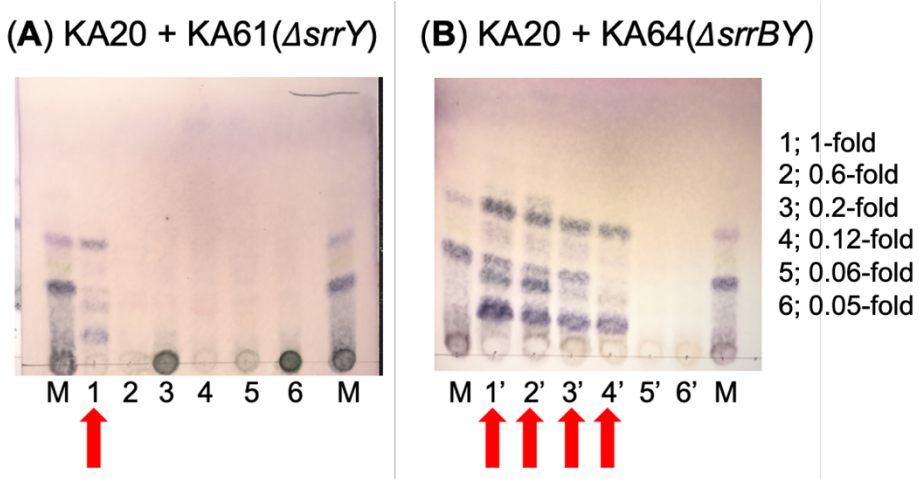

Figure 2.3.6 Effect of *srrB* mutation on SRB productivity.
Two strains for SRB donors, KA61 (Δ*srrY*) (A) and KA64 (Δ*srrBsrrY*) (B), were cultured for 30 h, and then extracted with ethyl acetate to obtain culture extracts. Antibiotic production was detected in lanes 1 (for KA61) and 1'-4' (for KA64). TLC was developed with CHCl3-MeOH = 15:1 (v/v) and stained with anisaldehyde-H_2SO_4.

2.3.2 *srrB* and *srrY* are expressed under the SRB/SrrA regulatory system, and SrrB then represses *srrY* expression at the later stage

To analyze the role of *srrB* in the SRB/SrrA regulatory system in *S. rochei*, I performed comparative transcriptional analysis of the three key regulatory genes, *srrA*, *srrB*, and *srrY*, in the parent and three mutants (*srrA, srrB*, and *srrA-srrB*). Transcription of *srrY* in the parent appeared around 18 h and diminished after 32 h (**Figure 2.3.7 A**), while that in the *srrB* mutant KA07 continued until the later stage (**Figure 2.3.7 C**). On the other hand, *srrB* transcription in the parent appeared around 16 h and prolonged until the late stage of fermentation (**Figure 2.3.7 A**). In the *srrA* mutant KA12, transcription of both *srrY* and *srrB* appeared at 12 h or earlier (**Figure 2.3.7 B**), whereas *srrY*transcription in the *srrA-srrB* mutant TS03 was detected through all time periods (12–36 h) (**Figure 2.3.7 D**).

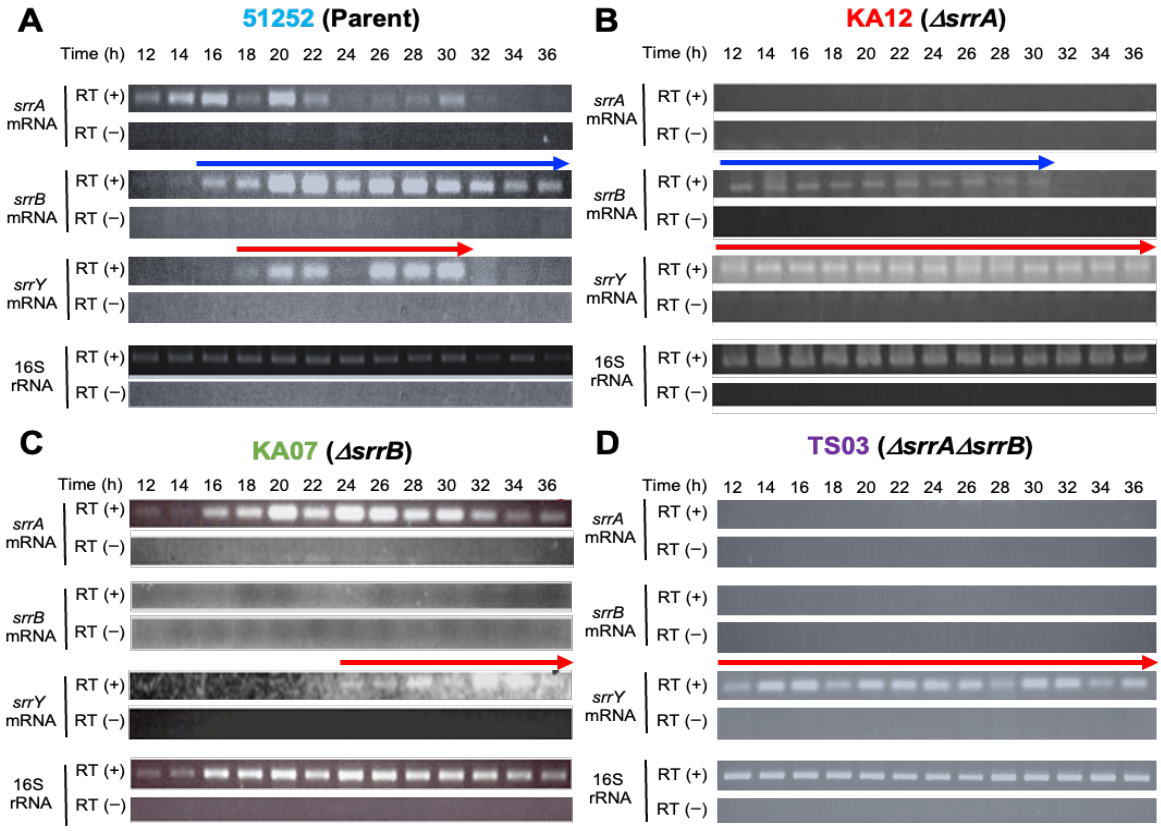

Figure 2.3.7 Time-course RT-PCR analysis of strains 51252 (A), KA12 (B), KA07 (C), and TS03 (D). Three upper panels represent *srrA* mRNA, *srrB* mRNA, and *srrY* mRNA. The lowest panels represents 16S rRNA gene as a control. RT (+) indicates the treatment of total RNA with Transcriptor Reverse Transcriptase, while RT (–) dues no treatment of transcriptase. Red arrow indicates transcription of *srrY*, while blue arrow does transcription of *srrB*.

These findings together with our previous result [**20**] showed that SRB/*srrA* regulatory system controls transcription of both *srrY* and *srrB*, and SrrB represses *srrY* transcription at the later stage.

2.3.3 SrrA binds to the promoter region of *srrB*

A transcriptional start point (TSS) of *srrB* was determined be 401-bp upstream of its translational start codon by 5′-RACE (**Figure 2.3.8**).

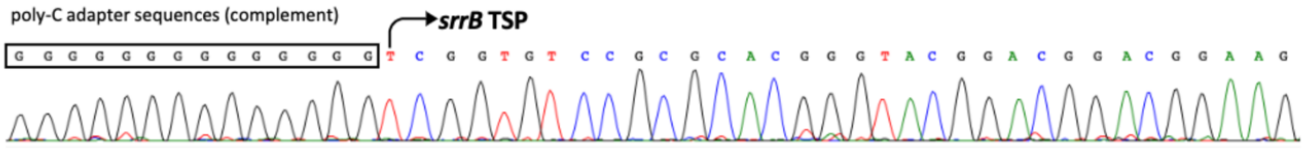

Figure 2.3.8 Determination of transcriptopnal start site (TSS) of *srrB* by 5' RACE system. Complement sequence of poly-C adapter is indicated by a box. TSS of *srrB* is indicated by a bent arrow.

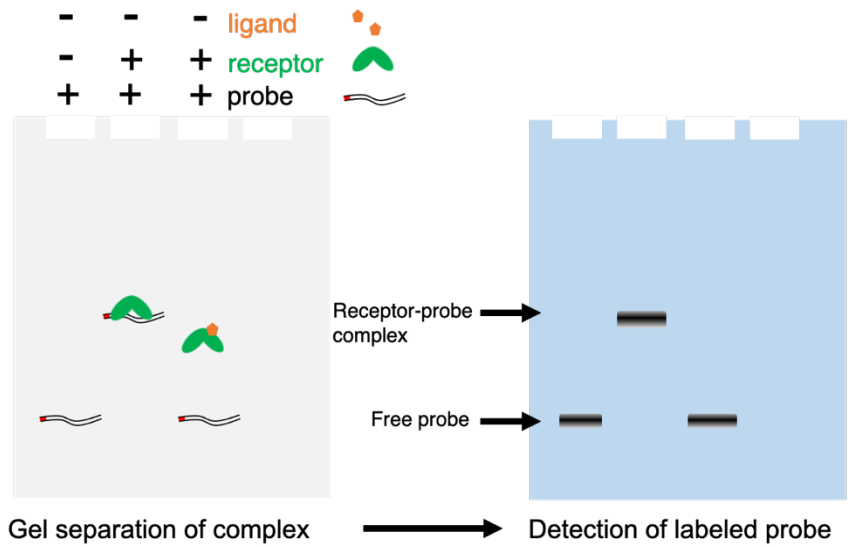

Figure 2.3.9 Illustration of Gel shift assay

To determine whether SrrA binds to the upstream promoter region of *srrB*(*srrBp*), gel shift assay was performed using ^{32}P-labeled probe B1 (nt 140,677-141,240 of pSLA2-L) that contained the upstream region of *srrB* (**Figure 2.3.10 A**). **Figure 2.3.9** indicates the schematic diagram of gel shift assay. The band shift of ^{32}P-labeled probe will be

observed in the presence of its cognate binding protein such as SrrA, whereas its gel retardation will be inhibited in the presence of SRB molecules, which allows to form SrrA-SRB complex and then leads to dissociate from the binding sequence for SrrA on the ^{32}P-labeled probe. SrrA protein was overexpressed in *E. coli* as described previously [**20**]. A band shift of probe B1 was observed in the presence of SrrA protein in a concentration-dependent manner (**Figure 2.3.10 B**). Competition experiments using unlabeled probes B1 and B2 (nt 140,201-140,585 of pSLA2-L) (**Figure 2.3.10 C**) were performed to determine the specific binding of SrrA to the region of probe B1. A band shift disappeared in the large excess of unlabeled probe B1, whereas probe B2 gave no effect on band shift (**Figure 2.3.10 C**). Addition of SRB led to dissociation of SrrA from probe B1 (**Figure 2.3.10 C**), indicating that the *srrB* transcription is controlled by SRB/SrrA regulatory system. DNase I footprinting experiment was performed to identify the SrrA binding sequence in the upstream of *srrB* (**Figure 2.3.11 A**). Positions −36 to −11 of the non-template strand was protected by SrrA (**Figure 2.3.10 D**).

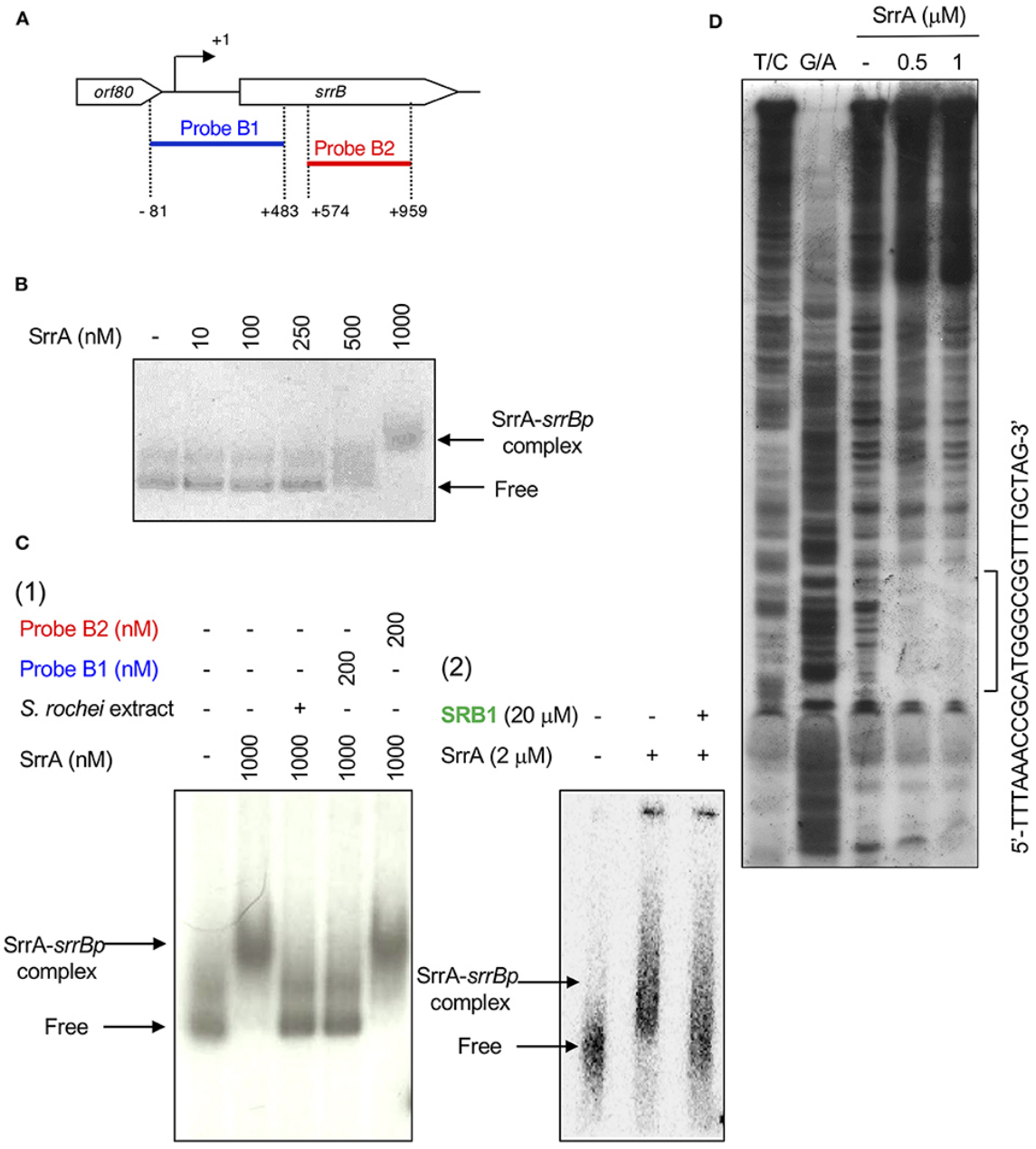

Figure 2.3.10 Gel shift assay and DNase I footprinting analysis of SrrA-binding in the upstream region of *srrB*. (**A**) Location of the two probes B1 and B2. The TSS of *srrB* is numbered +1. (**B**) The concentration-dependent binding of SrrA to the upstream promoter region of *srrB* (*srrBp*). The ^{32}P-labeled probe B1 (1 nM) was mixed with various concentration of SrrA (0–1,000 nM). (**C**) (1) Competition experiments to investigate specific binding of SrrA to the upstream region of *srrB*. Each reaction mixture contained 0.5 nM ^{32}P-labeled probe B1 (lane 1) and 1,000 nM SrrA (lane 2). Then, *S. rochei* culture extract (lane 3), 200 nM unlabeled probe B1 (lane 4) or unlabeled probe B2 (lane 5) was added. (2) Effect of endogenous SRB to investigate specific binding of SrrA to the upstream region of *srrB*. Each reaction mixture contained 0.5 nM ^{32}P-labeled probe B1 (lane 1) and 2,000 nM SrrA (lane 2). Then, 20 μM synthetic SRB1 [(1′*R*)-isomer; **7**] [**12**](lane 3) was added. (**D**) DNase I footprinting analysis of SrrA-binding site on the upstream of *srrB*. Probe B1 was end labeled on the non-template strand. Each reaction mixture contained 2 nM labeled DNA and SrrA (0.5 and 1 μM). Sequencing ladders were generated by Maxam-Gilbert sequencing of the labeled probe B1. Capital letters at right side indicate SrrA-binding sequences.

The protected region overlapped with a possible *srrB* promoter containing a palindromic sequence (asterisks in **Figure 2.3.11 B**), whose sequence well-matched with the SrrA-binding sequence of *srrY* [**20**]. Taking account of transcriptional analysis above mentioned, SrrA binds to the upstream regions of both *srrB* and *srrY* to repress their transcription at the early growth phase (~16 h).

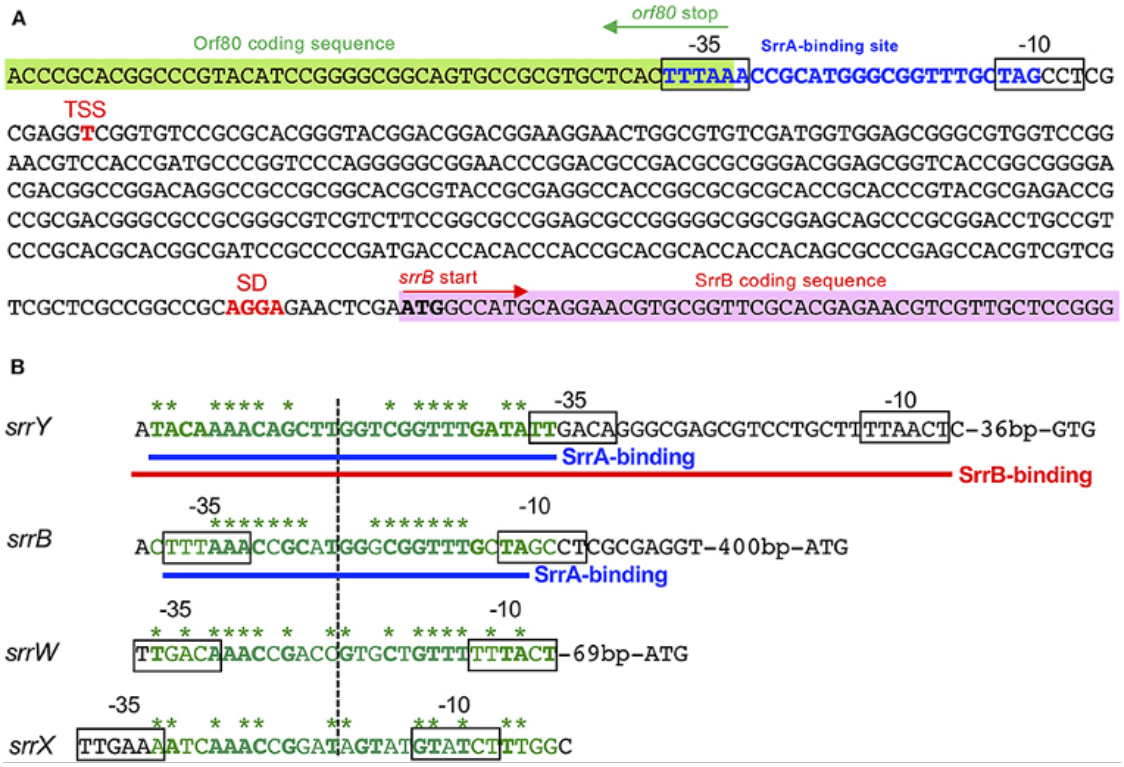

Figure 2.3.11 SrrA/SrrB binding sequences. **(A)** Characterization of the upstream region of *srrB*. Putative *srrB*promoter regions (−35 and −10) are boxed. Shine-Dalgarno (SD) sequence and transcriptional start site (TSS) are shown as red boldface letters. SrrA-binding sequence is shown as blue boldface letters. Pink and green highlights indicate SrrB and Orf80 coding sequences, respectively. **(B)** Comparison of the binding sequences for SrrA and SrrB. The confirmed SrrA- and SrrB-binding sequences are shown as blue and red underlines, respectively. Possible SrrA-binding sites at upstream of *srrW* and *srrX* are deduced from sequence data. For comparison of consensus sequence, SrrA-binding sites at the upstream of *srrY* (SrrA-*srrY*) are shown as green. Bases identical with SrrA-*srrY* are shown in boldface letters. Complementary bases are indicated as asterisks. The center of palindromes is shown as a vertical dashed line.

2.3.4 SrrB represses *srrY* transcription at the later stage of fermentation by binding to the promoter region of *srrY*

SrrB protein was overexpressed in the *E. coli* BL21(DE3)pLysS/pKAR3036 recombinant with IPTG induction, purified by Ni-NTA agarose and digested by enterokinase (**Figure 2.3.12**). To analyze whether SrrB binds to the promoter region of *srrY* (*srrYp*), gel shift assay was performed using probe Y1 (positions −452 to +100 from TSS of *srrY*) (**Figure 2.3.13 A**) containing the promoter region of *srrY*. The addition of SrrB protein gave a shifted band of probe Y1 in a concentration-dependent manner (**Figure 2.3.13 B**).

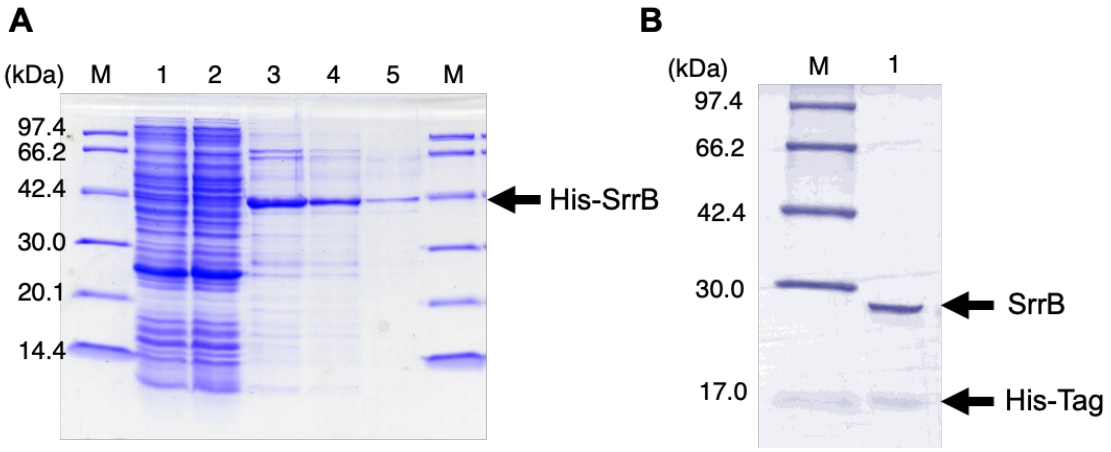

Figure 2.3.12 SDS-PAGE of SrrB protein expressed in *E. coli* BL21(DE3)pLysS.
(**A**) Purification of His-SrrB protein. Lane M, protein molecular weight markers; lanes 1 and 2, cell-free extract; lane 2, purified 41.0 kDa-sized His-SrrB prepared with the aid of a Ni^{2+}- nitrotriacetic acid agarose (Qiagen) (1st elution); lane 3. purified His-SrrB (2nd elution); purified His-SrrB (3rd elution). (**B**) Removal of His-Tag by enterokinase treatment. Lane M, protein molecular weight markers; lanes 1, purified SrrB digested with enterokinase. Marker sizes (kDa) are indicated on the left. All proteins were stained with Coomassie Brilliant Blue R250.

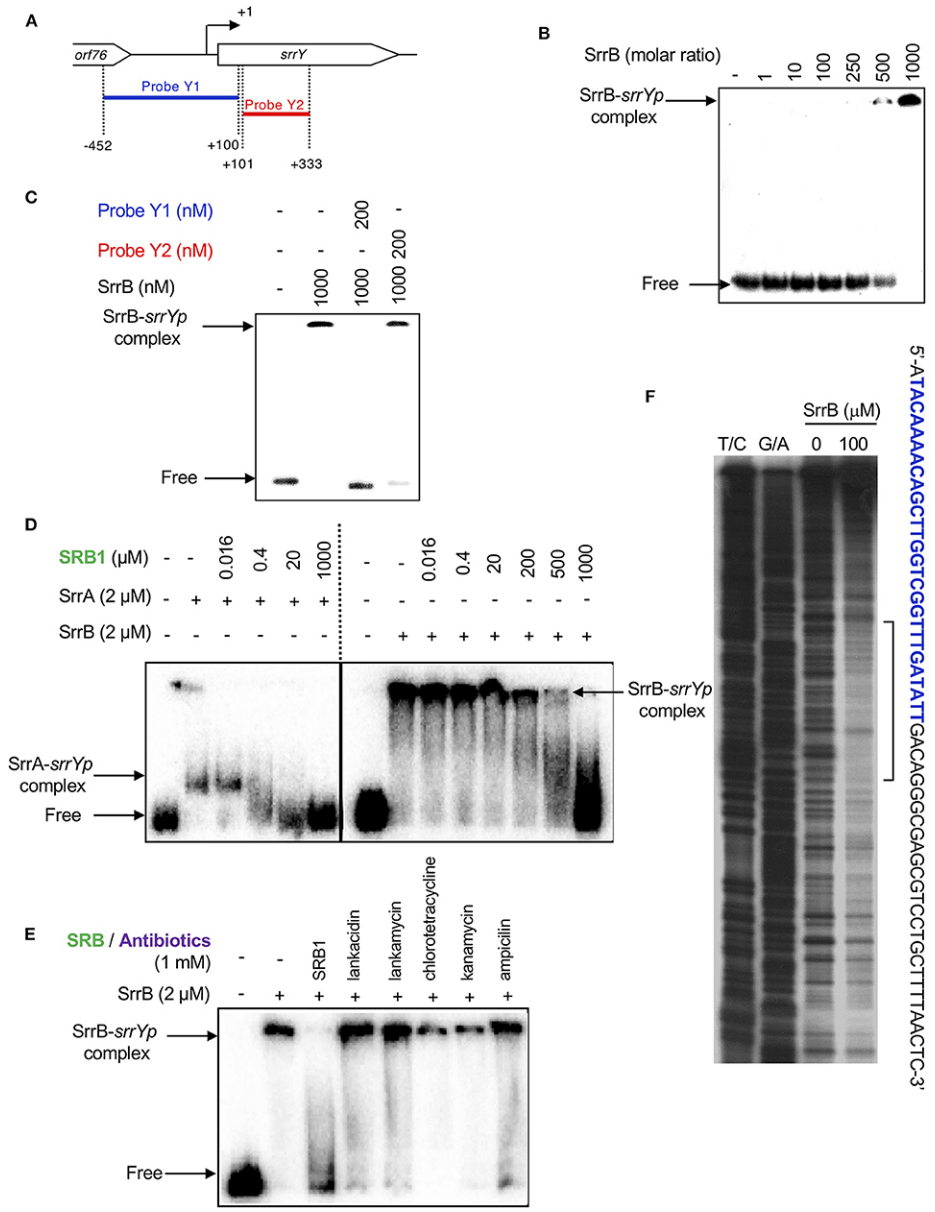

Figure 2.3.13. Gel shift assay and DNase I footprinting analysis of SrrB-binding in the upstream region of *srrY*. **(A)** Location of the two probes, probe Y1 and Y2. **(B)** The concentration-dependent binding of SrrB to the upstream promoter region of *srrY* (*srrYp*). Labeled probe Y1 (1 nM) was mixed with various concentration of SrrB (0–1,000 nM). **(C)** Competition experiments to investigate specific binding of SrrB to the upstream region of *srrY*. Each reaction mixture contained 1 nM ^{32}P-labeled probe Y1 and 1,000 nM SrrB. Then, 200 nM unlabeled probe Y1 (lane 3) or unlabeled probe Y2 (lane 4) was added. **(D)** Effect of SRB1 on the binding of SrrA (Right panel) and SrrB (left panel). Each reaction mixture contained 0.5 nM probe Y1 and 2,000 nM recombinant protein. To the reaction mixture, various concentration of synthetic SRB1 was added. **(E)** Effect of endogenous metabolites in *S. rochei* and other antibiotics on the binding of SrrB. To the same reaction mixture described for panel D, various compounds including SRB1, LC, LM, chlorotetracycline, kanamycin, and ampicillin (each 1 mM) were separately added. **(F)** DNase I footprint analysis of SrrB-binding site on the upstream of *srrY*. Probe Y1 was end labeled on the non-template strand. Each reaction mixture contained 2 nM labeled DNA and SrrB (100 nM). Sequencing ladders were generated by Maxam-Gilbert sequencing of the labeled probe Y1. Capital letters at right side indicate SrrB-binding sequences, among which blue letters indicate SrrA-binding sequences.

Competitive experiments (**Figure 2.3.13 C**) revealed that SrrB specifically binds to probe Y1, not to probe Y2 (positions +101 to +333 from TSS of *srrY*). The pseudoreceptors hitherto studied are insensitive to endogenous signaling molecules and interact with endogenous antibiotics [**6**][**17**] (details are described in Discussion Section). I tested the effects of various signaling-molecule/antibiotics on the binding of SrrB to *srrYp* through gel shift analysis using endogenous signaling molecule SRB, endogenous antibiotics (lankamycin and lankacidin), and other exogenous antibiotics (**Figure 2.3.13 D, E**). Dissociation of SrrB from *srrYp* could be caused by SRB, however, a higher concentration of 1 mM was required (500-fold excess against SrrB protein). The sensitivity of SrrB against SRB was 50-fold lower compared with the signaling molecule receptor SrrA (**Figure 2.3.13 D**). Dissociation of SrrB from *srrYp* was not caused by endogenous antibiotics lankamycin and lankacidin in *S. rochei* and neither by exogenous antibiotics (chlorotetracycline, kanamycin, ampicillin) at even 1 mM concentration (500-fold excess against SrrB protein) (**Figure 2.3.13 E**). I further performed DNase I footprinting experiment to identify the SrrB binding sequence in the upstream of *srrY*. As shown in **Figure 2.3.13 F**, positions −61 to −4 of non-template strand were protected by SrrB. Although SrrB covers larger upstream region (58 bp) than SrrA does (28 bp; blue letters in **Figure 2.3.13 F**, both SrrA and SrrB could bind to the promoter region of *srrY* (**Figure 2.3.13 B**).

2.4 Discussion

In this study, I revealed that SrrB protein acts as a negative regulator by binding to the promoter region of the target gene *srrY* to repress lankacidin and lankamycin production in *S. rochei*. Expression of *srrB* is controlled by SRB/SrrA regulatory system. As shown in General Introduction, TetR-type receptors have a conserved DNA-binding helix-turn-helix motif in the N-terminus and a ligand-binding pocket in the C-terminus [**42**] (**Figure 1.5** and **2.1.2**). This family protein is further classified into two sub-groups, the signaling molecule receptors and the pseudo-receptors. The signaling molecule receptors have a helix-turn-helix DNA-binding motif in the N-terminus and a ligand-binding Trp residue in the C-terminus. And they usually locate adjacent to the signaling molecule synthase genes [**43**], which allows us to predict signaling molecule/receptor systems in *Streptomyces* species [**44**]. On the other hand, the pseudo-receptors also have a conserved DNA-binding motif like the signaling molecule receptors, however, their genetic locus is independent to the signaling molecule synthase genes. As I have already described in General Introduction and Table 1.1, many of them act as negative regulators for antibiotic production; for example, TylQ for tylosin production in *S. fradiae* [24], BarB for virginiamycin in *S. virginiae* [**85**], ScbR2 for coelimycin P-1 in *S. coelicolor* [28], AlpW for orange pigment kinamycin in *S. ambofaciens* [**38**], and AvaR2 for avermectin in *S. avermitilis* [**41**].

In general, the pseudo-receptors are insensitive to endogenous signaling molecules. BarB has no binding affinity to virginia butanolides in *S. virginiae* [**85**]. Surprisingly, ScbR2 from *S. coelicolor* does not bind to the signaling molecules SCB1-3 but binds to two endogenous antibiotics, actinorhodin and undecylprodigiosin [**30**], and exogenous antibiotic jadomycin [86]. In *S. venezuelae*, JadR2 binds to endogenous jadomycin and chloramphenicol as ligands [**30**]. Thus, ScbR2 and JadR2 bind to multiple antibiotics, and coordinate their biosynthesis [**10**][**36**]. In *S. avermitilis*; AvaR2 binds to the endogenous signaling molecule avenolide, but not to oligomycin and avermectin [**41**]. Its mutational analysis revealed that AvaR2 plays a negative regulatory role in avermectin production and cell growth [**41**]. In *S. rochei*, SrrB-*srrYp* complex was disrupted by endogenous signaling molecule SRB at 1 mM concentration, although its minimum dissociation concentration for SrrB was 50-fold higher than that for SrrA, the SRB receptor. SrrB

showed no binding activity to endogenous polyketide antibiotics lankamycin or lankacidin in *S. rochei* and neither to exogenous antibiotics including aromatic polyketide chlortetracycline, aminoglycoside antibiotic kanamycin, and β-lactam antibiotic ampicillin even at 1 mM concentration (500-fold excess against SrrB). Thus, functions of the pseudo-receptors are variable in *Streptomyces* species (**Figure 2.4.1**).

Pseudo-receptor	Signaling molecules	exogenous antibiotic ligands	exogenous antibiotic ligands
AvaR2	Avenolide	oligomycin and avermectin B1	jadomycin B, apramycin, hygromycin B, kanamycin and streptomycin
JadR2	SVB1 **not tested**	jadomycin and chloramphenicol	not determined
ScbR2	SCB1	actinorhodin and undecylprodigiosi	jadomycin
SrrB	**SRB1** **could bind, but almost insensitive (1 mM)**	**lankacidin and lankamycin**	**kanamycin, chlortetracyclin and ampicillin**

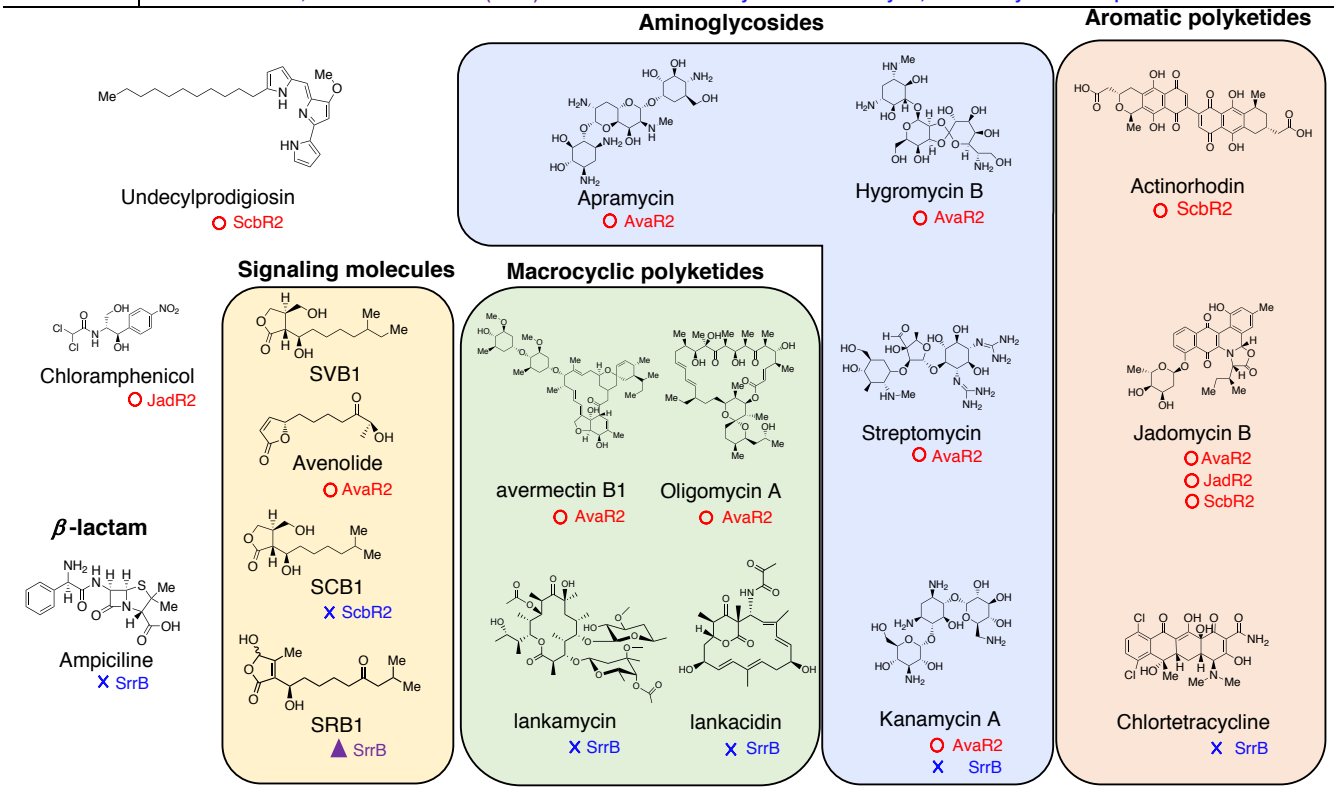

Figure 2.4.1 Ligands for the pseudo-receptor
Red letters indicate that the compound functions as a ligand. Blue letters indicate that the compound does not function as a ligand. Purple letters indicates that compound could bind, but almost insensitive (1 mM)

The possible regulatory pathway in *S. rochei* is shown in **Figure 2.4.2**. At the early growth phase, SrrA represses transcription of both *srrY* and *srrB* (panel A). When SRB reaches a critical concentration, SrrA-SRB complex dissociates from both promoter regions to induce expression of *srrY* and *srrB* (panel B). Then SrrB represses *srrY* transcription at the later stage fermentation (panel C), suggesting a transient expression of *srrY* by two receptor proteins SrrA and SrrB in *S. rochei*. A similar regulatory pathway was proposed for kinamycin production in *S. ambofaciens* [**38**]

although its ligand has not yet been identified. In the early stage of growth, the signaling molecule receptor AlpZ represses both transcription of *alpV* (an SARP-type activator gene) and *alpW* (a pseudo-receptor gene). When an unidentified ligand interacts with AlpZ, this protein dissociates from the promoter regions in both *alpV* and *alpW*, leading to kinamycin production. At the later stage of fermentation, AlpW represses *alpV* transcription again to cease kinamycin production. Another interesting features in the *S. rochei* regulatory pathway is the presence of *srrY-srrC* cistron (**Figure 2.4.2**).

The *srrC* mutant showed no sporulation, suggesting that *srrC* acts as a positive regulator for morphological differentiation [**19**]. As shown in **Figure 2.4.2**, *srrB* negatively regulates the transcription of both *srrY* and *srrC*, which leads to transient controls for antibiotic production and morphological differentiation, respectively. The *srrB* mutation increased the titers of antibiotics as well as SRBs. This result well agreed with preliminary gel shift assay that both SrrA and SrrB bind to the upstream region of SRB biosynthesis gene *srrX* (data not shown). Large excess of SRBs has no effect on antibiotic overexpression in *S. rochei* [**12**], hence, exact mechanism of the *srrX* repression by SrrB at the later stage remains to be clarified.

In conclusion, I have extensively characterized the role of the pseudo-receptor SrrB for antibiotic production in *S. rochei*. Further understanding and manipulation of the regulatory system in *Streptomyces* will lead to a natural product discovery with notable biological activities.

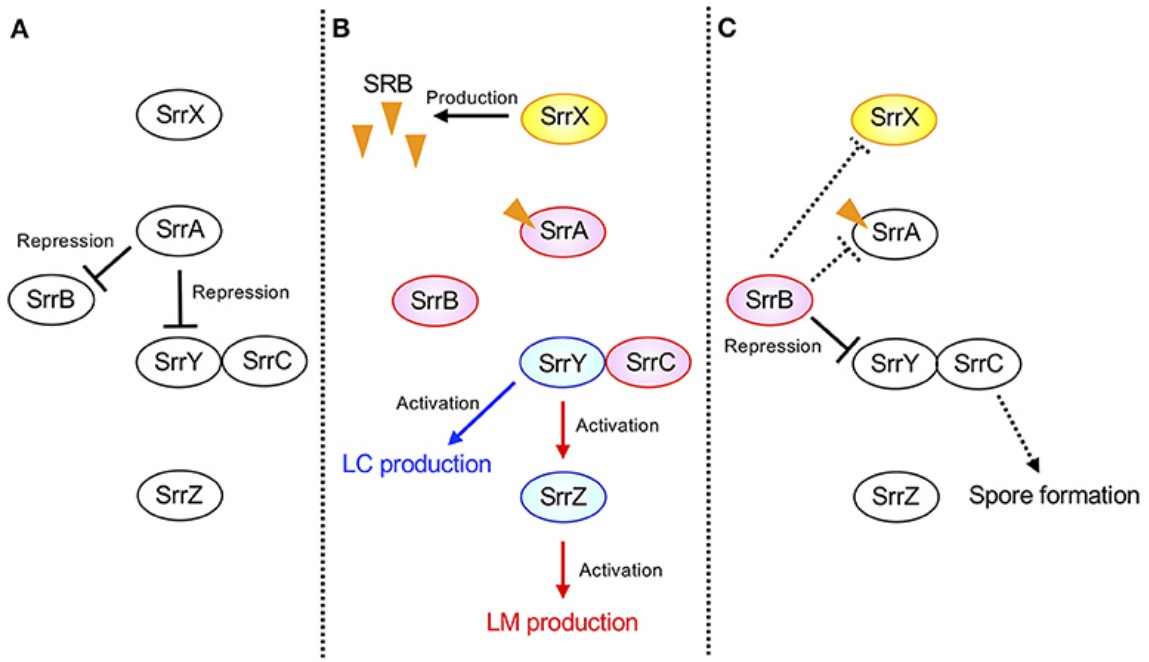

Figure 2.4.2 Model of transient *srrY* expression for lankamycin and lankacidin production in *S. rochei*. **(A)** SrrA represses both *srrY* and *srrB* expression in the early stage of growth. **(B)** Dissociation of SrrA from the promoter region of both *srrY* and *srrB* by SRB in middle stage of growth. **(C)** Repression of *srrY* by SrrB in the late stage of growth. Solid lines indicate the confirmed regulatory pathway hitherto. Additional dashed lines were suggested by unpublished results. Orange triangles indicate the signaling molecules SRBs.

Chapter 3

Discovery of novel compounds by overexpression of a *Streptomyces* antibiotic regulatory protein (SARPs)

3.1 Introduction

As shown in Chapter 1, SARPs (*Streptomyces* antibiotics regulatory proteins) are main targets of the signaling molecule receptors, and are responsible for the direct activation of secondary metabolite BGCs [**16**][**21**][**53**]. Furthermore, SARPs can sometimes control other secondary metabolite BGCs as pleiotropic actions [**87**]. Hence, overexpression of SARPs in *Streptomyces* strains will be an appropriate genome mining strategy for activation of "cryptic" secondary metabolite BGCs.

S. rochei 7434AN4 carries 15 SARP genes, among which three genes (*srrY*, *srrZ*, and *srrW*) were located on pSLA2-L and others were on the chromosome (**Table 3.1.1**).

Table 3.1.1 SARP-type activator genes on the *S. rochei* chromosome and a linear plasmid pSLA2-L.

No.	SRO	Start	End	Direction	AA	Type	Products	*E* value	identities
Chromosome									
1	SRO_732	775,656	776,525	+	291	small SARP, CSR	PKS	3E-20	31
2	SRO_1189	1,323,183	1,324,307	-	376	small SARP, CSR	NRPS,Lantipeptide	2E-23	35
3	SRO_1564	1,764,539	1,767,568	+	1011	large SARP, stand-alone	unkonown	4E-26	36
4	SRO_1851	2,097,725	2,098,522	+	267	Small SARP, stand-alone	Azoxyalken KA57-A	6E-21	32
5	SRO_2506	2,837,984	2,841,157	-	1059	large SARP, CSR	NRPS	2E-20	31
6	SRO_3163	3,534,658	3,537,678	-	1008	large SARP, stand-alone	**YM3163-A** (This chapter)	3E-23	34
7	SRO_3164	3,537,850	3,538,644	-	266	Small SARP, stand-alone	unknown	3E-21	31
8	SRO_3350	3,728,856	3,732,182	-	1110	large SARP, stand-alone	unknown	2E-31	38
9	SRO_4200	4,640,132	4,643,095	-	989	large SARP, stand-alone	unknown	3E-24	34
10	SRO_6312	6,944,375	6,945,175	+	268	small SARP, CSR	NRPS	6E-26	31
11	SRO_6387	7,028,269	7,030,383	-	706	large SARP, stand-alone	unknown	4E-31	34
12	SRO_7232	8,026,047	8,029,616	-	1191	large SARP, CSR	Pentamycin	1E-21	34
pSLA2-L									
1	SrrW	111,359	112,228	-	289	small SARP, CSR	unknown	5E-32	36
2	SrrY	133,442	134272	-	276	small SARP, stand-alone	Lankacidin, Lankamycin	1E-31	35
3	SrrZ	129,701	130,522	-	273	small SARP, stand-alone	Lankamycin	4E-39	38

Our laboratory has revealed that two SARP genes, *srrY* and *srrZ*, act as activators for the production of lankamycin(**1**) and lankacidins (**2-6**) (**Figure 1.6**), both of which are coded on pSLA2-L [**20**][**21**].

Hence, some of the 12 SARPs may function as activators for cryptic secondary metabolite BGCs coded on the *S. rochei* chromosome. Our laboratory has isolated three "silent" secondary metabolites through gene inactivation of transcriptional repressors and/or major BGCs from mutants of *S. rochei* 7434AN4; for example, a 28-membered polyene macrolide pentamycin, two C_{10}-aliphatic polyketides citreodiol and *epi*-citreodiol, and an azoxyalkene compound KA57-A (**Figure 3.1.1**) [**88**][**89**]. *In vivo* overexpression of SARP-type activators might be providing an excellent potential for natural product discovery from the *Streptomyces* genome.

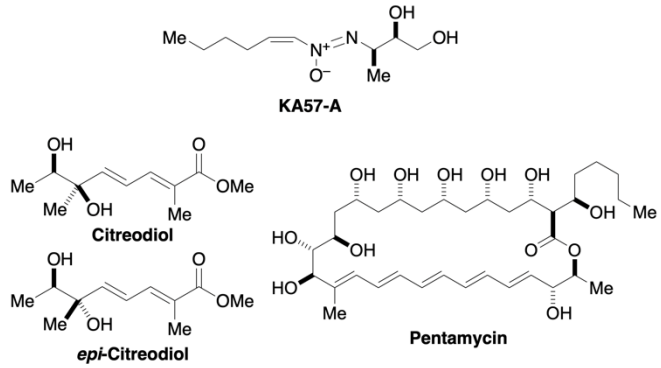

Figure 3.1.1 Chemical structures of "silent" secondary metabolites obtained through various genome mining approaches in *Streptomyces rochei* 7434AN4. Me, methyl

In this chapter, I performed the overexpression of SARP genes to activate silent secondary metabolite BGCs in *S. rochei*. The recombinant of SARP homolog, SRO_3163, accumulated a UV-active compound YM3163-A (**Figure 3.1.2**), which was not detected in the parent strain and other SARP recombinants. Extensive NMR analysis revealed that YM3163-A is a novel enamide, 2-(cyclohex-2-en-1-ylidene)acetamide, and its structure was confirmed by chemical synthesis.

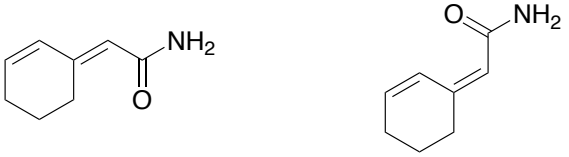

YM3164-A (*E*)-isomer (**9a**) YM3164-A (*Z*)-isomer (**9b**)

Figure 3.1.2 Chemical structures of novel metabolites isolated from the SRO_3163 rebombinant.

3.2 Material and Methods

3.2.1 Strains, plasmids, and oligonucleotides, and culture conditions

Table 3.2.1 Bacterial strains, plasmids, and oligonucleotides used in this chapter.

Strains/plasmids/oligonucleotides	Description	Source/References
Bacterial strains		
Streptomyces rochei 51252	pSLA2-L	[65]
Streptomyces rochei KA20	*kan*::*srrX* and in-frame deletion of *srrB* in 51252	[12]
Escherichia coli XL1-Blue	*recA1 endA1 gyrA96 thi-1 hsdR17 supE44 relA1 lac* [F' *proAB lacIqZΔ*(*M15* Tn10 (Tetr))	Stratagene
Plasmids		
pIJ8600	Integrative *E. coli-Streptomyces* shuttle vector, inducible *tipA* promoter, *apr, tsr*	[79]
pKAR3049	1.2 kb *Nde*I-*Bam*HI PCR fragment containing *srrY* in pIJ8600	[20]
pYMR3163	3.0 kb *Nde*I-*Xba*I PCR fragment containing *SRO_3163* in pIJ8600	This study
Oligonucleotides (5' - 3')		
SRO3163f	AATCATATGCGCTTCAACATCCTCGGCTC	This study
SRO3163r	ATCTCTAGACCACGAGCCACCGGTCACGGC	This study

All the strains and plasmids used in this study were listed in **Table 3.2.1**. *S. rochei* strain 51252 that carries only pSLA2-L was used as a reference strain for production of lankamycin and lankacidin **(Figure 1.6)** [**65**]. Strain KA20, an *srrX*-deficient mutant of 51252, was used as a host strain for overexpression of the SARP genes [**19**]. YM medium was used for secondary metabolites production. For protoplast preparation, *S. rochei* strains were cultured in YEME liquid medium [**77**]. Protoplasts were regenerated on R1M solid medium [**78**]. DNA manipulations for *Streptomyces* [**77**] and *E. coli* [**75**] were carried out according to the described protocols. The basic experimental instructions including plasmid isolation from *E. coli,* total DNA preparation for *Streptomyces,* and Southern hybridization are shown in Chapter Sections 2.2.1-2.2.3, respectively.

3.2.2 Construction of SRO_3163-overexpression vector

A 3.0-kb PCR fragment containing *SRO_3163* (nt 3,534,658–3,537,678 (complement) of the chromosome) was amplified using total DNA and two primers, SRO3163f and SRO3163r (**Table 3.2.1**). The PCR fragment was digested with *Nde*I and *XbaI* and cloned into pIJ8600 [**79**], a thiostrepton-inducible *E. coli-Streptomyces* shuttle vector carrying a *tipA* promoter, to give pYMR3163. This plasmid was transformed into *S. rochei* KA20 in the presence of apramycin (10 μg/ml) to give a recombinant, *S. rochei*

KA20/pYMR3163. Empty vector pIJ8600 was transformed to obtain the recombinant, *S. rochei* KA20/pIJ8600, in a similar manipulation for negative control.

3.2.3 Analysis of metabolites

The recombinants were separately inoculated in YM liquid medium supplemented with apramycin (10 μg/ml). After 24-h cultivation at 28°C, thiostrepton was supplemented at a final concentration of 10 μg/ml and further cultivated for 2 days. The culture broth was extracted twice with equal volume of EtOAc. Metabolites from the recombinants were analyzed by high performance liquid chromatography (HPLC) and thin-layer chromatography (TLC). The crude extract was dissolved in acetonitrile, applied on a reverse-phase HPLC column (Cosmosil Cholester 4.6 x 250 mm; Nacalai Tesque, Kyoto, Japan), eluted with two different solvent systems either acetonitrile/phosphate buffer (10 mM, pH 8.2) (3:7, v/v) or 10% aqueous acetonitrile with 0.1% trifluoroacetic acid at a flow rate of 1.0 ml/min, and then monitored at 230 and 268 nm with a JASCO MD-2010 multi-wavelength photodiode array detector. TLC was developed with $CHCl_3$/MeOH (15:1, v/v), monitored under UV light at 254 nm, and baked after staining with anisaldehyde-H_2SO_4.

3.2.4 Isolation of metabolites

Ten liter culture of the recombinant *S. rochei* KA20/pYMR3163 was extracted twice with equal volume of EtOAc. The combined organic phase was dried (Na_2SO_4), filtered, and concentrated *in vacuo*. The resulting residue was passed through Sephadex LH-20 (GE Healthcare, Chicago, USA) with methanol. The fractions containing YM3163-A were combined, and further purified by silica gel chromatography with two different solvent systems of $CHCl_3$-methanol = 50:1-10:1 (v/v) and toluene-EtOAc = 1:3 (v/v) to give YM3163-A (2.9 mg) as a colorless oil.

High resolution ESI-MS: observed *m/z* 160.0730 $[M+Na]^+$ (calcd for $C_8H_{11}NONa$, 160.0733). The ^1H- and ^{13}C-NMR assignments were shown in **Table 3.2.2**.

Table 3.2.2 ^{1}H and ^{13}C data of YM3163-A (**9ab**)[a]

Position	(*E*)-isomer **9a**		(*Z*)-isomer **9b**	
	δ_C[a]	δ_H (coupling, *J* in Hz)	δ_C[a]	δ_H (coupling, *J* in Hz)
1	168.9 (s)	–	168.5 (s)	–
2	116.1 (d)	5.52 (s, 1H)	114.4 (d)	5.42 (s, 1H)
3	151.4 (s)	–	149.7 (s)	–
4	26.2 (t)	2.99 (dt, 1.5 and 2.5, 2H)	32.5 (t)	2.36 (dt, 1.5 and 2.5, 2H)
5	21.9 (t)	1.72 (m, 2H)	22.7 (t)	1.79 (m, 2H)
6	25.6 (t)	2.20 (m, 2H)	26.1 (t)	2.22 (m, 2H)
7	137.2 (d)	6.18 (dt, *J* = 10 and 5, 1H)	137.2 (d)	6.18 (dt, *J* = 10 and 5, 1H)
8	130.1 (d)	6.07 (d, *J* = 10, 1H)	125.1 (d)	7.47 (d, *J* = 10, 1H)
1-NH_2	–	N.D.[c]	–	N.D.[c]

[a] The ^{13}C-NMR (150 MHz) and ^{1}H-NMR (600 MHz) were taken in $CDCl_3$, and the internal solvent signal (δ_C = 77.0) and tetramethylsilane (δ_H = 0.00) were used as references for chemical shifts.
[b] Multiplicity is shown in parenthesis.
[c] N.D.; Not detected.

3.2.5 Spectroscopic instruments

Structural elucidation was performed by electrospray ionization-mass spectrometry (ESI-MS) and nuclear magnetic resonance (NMR). ESI-MS analysis was performed by a LTQ Orbitrap XL mass spectrometer (Thermo Fisher Scientific, Waltham, MA, USA). NMR spectra were recorded on JEOL ECA-500 and ECA-600 spectrometers equipped with a field gradient accessory. Deuterochloroform (99.9 atom %; Kanto Chemical, Co., Inc., Tokyo, Japan) was used as a solvent for ^{1}H- and ^{13}C-NMR. The resident solvent signal (δ_C = 77.0) and the internal standard signal of tetramethylsilane (δ_H = 0.00) were used as references for chemical shifts.

3.2.6 Synthesis of YM3163-A

Ethyl 2-(cyclohex-2-en-1-ylidene)acetate [(*E*)-isomer **12a**, (*Z*)-isomer **12b**]

To a suspension of sodium hydride (55%, 445 mg, 10.2 mmol) in THF (10 mL) was dropwisely added ethyl diethylphosphonoacetate **10** (2.20 g, 9.81 mmol) in THF (7 mL) at 0 °C, and the mixture was stirred at 0°C for 45 min. A solution of 2-cyclohexen-

1-one **11** (807 mg, 8.39 mmol) in THF (7 mL) was added dropwisely to the mixture at 0°C, and then the mixture was stirred at 50°C for 3 h. Saturated aqueous NH_4Cl (10 mL) was dropwisely added at 0°C, and the mixture was extracted with ether twice. The combined organic phase was washed with brine, dried (Na_2SO_4), filtered, and concentrated to dryness. The residue was purified over silica gel with hexane-EtOAc (10:1, *v*/*v*) to give ester **12ab** (204 mg, 15%) as a diastereomer mixture.

(*E*)-isomer **12a**; ^{1}H-NMR ($CDCl_3$): d = 1.27 (t, *J* = 7.0 Hz, 3H), 1.72 (quintet, *J* = 6.5 Hz, 2H), 2.22 (m, 2H), 2.96 (dt, *J* = 1.5 and 6.5 Hz, 2H), 4.15 (q, *J* = 7.5 Hz, 2H), 5.56 (s, 1H), 6.10 (d, *J* = 10 Hz, 1H), 6.22 (m, 1H); ^{13}C-NMR ($CDCl_3$): d = 14.1 (q), 22.4 (t), 26.0 (t), 32.3 (t), 59.6 (t), 114.9 (d), 130.2 (d), 138.2 (d), 153.9 (s), 166.5 (s).

(*Z*)-isomer **12b**; ^{1}H-NMR ($CDCl_3$): d = 1.28 (t, *J* = 7.0 Hz, 3H), 1.78 (quint, *J* = 6.5 Hz, 2H), 2.19 (m, 2H), 2.39 (t, *J* = 6.0 Hz, 2H), 4.15 (q, *J* = 7.5 Hz, 2H), 5.58 (s, 1H), 6.22 (m, 1H), 7.46 (d, *J* = 9.5 Hz, 1H); ^{13}C-NMR ($CDCl_3$): d = 14.1 (q), 21.6 (t), 25.4 (t), 31.3 (t), 59.4 (t), 113.0 (d), 125.1 (d), 137.8 (d), 152.4 (s), 163.5 (s).

High resolution APCI-MS: observed *m*/*z* 167.1065 $[M+H]^+$ (calcd for $C_{10}H_{15}O_2$, 167.1067).

2-(Cyclohex-2-en-1-ylidene)acetamide [(*E*)-isomer **9a**, (*Z*)-isomer **9b**]

A mixture of ester **12ab** (220 mg, 1.32 mmol) and 1 M NaOH (8 ml) in EtOH–H_2O (15 ml; 2:1 *v*/*v*) was stirred at room temperature for 31 h. The mixture was cooled to 0°C, and acidified by 2 M HCl. The mixture was extracted with ether twice, and the combined organic phase was washed with brine, dried (Na_2SO_4), filtered and concentrated to dryness. The residue was chromatographed over silica gel with hexane–EtOAc (2:1, *v*/*v*) to give carboxylic acid (150 mg, 82%) as a colorless solid. To carboxylic acid (150 mg, 1.09 mmol) in dry dichloromethane (10 ml) was added thionyl chloride (1.60 ml, 22.2 mmol) at 0 °C, and the mixture was stirred at room temperature for 19 h. The mixture was concentrated *in vacuo*, and then the residue was carefully dissolved in 28% aqueous NH_3 (20 mL, 296 mmol) at 0°C. The mixture was stirred at 0 °C for 10 min and at room temperature for 24 h. The mixture was cooled to 0 °C, and acidified by addition of 2 M HCl. The mixture was extracted with ether twice, and the combined organic phase was washed with brine, dried (Na_2SO_4), filtered and concentrated to dryness. The residue was purified over silica gel with $CHCl_3$–MeOH (25:1, *v*/*v*) to give amide **9ab** (68 mg, 46% in 2 steps) as a diastereomer mixture.

The ^{1}H- and ^{13}C-NMR data of synthetic **9ab** were identical with those of natural YM3163-A (**9ab**). High resolution ESI-MS: observed *m*/*z* 160.0731 $[M+Na]^{+}$ (calcd for $C_8H_{11}NONa$, 160.0733).

3.2.7 Antimicrobial activity

The antimicrobial activity of YM3163-A was determined by the agar dilution method. Growth of test strain *Micrococcus luteus* was judged after 24 h incubation at 28°C.

3.3 Results

3.3.1 Sequence analysis of SARPs in *S. rochei*

As shown in **Figure 3.3.1**, the characteristic N-terminal Helix-Turn-Helix (HTH) DNA-binding and bacterial transcriptional activator domain (BTAD) motifs were well conserved among fifteen SARPs of *S. rochei* and a well-studied SARP, ActII-ORF4 [**89**]. SARP-type activators are classified based on their size and domain organization; "small" SARPs have only HTH DNA-binding and BTAD motifs, whereas "large" SARPs have additional functional domains such as ATPase domain and tetratricopeptide repeats at the C-terminal region [**51**]. In many cases, SARP genes are coded at secondary metabolite BGCs (termed as "cluster-situated regulators"; CSRs). On the other hand, SARP genes apart from any BGCs are also found in some extent (termed as "stand-alone" type).

The genetic characterization of SARPs in *S. rochei* and their possible target(s) was shown in **Table 3.1.1** and **Figure 3.3.2**. Our group has revealed the function of three SARPs coded on pSLA2-L. Two SARP-type genes, *srrY* (*orf75*) and *srrZ* (*orf71*), are located apart from BGCs for lankacidin (*lkc*; *orf4-orf23*) and lankamycin (*lkm*; *orf24-orf53*) (*srrY* and *srrZ* are 22 kb and 18 kb away from the *lkm* cluster), however, they act as transcriptional activators for their biosynthesis. Although *srrW* (*orf55*) locates at the right end of the *lkm* cluster, its mutation and overexpression resulted in no effect on lankamycin production. Thus, it is almost difficult to predict the role of SARPs in view of their location against BGCs. Hence, I planned to perform random overexpression of SARPs, which will give rise to transcriptional activation of "cryptic" secondary metabolite BGCs.

Figure 3.3.1 Alignment of amino acid sequences of fifteen SARP-type activators in *Streptomyces rochei* 7434AN4. Query sequence is ActII-ORF4 from *Streptomyces coelicolor*. Conserved amino acids are marked with asterisks (identical), colons (highly similar), and periods (weakly similar). The orange background indicates the DNA binding domain. The blue background indicates the conserved BTAD (bacterial transcriptional activator domain).

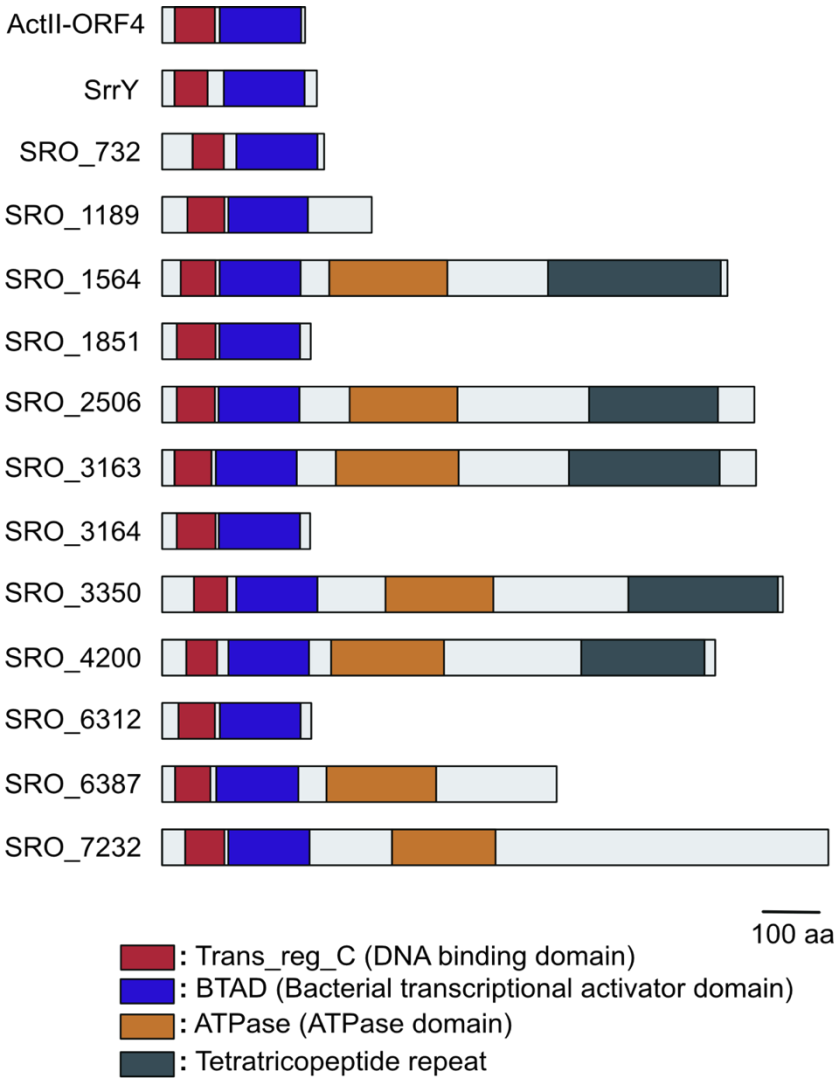

Figure 3.3.2 Domain organization of fifteen SARP-type activators in *Streptomyces rochei* 7434AN4. Query sequence is ActII-ORF4 from *Streptomyces coelicolor*.

3.3.2 Overexpression of SARP-encoding genes in *S. rochei*

SARP genes coded on the *S. rochei* chromosome were cloned into an integrative thiostrepton-inducible vector pIJ8600 [**79**], and their recombinants were incubated. Metabolite analysis in the recombinants was performed by HPLC (**Figure 3.3.3**). Strain KA20 (deletion of *srrX*) was used as a host for overexpression vector, hence, this mutant has no production of two dominant antibiotics lankacidin and lankamycin (**Figure 1.6**) in *S. rochei*. A recombinant KA20/pIJ8600 was used as a negative control strain, and it showed no significant metabolites production when compared with the parent strain 51252 (**Figure 3.3.3 A**). On the other hand, a recombinant of an SARP homolog gene, *SRO_3163*, showed two distinct peaks at 14.0 and 15.5 min on HPLC chromatogram at 268 nm, which were not detected in the parent strain 51252 and other SARP recombinants including *srrY* overexpression (**Figure 3.3.3 B**). In TLC analysis, a distinct UV active spot (termed as YM3163-A) was detected at Rf = 0.55 in $CHCl_3$-MeOH=15:1, which was then homogeneity purified.

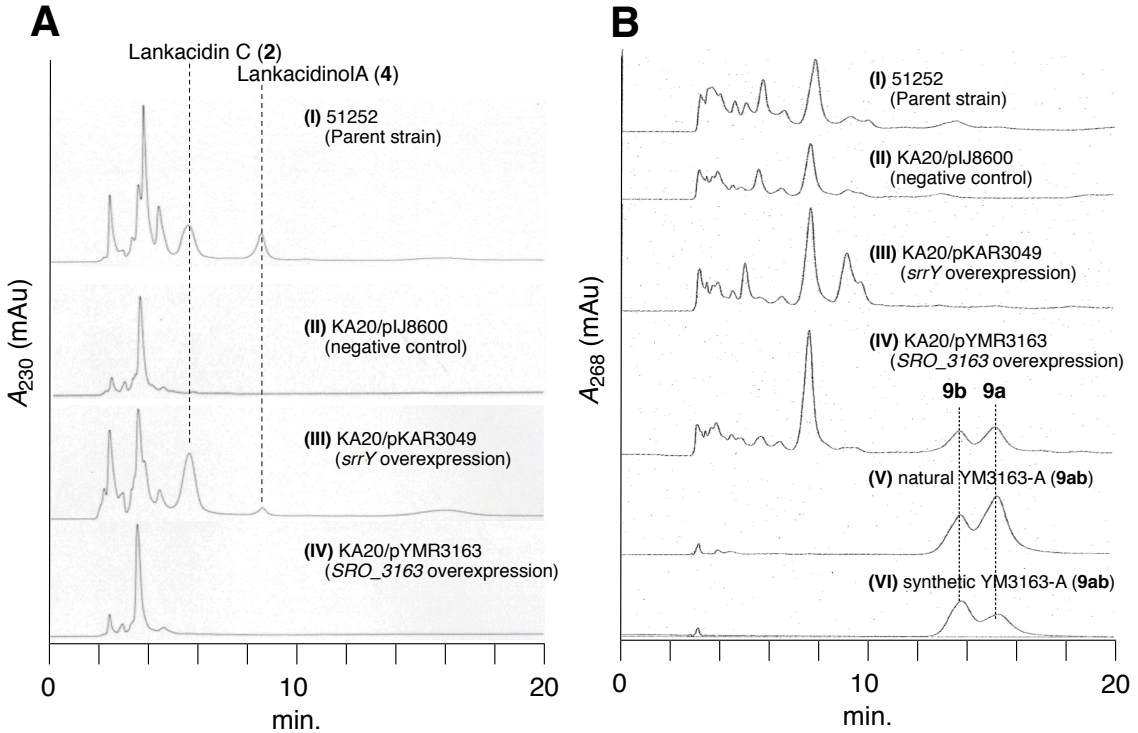

Figure 3.3.3 HPLC analysis of metabolites produced by *S. rochei* strains.
(**A**) HPLC chromatograms at 230 nm acquired using photodiode array detector. (I) Strain 51252 (parent), (II) recombinant KA20/pIJ8600 (control), (III) recombinant KA20/pYMR3163 (*SRO_3163* overexpression), and (IV) recombinant KA20/pKAR3049 (*srrY* overexpression). The crude extracts were applied on a COSMOSIL Cholester column (4.6 x 250 mm, Nacalai Tesque) and eluted with a mixture of acetonitrile-10 mM sodium phosphate buffer (pH 8.2) (3:7, v/v) at a flow rate of 1.0 ml/min.
(**B**) HPLC chromatograms at 268 nm acquired using photodiode array detector. (I) Strain 51252, (II) recombinant KA20/pIJ8600, (III) recombinant KA20/pKAR3049, (IV) recombinant KA20/pYMR3163, (V) natural YM3163-A (**9,10**), and (VI) synthetic YM3163-A (**9,10**). Either the crude extracts or YM3163-A was applied on a COSMOSIL Cholester column (4.6 x 250 mm, Nacalai Tesque) and eluted with 10% aqueous acetonitrile supplemented with 0.1% trifluoroacetic acid at a flow rate of 1.0 ml/min.

3.3.3 Isolation and structural elucidation of UV-active compound accumulated in the recombinant harboring *SRO_3163* gene

Compound YM3163-A was purified by Sephadex LH20 with MeOH and silica gel chromatography with $CHCl_3$-MeOH=50:1. In its ESI-MS analysis, a distinct molecular ion peak was detected at *m/z* 160.0730 as a sodium ion adduct, and its molecular formula was predicted to be $C_8H_{11}NO$. Although its molecular formula was deduced to be $C_8H_{11}NO$, 15 carbons were detected in its ^{13}C-NMR, suggesting that YM3163-A is an inseparable mixture in the 4:3 ratio (an enhanced signal at δ_C = 137.2 was possibly overlapped). In the major isomer, carbon signals were classified into 3 methylene, 3 methine, and 2 quaternary carbons. The ^{1}H- and ^{13}C-NMR assignments and key correlations were displayed in **Table 3.2.2** and **Figure 3.3.4**, respectively (1D and 2D spectral charts were shown in **Figures S1-6** (see Appendix)).

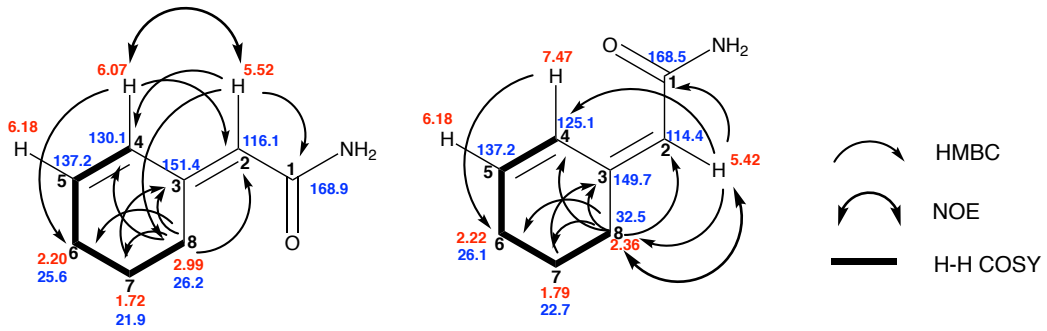

YM3163-A (*E*)-isomer (**9a**) YM3163-A (*Z*)-isomer (**9b**)

Figure 3.3.4 Key HMBC, ^{1}H-^{1}H COSY, and NOE correlations of YM-3163-A (*E*)-isoler **9** and (*Z*)-isomer **10**. The δ_H and δ_C values are shown underlined (red) and in italics (blue), respectively.

In the major isomer (see **Figure 3.3.4** left panel), a doublet olefin proton H-4 (δ_H = 6.07) showed two HMBC correlations with a deshielded methine carbon C-2 (δ_C = 116.1) and a methylene carbon C-6 (δ_C = 25.6). Sequential H-H COSY correlations were observed from H-4 through H-5 (δ_H = 6.18), H-6 (δ_H = 2.20), H-7 (δ_H = 1.72), and H-8 (δ_H = 2.99). Methylene protons H-7 showed a HMBC correlation with a quaternary carbon C-3 (δ_C = 151.4). Methylene protons H-8 showed five HMBC correlations with a methylene carbon C-7 (δ_C = 21.9) and a deshielded methine carbon C-4 (δ_C = 130.1), together with C-6, C-3, and C-2. Furthermore, an olefinic methine proton H-2 showed three HMBC correlations with a quaternary carbon C-1 (δ_C = 168.9), C-8 (δ_C =26.2), and C-4. Based on the degree of unsaturation, YM3163-A contains the cyclic skeleton together with two olefins and one ketone moiety. HMBC and COSY correlations above mentioned indicated the presence of cyclohexene ring. Finally, all spectral data (**Table 3.2.2**) deduced to be a novel enamide, 2-(cyclohex-2-en-1-ylidene)acetamide (**9ab**, **Figure 3.1.2**). The minor isomer (see **Figure 3.3.4** right panel) was determined to be its stereoisomer in a similar fashion. To determine the *E*/*Z*-stereochemistry of YM3163-A, NOE experiment was performed.

As shown in **Figures 3.3.5**, the major isomer **9a** showed a significant NOE value between H-2 and H-4, while the minor isomer **9b** showed NOE between H-2 and H-8. Thus, the major isomer was determined to be (*E*)-isomer (**9a**; **Figure 3.3.4 left**), while the minor was (*Z*)-isomer (**9b**; **Figure 3.3.4 right**). Comparing ^{1}H-NMR chemical shifts of **9ab**, methylene protons H-8 (d_H = 2.99) of **9a** showed a downfield shift by the effect of carbonyl moiety of C-1. On the other hand, methine proton H-4 (d_H = 7.47) of **9b** showed a downfield shift. These results well supported the *E*/*Z* stereochemistry of YM3163-A.

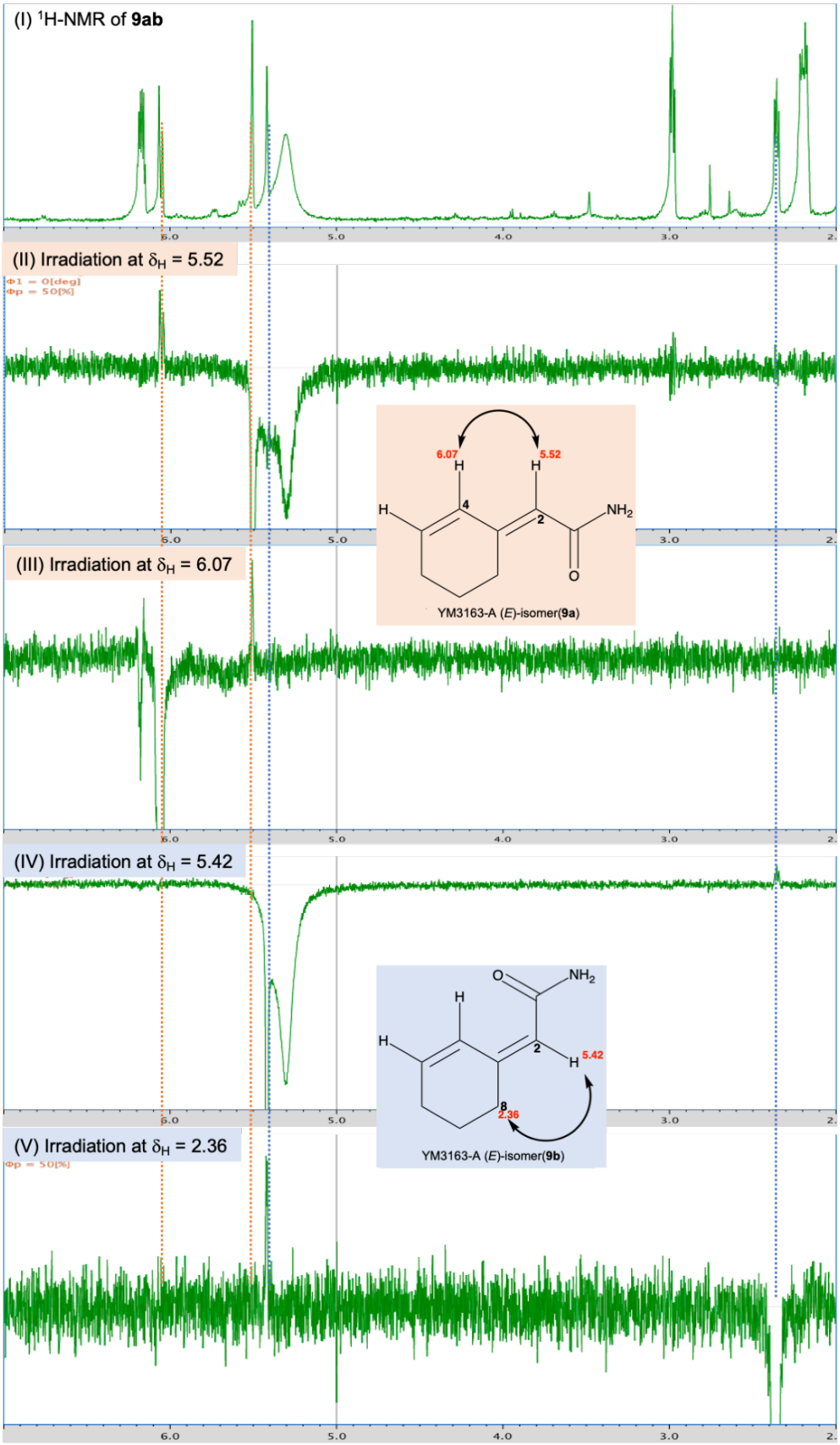

Figure 3.3.5 Differential NOE analysis of natural **9ab**. (I) 1H-NMR of **9ab**, (II) Irradiation at δ_H = 5.52, (III) Irradiation at δ_H = 6.07, (IV) Irradiation at δ_H = 5.42, and (V) Irradiation at δ_H = 2.36.

3.3.4 Chemical synthesis of YM3163-A and its biological evaluation

The structure of **9ab** was finally confirmed through chemical synthesis (**Figure3.3.6**).

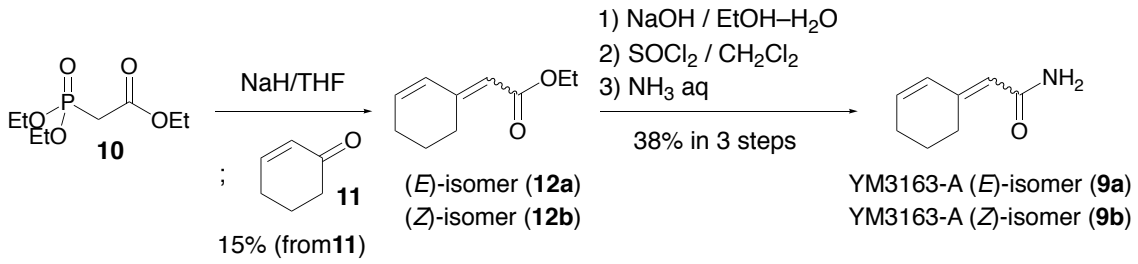

Figure 3.3.6 Synthesis of YM3163-A

2-Cyclohexen-1-one (**11**) was subjected to Horner-Wadsworth-Emmons reaction using ethyl diethylphosphonoacetate (**10**) to give α,β-unsaturated ester **12ab** as a diastereomeric mixture with a ratio of *E*/*Z* = 2:3. The yield was only 15% since the substrate contains a reactive α,β-unsaturated ketone. Ester **12ab** was then converted to amide **9ab** in the following three steps; **12ab** was subjected to alkaline hydrolysis to give the corresponding carboxylic acid, which was treated with thionyl chloride and then with aqueous ammonia to give amide **9ab** in 38% yield (3 steps). Their ^{1}H- and ^{13}C-NMR spectra (**Figures S7** and **S8**(see Appendix)) were comparable with those of natural **9ab** (**Figures S1** and **S2**(see Appendix)). The *E*/*Z* ratio of synthetic **9ab** was estimated to be 2:3, which was opposite to that of natural **9ab** (*E*/*Z* = 4:3). According to the peak intensity of synthetic **9ab** in its HPLC chromatogram, (*Z*)-isomer **9b** elutes at 14.0 min and then (*E*)-isomer **9a** does at 15.5 min (**Figure 3.3.3 B**).

Antimicrobial activity of **9ab** was evaluated using *Micrococcus luteus* as an indicator microorganism. This compound showed no inhibitory zone even at 5 mM.

3.4 Discussion

In this chapter, I focused on the function of SARP-type activator genes for activation of cryptic secondary metabolite BGCs in *S. rochei*. Overexpression of *SRO_3163* gene led to accumulate a novel enamide, 2-(cyclohex-2-en-1-ylidene)acetamide (**9ab; Figure 3.1.2**), that could not be produced in the parent strain. YM3163-A is a novel cyclohexene-containing enamide in nature. At this stage, its biosynthetic origin and genes are uncertain, indicating its novel biosynthetic machinery. The neighboring loci of *SRO_3163* (**Table 3.4.1**) contains three biosynthetic genes for futalosine; *SRO-3159,* coding a menaquinone biosynthesis protein MqnA (93% similarity and 87% identity to SCO4506), *SRO_3156*, coding a dehydroxanthine futalosine cyclase MqnC (98% similarity and 93% identity to SCO4550), and *SRO_3180*, coding an aminofutalosine synthase MqnE (99% similarity and 94% identity to SCO4494) [90][91]. However, the chemical structure of futalosine is not related with that of YM3163-A.

Table 3.4.1 The neighboring loci of *SRO_3163*

SRO	Start	End	AA length	deduced function
SRO_3150	3524307	3524930	208	polypeptide deformylase
SRO_3151	3524931	3526214	428	electron transfer oxidoreductase
SRO_3152	3526312	3526842	177	acetyltransferase
SRO_3153	3526925	3527260	112	PASTA domain-containing protein
SRO_3154	3527292	3527939	216	ubiquinone/menaquinone biosynthesismethyltransferase
SRO_3155	3528073	3528675	201	Uncharacterized protein
SRO_3156	3528683	3529882	400	radical SAM domain-containing protein
SRO_3157	3529925	3530647	241	type IV peptidase
SRO_3158	3530644	3531147	168	Putative uncharacterized protein
SRO_3159	3531694	3532542	283	menaquinone biosynthetic enzyme
SRO_3160	3532830	3533033	68	cold shock protein scoF
SRO_3161	3533209	3533877	223	methyltransferase
SRO_3162	3534049	3534228	60	Uncharacterized protein
SRO_3163	3534658	3537678	1007	transcriptional regulator, SARP family protein
SRO_3164	3537850	3538644	265	regulatory protein
SRO_3165	3538760	3539563	268	biotin carboxylase
SRO_3166	3539716	3539904	63	DNA-binding protein
SRO_3167	3539901	3540152	84	toxin-antitoxin system, toxin component
SRO_3168	3540149	3540958	270	DNA-binding protein
SRO_3169	3541121	3541570	150	regulatory protein
SRO_3170	3542026	3542361	112	Uncharacterized protein
SRO_3171	3542436	3543197	254	Uncharacterized protein (Precursor)
SRO_3172	3543405	3545327	641	long-chain-fatty acid CoA ligase
SRO_3173	3545592	3546434	281	dehydratase
SRO_3174	3546481	3547326	282	Prolipoprotein diacylglyceryl transferase (Precursor)
SRO_3175	3547654	3548292	213	TetR-family transcriptional regulator
SRO_3176	3548419	3548742	108	membrane protein
SRO_3177	3548811	3549335	175	acetyltransferase
SRO_3178	3549352	3550110	253	uracil DNA glycosylase superfamily protein
SRO_3179	3550194	3550463	90	Uncharacterized protein (Precursor)
SRO_3180	3550480	3551643	388	radical SAM protein

This result indicated that SRO_3163 protein acts as a stand-alone SARP to activate uncharacterized gene set for the biosynthesis of YM3163-A, whose cluster has not yet been identified. Occasionally, YM3163-A was detected as a trace amount in a plasmid-less mutant YN-P145 [**91**]. This mutant has a large deletion on the chromosome; 602,866-bp from the right end and 912,581-bp from the left end [**67**][**92**](**Figure 3.4.1**). Production of YM3163-A in strain YN-P145 strongly indicated that BGC for YM3163-A possibly locates between *SRO_0580* and *SRO_6743* in the chromosome and not on three linear plasmids. Identification of BGC for YM3163-A is in progress in our laboratory.

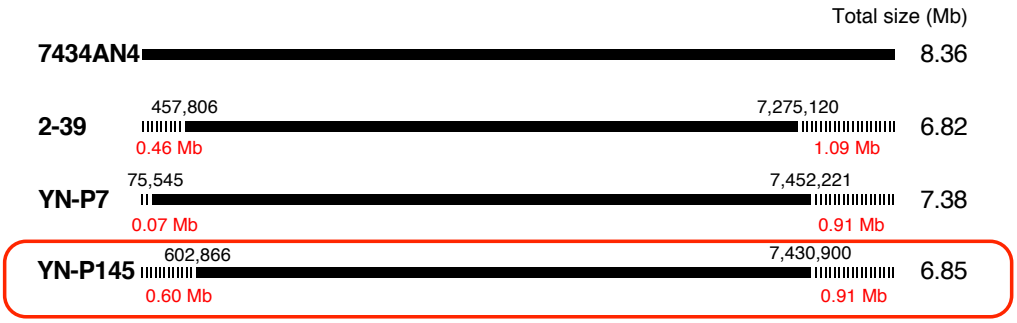

Figure 3.4.1 Chromosomal deletion amoung three plasmidless mutants (2-39, YN-P7, and YN-P145) of *S. rochei* Total chromosomal size of *S. rochei* 7434AN4 is 8,364,802 bp.

Thus, *in vivo* overexpression of activators is one of the powerful strategies for genome mining. Recently, Krause et al. reported that cross-overexpression of the SARP-type gene *papR2* from *Streptomyces pristinaespiralis* in *Streptomyces lividans* led to activate the silent undecylprodigiosin gene cluster [**50**]. Together with our present finding, an SARP-guided activation strategy will be advantageous to occasional discovery of microbial natural products.

Chapter 4. Conclusion

To understand the gross regulatory cascade for secondary metabolite production and develop the global genome mining approaches for natural product discovery, I performed the functional analysis of the transcriptional repressor (pseudo-receptor) SrrB (Chapter 2) and the SARP-type activator SRO_3163 in *S. rochei* 7434AN4 (Chapter 3).

As described in General Introduction, most important features in *Streptomyces* is a potential of vast array of secondary metabolite production, however, most of secondary metabolite BGCs (ca. 80-90%) are silent under normal laboratory culture conditions. Activation of silent secondary metabolite BGCs is challenging and practical tool for natural product discovery from microbial sources. Many researchers developed the genome mining strategies to discover novel natural products from microorganism [**16**][**68**][**69**][**93**][**94**]. The followings are genome mining methods relevant to this study; (1) blockage of major secondary metabolite gene cluster(s), (2) inactivation of the repressor gene(s), (3) combination of strategies (1) and (2), (4) extensive chromosomal deletion *via* removal of *tpg-tap* gene pair, (5) addition of chemical elicitor(s), including signaling molecules, and (6) overexpression of the activator gene(s) (among them, strategy (2) was focused in Chapter 2, and strategy (6) was in Chapter 3).

Strategy (1) ; Blockage of major secondary metabolite gene cluster(s)

Comparative analysis of metabolic profiles among wild-type and mutant strains is widely used to identify the cryptic metabolites of interests. Inactivation of major secondary metabolite gene cluster(s) sometimes improves the metabolic titer of other metabolites expressed poorly or silent (**Figure 4.1**). For example, *S. rochei* mutant FS18,

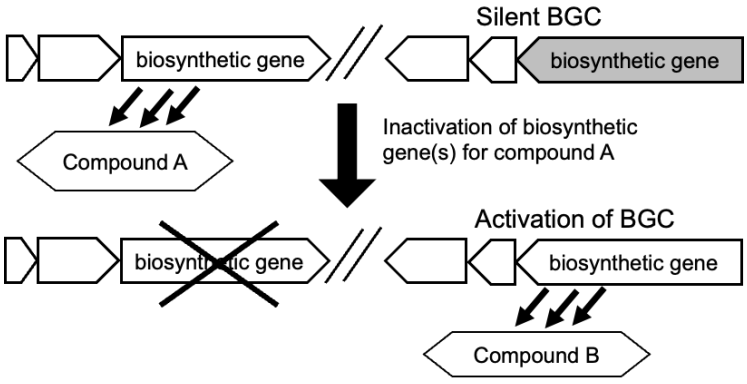

Figure 4.1 (Strategy 1) Blockage of major biosynthetic pathway

a gene disruptant of *lkcA* encoding an NRPS (nonribosomal peptide synthetase)/PKS

(polyketide synthase) hybrid enzyme involved in lankacidin biosynthesis, showed complex metabolic changes when compared with the parent strain and other mutants of lankacidin biosynthesis [**88**]. This strain failed to produce lankacidin and its derivatives due to the mutation in the early step of lankacidin biosynthesis, however, accumulated large amounts of three UV-active compounds, a 28-membered pentaene macrolide pentamycin, and a diastereomeric mixture of citreodiol and *epi*-citreodiol (**Figure 3.1.1**) [**88**].

Strategy (2) ; Inactivation of the repressor gene(s)

As I described in this thesis (Chapter 2), inactivation of transcriptional repressor genes can lead to activate cryptic secondary metabolite BGCs and/or titer improvement (**Figure 4.2**). Merit of this strategy is a simple genetic manipulation rather than strategy (6) since supplementation of antibiotics are necessary for the maintenance of heterologous vector in the cell.

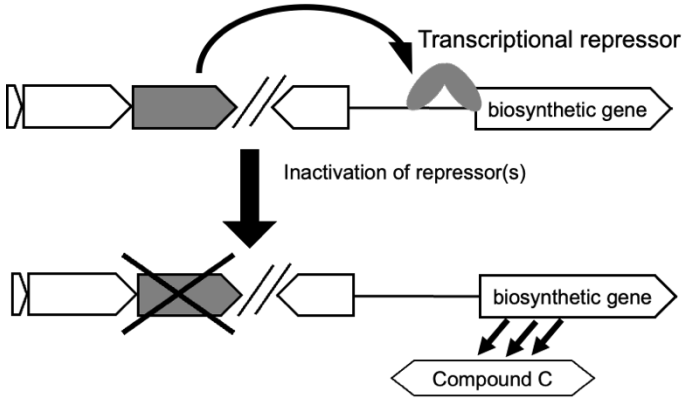

Figure 4.2 (Strategy 2) Inactivation of transcriptional repressors

Strategy (3) ; Combination of strategies (1) and (2)

Two strategies above mentioned are combined to develop more efficient approach for activation of silent clusters (**Figure 4.3**).

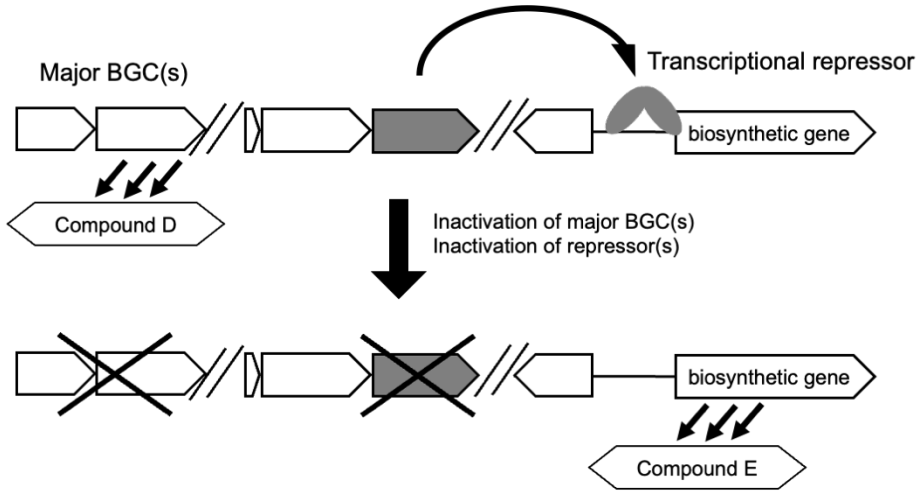

Figure 4.3 (Strategy 3) Combination of strategies 1 and 2

Mutant KA57 of *S. rochei* carries multiple mutations on the transcriptional repressor gene *srrB* together with two biosynthesis genes for lankacidin (*lkc*) and lankamycin (*lkm*). Occasionally, strain KA57 accumulates an azoxyalkene compound KA57-A (**Figure 3.1.1**) that is not detected in any other single or double mutants as well as the parent strain [**89**]. Advantage in this strategy is that target clusters are almost random and unpredictable, although multiple mutations are necessary.

Strategy (4) ; Extensive chromosomal deletion *via* removal of *tpg-tap* gene pair

Telomere deletion frequently occurs in the linear chromosome of *Streptomyces*. *Streptomyces rochei* 7434AN4, which carries three linear plasmids pSLA2-L, pSLA2-M, and pSLA2-S, showed telomere deletion concomitant with a loss of linear plasmids pSLA2-L and pSLA2-M [**92**]. Plasmid-complementation/curing experiment together with Southern hybridization and our complete nucleotide sequence analysis of *S. rochei* 7434AN4 revealed that the linearity of the *S. rochei* chromosome is maintained by *tap-tpg* gene pair from either of pSLA2-L or pSLA2-M [**92**]. Due to the presence of secondary metabolite BGCs at the arm region of the chromosome, telomere deletion in *S. rochei* 7434AN4 may affect their metabolite-producing properties (**Figure 4.4**). In fact, some secondary metabolites were detected in the three plasmid-less, chromosomal deletion mutants, 2-39, YN-P7, YN-P145 [**91**].

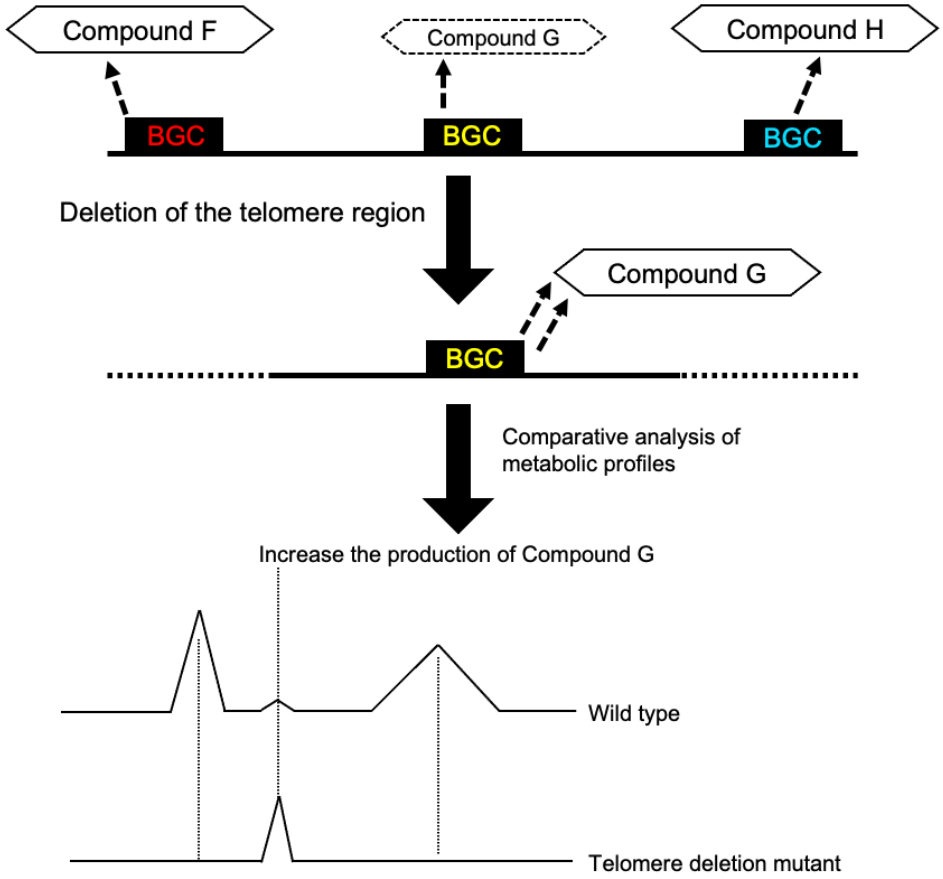

Figure 4.4 (Strategy 4) Extensive chromosomal deletion *via* removal of *tpg-tap* gene pair

Strategy (5) ; Addition of chemical elicitor(s), including signaling molecules

Streptomyces strains generally have multiple signaling-molecule receptor genes, suggesting that they have a potential to recognize heterologous signaling molecules as chemical elicitors (**Figure 4.5**). About 60% of *Streptomyces* strains can use γ-butyrolactones as signaling molecules to induce secondary metabolite production [**8**][**95**]. In addition, 24% of 51 actinomycetes exhibit avenolide activity for induction of secondary metabolites [**96**]. Hence, butanolide-type signaling molecules SRBs can share unique distribution in *Streptomyces*, and SRBs may contribute as "genetic engineering-free" genome mining tools in heterologous *Streptomyces*. Extensive heterologous addition of SRBs in various Actinomycetes is in progress in our laboratory.

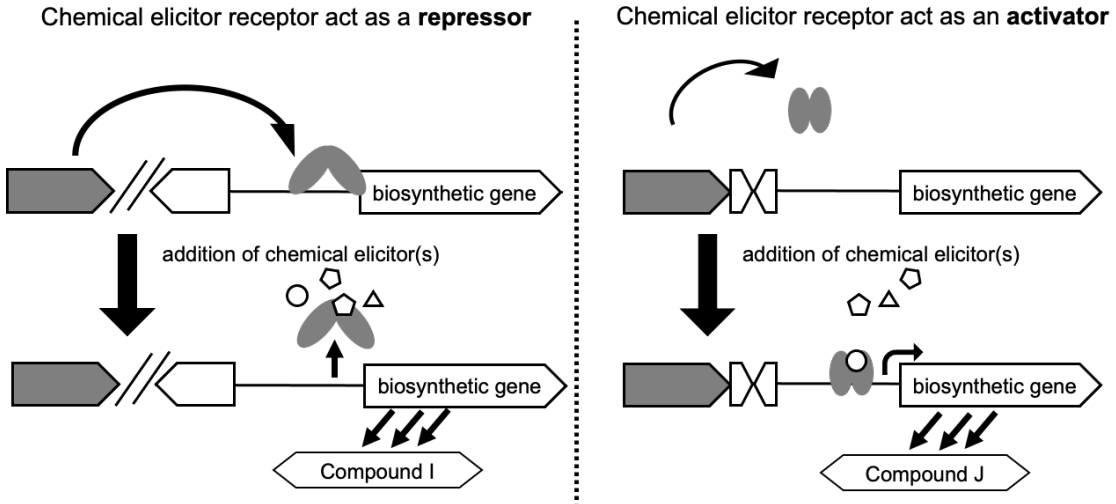

Figure 4.5 (Strategy 5) Addition of chemical elicitor(s), including signaling molecules

Strategy (6) ; Overexpression of the activator gene(s)

As I described in this thesis (Chapter 3), *in vivo* overexpression of pathway-specific activator genes including SARP genes is one of the intuitive approach to activate silent secondary metabolite BGCs, since they only require simple genetic manipulation; introduction of one SARP-gene expression construct into the strains of interests (**Figure 4.6**). As described in Chapter 3, any transcriptional activator genes including SARP genes are located on the secondary metabolite BGCs, hence, I can predict the secondary metabolite production in some extent.

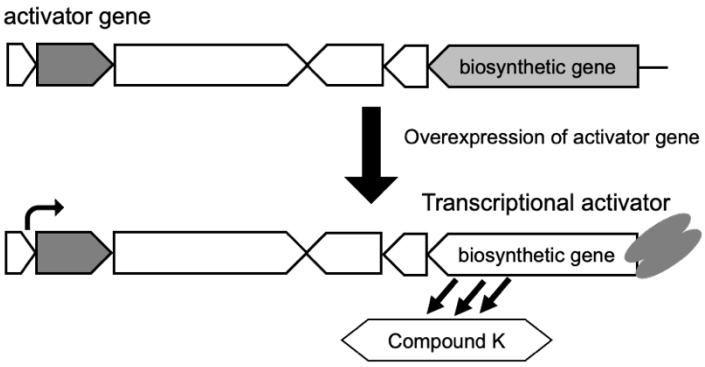

Figure 4.6 (Strategy 6) Overexpression of the activator gene(s)

Along with my extensive analysis of the SARP-type activator gene *SRO_3163* (Chapter 3), I also attempted overexpression of other SARP genes (8 genes of 12; SRO_732, SRO_1189, SRO_1851, SRO_2506, SRO_3163, SRO_3164, SRO_6312,

and SRO_6387) coded on the *S. rochei* chromosome, however, their recombinants have no inducing activity of cryptic BGCs at this stage. For example, a recombinant of *SRO_1851*, which locates at the border of BGC for azoxyalkene KA57-A (**Figure 3.1.1**), could not induce the production of KA57-A (data not shown). In view of the type of promoter (inducible or constitutive) together with a choice of culture medium, genome mining through *in vivo* overexpression may be conditional. Involvement of other activation elements could not be ruled out for constant expression of BGCs in the producing microorganism. Multiple overexpression of SARP genes may lead to extensive natural product discovery.

In this thesis, I extensively analyzed the regulatory genes to understand the regulatory cascade and attempted to develop the genome mining approaches for natural product discovery. More recently, I reported that a mutant strain of *S. rochei*, in which two regulatory genes, *srrY* (SARP-type activator) and *srrC* (a *tetR*-type repressor) were inactivated, produced three gamma-butyrolactone compounds, which were not detected in the parent strain (**Figure 4.7**) [**97**]. Thus, decipheringthe complex regulatory network may lead to activate silent metabolic gene clusters in the original strain. Recent advances in genome mining approaches described in this thesis will provide an opportunity for bioactive natural product discovery.

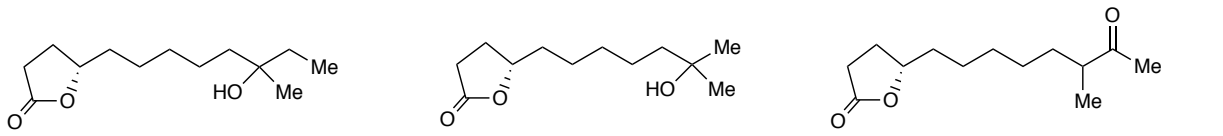

4,10-dihydroxy-10-methyldodecan-4-olide 4,10-dihydroxy-10-methylundecan-4-olide 4-hydroxy-11-oxo-10-methyldodecan-4-olide

Figure 4.7 Three butylolactone were isolated from the regulatory gene mutant strain *S. rochei*

Acknowledgments

This thesis study has been carried out at the Cell Biochemistry Laboratory, Unit of Biotechnology, Division of Biological and Life Sciences, Graduate School of Integrated Sciences for Life, Hiroshima University.

I am deeply grateful to Associate Professor Kenji Arakawa for their excellent guidance, encouragement and for providing me this study opportunity as a Ph.D. student. I would like to thank my first supervisor, Prof. Kozo Ochi (Hiroshima institute of technology), for his support. I also want to thank Prof. Tsunehiro Aki, Prof. Seiji Kawamoto, Prof. Hisato Kuniyoshi and Prof. Nobukazu Tanaka for their advice on my doctoral thesis. I appreciate Dr. Kuninobu Inada for advice on molecular biology. I would like to thank Mrs. Tomoko Amimoto for help technical support on MS analysis. I would like to thank Mr. Hitoshi Fujitaka for help technical support on NMR analysis. I thank all the members of the Cell Biochemistry laboratory and the Marine Biotechnology laboratory for their kindness and friendship. I would like to thank for Japan Society for the Promotion of Science (JSPS). I was supported by a JSPS Research Fellowship for Young Scientists. Finally, I would like to express my gratitude to my family have been supporting to me.

References

[1] "2020 Antibacterial agents in clinical and preclinical development: an overview and analysis." Geneva: World Health Organization, **ISBN:** 978-92-4-002130-3(2021).
[2] Shore, C., Coukell, A. " Roadmap for antibiotic discovery." *Nature microbiology,***1**,16083(2016).

[3] Horinouchi, S., and Beppu, T. "Hormonal control by A-factor of morphological development and secondary metabolism in *streptomyces*." *Proc. Jpn. Acad. Ser. B. Phys. Biol. Sci*., **83**, 277–295(2007).

[4] Bibb, M. J. "Regulation of secondary metabolism in *streptomycetes*." *Curr. Opin. Microbiol*., **8**, 208–215(2005).

[5] Takano E. “Gamma-butyrolactones: *Streptomyces* signalling molecules regulating antibiotic production and differentiation.” *Curr. Opin. Microbiol.,* **9**, 287–294 (2006).

[6] Martín, J. F., and Liras, P. "Harnessing microbiota interactions to produce bioactive metabolites: communication signals and receptor proteins." *Curr. Opin. Pharmacol.,* **48**, 8–16(2019).

[7] Khokhlov, A.S., Tovarova, I.I., Borisova, L.N., Pliner, S.A., Shevchenko, L.N., Kornitskaia, EIa, Ivkina, N.S., Rapoport, I.A." The A-factor, responsible for streptomycin biosynthesis by mutant strains of Actinomyces streptomycini" *Dokl Akad Nauk SSSR,***177**,232-235(1967)

[8] Hara, O., and Beppu, T. “Mutants blocked in streptomycin production in *Streptomyces griseus*–the role of A-factor.” *J. Antibiot.*, **35**, 349–358(1982).

[9] Kondo, K., Higuchi, Y., Sakuda, S., Nihira, T., Yamada, Y. "New virginiae butanolides from *Streptomyces virginiae*." *J. Antibiot.*, **42**,1873-1876(1989)

[10] Sato, K., Nihira, T., Sakuda, S., Yanagimoto, M., Yamada, Y. "Isolation and structure of a new butyrolactone autoregulator from *Streptomyces* sp. FRI-5." *J. Ferment. Bioeng.*, **68**,170–173(1989).

[11] Kitani, S., Miyamoto, K.T., Takamatsu, S., Herawati, E., Iguchi, H., Nishitomi, K., Uchida, M., Nagamitsu, T., Omura, S., Ikeda, H., Nihira, T. "Avenolide, a Streptomyces hormone controlling antibiotic production in *Streptomyces avermitilis*." *Proc. Natl. Acad. Sci. USA*, **108**,16410–5(2011)

[12] Arakawa, K., Tsuda, N., Taniguchi, A. and Kinashi, H. "The butenolide signaling molecules SRB1 and SRB2 induce lankacidin and lankamycin production in *Streptomyces rochei*." *Chem. Bio. Chem.*, **13**, 1447–57(2012).

[13] Corre, C., Song, L., O'Rourke, S., Chater, K. F. and Challis, G.L. "2-Alkyl-4-hydroxymethylfuran-3-carboxylic acids, antibiotic production inducers discovered by *Streptomyces coelicolor* genome mining." *Proc. Natl. Acad. Sci. USA*, **105**, 17510–17515(2008).

[14] Ohnishi, Y., Kameyama, S., Onaka, H., and Horinouchi, S. "The A-factor regulatory cascade leading to streptomycin production in streptomyces griseus: identification of a target gene of the A-factor receptor." *Mol. Microbiol*., **34**, 102–111(1999).

[15] Ohnishi, Y., Yamazaki, H., Kato, J. Y., Tomono, A., and Horinouchi, S. "AdpA, a central transcriptional regulator in the A-factor regulatory cascade that leads to morphological development and secondary metabolism in *Streptomyces griseus*." *Biosci. Biotechnol. Biochem*., **69**, 431–439(2005).

[16] Arakawa, K. "Manipulation of metabolic pathways controlled by signaling molecules, inducers of antibiotic production, for genome mining in *Streptomyces* spp." *Antonie. Leeuwen*., **111**, 743–751(2018).

[17] Xu, G., and Yang, S. "Regulatory and evolutionary roles of pseudo γ-butyrolactone receptors in antibiotic biosynthesis and resistance." *Appl. Microbiol. Biotechnol*., **103**, 9373–9378(2019).

[18] Onaka, H., Ando, N., Nihira, T., Yamada, Y., Beppu, T., and Horinouchi, S. "Cloning and characterization of the A-factor receptor gene from *Streptomyces griseus*." *J. Bacteriol*., **177**, 6083–6092(1995).

[19] Arakawa, K., Mochizuki, S., Yamada, K., Noma, T., and Kinashi, H. "γ-Butyrolactone autoregulator-receptor system involved in lankacidin and lankamycin production and morphological differentiation in *Streptomyces rochei*. "*Microbiology,* **153**, 1817–1827(2007).

[20] Yamamoto, S., He, Y., Arakawa, K., and Kinashi, H. "γ-Butyrolactone-dependent expression of the SARP gene *srrY* plays a central role in the regulatory cascade leading to lankacidin and lankamycin production in *Streptomyces rochei*." *J. Bacteriol*., **190**, 1308–1316(2008).

[21] Suzuki, T., Mochizuki, S., Yamamoto, S., Arakawa, K., and Kinashi, H. "Regulation of lankamycin biosynthesis in *Streptomyces rochei* by two SARP genes, *srrY* and *srrZ*." *Biosci. Biotechnol. Biochem*., **74**, 819–827(2010).

[22] Bate, N., Butler, A. R., Gandecha, A. R., and Cundliffe, E. "Multiple regulatory genes in the tylosin biosynthetic cluster of *Streptomyces fradiae*." *Chem. Biol*., **6**, 617–624(1999).

[23] Bate, N., Stratigopoulos, G., and Cundliffe, E. "Differential roles of two SARP-encoding regulatory genes during tylosin biosynthesis. "*Mol. Microbiol*., **43**, 449–458(2002).

[24] Stratigopoulos, G., and Cundliffe, E. "Expression analysis of the tylosin-biosynthetic gene cluster: pivotal regulatory role of the tylQ product." *Chem. Biol*., **9**, 71–78(2002).

[25] Takano, E., Chakaraburtty, R., Nihira, T., Yamada, Y., and Bibb, M. J. "A complex role for the γ-butyrolactone SCB1 in regulating antibiotic production in *Streptomyces coelicolor* A3(2)." *Mol. Microbiol*." **41**, 1015–1028(2001).

[26] Takano, E., Kinoshita, H., Mersinias, V., Bucca, G., Hotchkiss, G., Nihira, T. "A bacterial hormone (the SCB1) directly controls the expression of a pathway-specific regulatory gene in the cryptic type I polyketide biosynthetic gene cluster of *Streptomyces coelicolor*." *Mol. Microbiol*., **56**, 465–479(2005).

[27] Hsiao, N. H., Nakayama, S., Merlo, M. E., de Vries, M., Bunet, R., Kitani, S. "Analysis of two additional signaling molecules in streptomyces coelicolor and the development of a butyrolactone-specific reporter system." *Chem. Biol*.,**16**, 951–960(2009).

[28] Gottelt, M., Kol, S., Gomez-Escribano, J. P., Bibb, M., and Takano, E. "Deletion of a regulatory gene within the cpk gene cluster reveals novel antibacterial activity in *Streptomyces coelicolor* A3(2)." *Microbiology*, **156**, 2343–2353(2010).

[29] Li, X., Wang, J., Li, S., Ji, J., Wang, W., and Yang, K. "ScbR- and ScbR2-mediated signal transduction networks coordinate complex physiological responses in *Streptomyces coelicolor.*" *Sci. Rep*. **5**,14831(2015).

[30] Xu, G., Wang, J., Wang, L., Tian, X., Yang, H., Fan, K. " "Pseudo" γ-butyrolactone receptors respond to antibiotic signals to coordinate antibiotic biosynthesis." *J. Biol. Chem*., **285**, 27440–27448(2010).

[31] Wang, J., Wang, W., Wang, L., Zhang, G., Fan, K., Tan, H. "A novel role of 'pseudo' γ-butyrolactone receptors in controlling γ-butyrolactone biosynthesis in streptomyces." *Mol. Microbiol*., **82**, 236–250(2011).

[31] Kinoshita, H., Ipposhi, H., Okamoto, S., Nakano, H., Nihira, T., and Yamada, Y. "Butyrolactone autoregulator receptor protein (BarA) as a transcriptional regulator in *Streptomyces virginiae*." *J. Bacteriol*., **179**, 6986–6993(1997).

[32] Kawauchi, R., Akashi, T., Kamitani, Y., Sy, A., Wangchaisoonthorn, U., Nihira, T. "Identification of an AfsA homologue (BarX) from *Streptomyces virginiae* as a pleiotropic regulator controlling autoregulator biosynthesis, virginiamycin biosynthesis and virginiamycin M1 resistance." *Mol. Microbiol.,* **36**, 302–313(2000).

[33] Yang, K., Han, L., and Vining, L. C. "Regulation of jadomycin B production in Streptomyces venezuelae ISP5230: involvement of a repressor gene, *jadR2*." *J. Bacteriol*., **177**, 6111–6117(1995).

[34] Wang, L., and Vining, L. C. "Control of growth, secondary metabolism and sporulation in *Streptomyces venezuelae* ISP5230 by *jadW1*, a member of the *afsA* family of γ-butyrolactone regulatory genes." *Microbiology,* **149**, 1991–2004(2003).

[35] Wang, L., Tian, X., Wang, J., Yang, H., Fan, K., Xu, G. "Autoregulation of antibiotic biosynthesis by binding of the end product to an atypical response regulator." *Proc. Natl. Acad. Sci. U.S.A*., **106**, 8617–8622(2009).

[36] Zou, Z., Du, D., Zhang, Y., Zhang, J., Niu, G., and Tan, H. "A γ-butyrolactone-sensing activator/repressor, JadR3, controls a regulatory mini-network for jadomycin biosynthesis." *Mol. Microbiol*., **94**, 490–505(2014).

[37] Aigle, B., Pang, X., Decaris, B., and Leblond, P. "Involvement of AlpV, a new member of the Streptomyces antibiotic regulatory protein family, in regulation of the duplicated type II polyketide synthase alp gene cluster in *Streptomyces ambofaciens*." *J. Bacteriol*., **187**, 2491–2500(2005).

[38] Bunet, R., Mendes, M. V., Rouhier, N., Pang, X., Hotel, L., Leblond, P. "Regulation of the synthesis of the angucyclinone antibiotic alpomycin in *Streptomyces ambofaciens* by the autoregulator receptor AlpZ and its specific ligand." *J. Bacteriol*. **190**, 3293–3305(2008).

[39] Bunet, R., Song, L., Mendes, M. V., Corre, C., Hotel, L., Rouhier, N. "Characterization and manipulation of the pathway-specific late regulator AlpW reveals Streptomyces ambofaciens as a new producer of kinamycins." *J. Bacteriol*., **193**, 1142–1153(2011).

[40] Wang, J. B., Zhang, F., Pu, J. Y., Zhao, J., Zhao, Q. F., and Tang, G. L. "Characterization of AvaR1, an autoregulator receptor that negatively controls avermectins production in a high avermectin-producing strain." *Biotechnol. Lett*., **36**, 813–819(2014).

[41] Zhu, J., Sun, D., Liu, W., Chen, Z., Li, J., and Wen, Y. "AvaR2, a pseudo γ-butyrolactone receptor homologue from *Streptomyces avermitilis*, is a pleiotropic

repressor of avermectin and avenolide biosynthesis and cell growth." *Mol. Microbiol*., **102**, 562–578(2016).

[42] Yu, Z., Reichheld, S. E., Savchenko, A., Parkinson, J., and Davidson, A. R. "A comprehensive analysis of structural and sequence conservation in the TetR family transcriptional regulators." *J. Mol. Biol*., **400**, 847–864(2010).

[43] Biarnes-Carrera, M., Breitling, R., and Takano, E. "Butyrolactone signaling circuits for synthetic biology." *Curr. Opin. Chem. Biol*., **28**, 91–98(2015).

[44] Niu, G., Chater, K. F., Tian, Y., Zhang, J., and Tan, H. "Specialized metabolites regulating antibiotic biosynthesis in *Streptomyces* spp." *FEMS Microbiol. Rev*., **40**, 554–573(2016).

[45] Okamoto, S., Nakamura, K., Nihira, T., and Yamada, Y. "Virginiae butanolide binding protein from Streptomyces virginiae. Evidence that VbrA is not the virginiae butanolide binding protein and reidentification of the true binding protein." *J. Biol. Chem.,* **270**,12319-26(1995).

[46] Kitani, S., Yamada, Y., and Nihira, T. "Gene replacement analysis of the butyrolactone autoregulator receptor (FarA) reveals that FarA acts as a Novel regulator in secondary metabolism of *Streptomyces lavendulae* FRI-5." *J. Bacteriol.,***183**, 4357-4363(2001).

[47] Zhou, S., Malet, N.R., Song, L., Corre, C., and Challis, G.L. "MmfL catalyses formation of a phosphorylated butenolide intermediate in methylenomycin furan biosynthesis." *Chem. Commun. (Camb).*, **56**,14443-14446(2020).

[48] Kumar, S., Stecher, G., Li, M., Knyaz, C., and Tamura, K. "MEGA X: molecular evolutionary genetics analysis across computing platforms." *Mol. Biol. Evol*., **35**, 1547–1549(2018).

[49] Wietzorrek, A., Bibb, M.J. "A novel family of proteins that regulates antibiotic production in streptomycetes appears to contain an OmpR-like DNA-binding fold." *Mol Microbiol,***25**,1181–84(1997).

[50] Krause, J., Handayani, I., Blin, K., Kulik, A., and Mast, Y., "Disclosing the Potential of the SARP-Type Regulator PapR2 for the Activation of Antibiotic Gene Clusters in *Streptomycetes*." *Front Microbiol.,***11,** 225(2020).

[51] Liu, G., Chater, K.F., and Chandra, G. "Molecular regulation of antibiotic biosynthesis in *Streptomyces*." *Microbiol. Mol. Biol. Rev.,***77**:112-143(2013).

[52] Takano, E., Gramajo, H.C., and Strauch, E. "Transcriptional regulation of the *redD* transcriptional activator gene accounts for growth-phase-dependent production of the antibiotic undecylprodigiosin in *Streptomyces coelicolor* A3(2)." *Mol. Microbiol.,* **6**, 2797–804(1992).

[53] Arias, P., Fernández-Moreno, M.A., and Malpartida, F. "Characterization of the pathway-specific positive transcriptional regulator for actinorhodin biosynthesis in *Streptomyces coelicolor* A3(2) as a DNA-binding protein." *J. Bacteriol.,* **181**,6958-6968(1999)

[54] Madduri, K., and Hutchinson, C.R. "Functional characterization and transcriptional analysis of a gene cluster governing early and late steps in daunorubicin biosynthesis in *Streptomyces peucetius*." *J. Bacteriol.,* **177**, 3879–3884(1995).

[55] Vasanthakumar, A., Kattusamy, K., and Prasad, R., "Regulation of daunorubicin biosynthesis in Streptomyces peucetius - feed forward and feedback transcriptional control." *J. Basic. Microbiol.*, **53**,636-644(2013)

[56] Chen, Y., Wendt-Pienkowski, E., and Shen, B. "Identification and utility of FdmR1 as a Streptomyces antibiotic regulatory protein activator for fredericamycin production in *Streptomyces griseus* ATCC 49344 and heterologous hosts." *J. Bacteriol*., **190**, 5587-5596(2008)

[57] Cundliffe, E. "Control of tylosin biosynthesis in *Streptomyces fradiae*." *J. Microbiol. Biotechnol.*, **18**,1485-1491(2008)

[58] Sheldon, P.J., Busarow, S.B., and Hutchinson, C.R. "Mapping the DNA-binding domain and target sequences of the Streptomyces peucetius daunorubicin biosynthesis regulatory protein, DnrI." *Mol. Microbiol.*, **44**, 449-460(2002).

[59] Tanaka, A., Takano, Y., Ohnishi, Y., and Horinouchi, S. "AfsR recruits RNA polymerase to the afsS promoter: a model for transcriptional activation by SARPs." *J. Mol. Biol.*, **369**, 322-333(2007).

[60] Arakawa, K., and Suzuki, T. "Regulation of secondary metabolites through signaling molecules in *Streptomyces*" in *Natural Products from Actinomycetes – Diversity, Ecology and Drug Discovery* -, Eds Ravishankar V. Rai and Jamuna A. Bai, in press, 2022, Springer Nature.DOI: 10.1007/978-981-16-6132-7

[61] Tang, L., Grimm, A., Zhang, Y.X., and Hutchinson, C.R. "Purification and characterization of the DNA-binding protein DnrI, a transcriptional factor of daunorubicin biosynthesis in *Streptomyces peucetius*." *Mol. Microbiol*., **22**, 801-813(1996)

[62] Novakova, R., Knirschova, R., Farkasovsky, M., Feckova, L., Rehakova, A., Mingyar, E., and Kormanec, J. "The gene cluster aur1 for the angucycline antibiotic auricin is located on a large linear plasmid pSA3239 in *Streptomyces aureofaciens* CCM 3239." *FEMS. Microbiol. Lett.,* **342**, 130-137(2013)

[63] Higashi, T., Iwasaki, Y., Ohnishi, Y., and Horinouchi, S. "A-factor and phosphate depletion signals are transmitted to the grixazone biosynthesis genes via the pathway-specific transcriptional activator GriR." *J. Bacteriol*., **189**, 3515-3524(2007)

[64] Mast, Y., Guezguez, J., Handel, F., and Schinko, E. "A Complex Signaling Cascade Governs Pristinamycin Biosynthesis in *Streptomyces pristinaespiralis.*" *Appl. Environ. Microbiol.,* **81**, 6621-6636(2015)

[65] Kinashi, H., Mori, E., Hatani, A., and Nimi, O. "Isolation and characterization of large linear plasmids from lankacidin-producing *Streptomyces* species." *J. Antibiot*., **47**, 1447–1455(1994).

[66] Mochizuki, S., Hiratsu, K., Suwa, M., Ishii, T., Sugino, F., Yamada, K. "The large linear plasmid pSLA2-L of *Streptomyces* rochei has an unusually condensed gene organization for secondary metabolism." *Mol. Microbiol*., **48**, 1501–1510(2003).

[67] Nindita, Y., Cao, Z., Fauzi, A.A., Teshima. A., Misaki, Y., Muslimin, R., Yang, Y., Shiwa, Y., Yoshikawa, H., Tagami, M., Lezhava, A., Ishikawa, J., Kuroda, M., Sekizuka, T., Inada, K., Kinashi, H., and Arakawa, K. "The genome sequence of Streptomyces rochei 7434AN4, which carries a linear chromosome and three characteristic linear plasmids." *Sci. Rep.,* **9**,10973(2019)

[68] Zerikly, M., and Challis, G.L. "Strategies for the discovery of new natural products by genome mining." *ChemBioChem,* **10**, 625-633(2009).

[69] Craney, A., Ahmed, S., and Nodwell, J. "Towards a new science of secondary metabolism." *J. Antibiot,* **66**, 387-400(2013).

[70] Ramos, J.L., Martínez-Bueno, M., Molina-Henares, A.J., Terán, W., Watanabe, K., Zhang, X., Gallegos, M.T., Brennan, R., and Tobes, R. "The TetR family of transcriptional repressors." *Microbiol. Mol. Biol. Rev.,* **69,** 326-356(2005)

[71] Laureti, L., Song, L., Huang, S., Corre, C., Leblond, P., Challis, G.L., and Aigle, B. "Identification of a bioactive 51-membered macrolide complex by activation of a silent polyketide synthase in *Streptomyces ambofaciens*." *Proc. Natl. Acad. Sci. USA.,* **108**, 6258-6263(2011)

[72] Olano, C., García, I., González, A., Rodriguez, M., Rozas, D., Rubio, J., Sánchez-Hidalgo, M., Braña, A.F., Méndez, C., and Salas, J.A. "Activation and identification of five clusters for secondary metabolites in *Streptomyces albus* J1074." *Microb. Biotechnol.,***7**, 242-56(2014)

[73] Du, D., Katsuyama, Y., Onaka, H., Fujie, M., Satoh, N., Shin-Ya, K., and Ohnishi, Y. "Production of a Novel Amide-Containing Polyene by Activating a Cryptic Biosynthetic Gene Cluster in Streptomyces sp. MSC090213JE08." *Chembiochem.,***17**, 1464-71(2016)

[74] Hall, T. A. "BioEdit: a user-friendly biological sequence alignment editor and analysis program for Windows 95/98/NT." *Nucl. Acids. Symp. Ser.,* **41**, 95–98(1999).

[75] Sambrook, J., Fritsch, E. F., and Maniatis, T. "*Molecular Cloning: A Laboratory Manual*." *Cold Spring Harbor Laboratory Press,* Cold Spring Harbor, NY (1989).

[76] Suwa, M., Sugino, H., Sasaoka, A., Mori, E., Fujii, S., Shinkawa, H., Nimi, O. and Kinashi, H. "Identification of two polyketide synthase gene clusters on the linear plasmid pSLA2-L in *Streptomyces rochei*." *Gene*., **246**, 123-131 (2000).

[77] Kieser, T., Bibb, M. J., Buttner, M. J., Chater, K. F., and Hopwood, D. A. "*Practical Streptomyces Genetic: A Laboratory Manual*." *The John Innes Foundation,* Norwich, UK(2000).

[78] Zhang, H., Shinkawa, H., Ishikawa, J., Kinashi, H., and Nimi, O. "Improvement of transformation system in Streptomyces using a modified regeneration medium." *J. Ferment. Bioeng*., **83**, 217–221(1997).

[79] Sun, J., Kelemen, G. H., Fernandez-Abalos, J. M., and Bibb, M. J. "Green fluorescent protein as a reporter for spatial and temporal gene expression in Streptomyces coelicolor A3(2)." *Microbiology*, **145**, 2221–2227(1999).

[80] Turner, S., Pryer, K. M., Miao, V. P., and Palmer, J. D. "Investigating deep phylogenetic relationships among cyanobacteria and plastids by small subunit rRNA sequence analysis." *J. Eukaryot. Microbiol*., **46**, 327–338(1999).

[81] Lane, D. J. "16S/23S rRNA sequencing," in *Nucleic Acid Techniques in Bacterial Systematics*, eds E. Stackebrandt and M. Goodfellow (New York, NY: John Wiley and Sons, 115–175(1991).

[82] Ishikawa, J., Niino, Y., and Hotta, K. "Construction of pRES18 and pRES19, streptomyces-escherichia coli shuttle vectors carrying multiple cloning sites." *FEMS Microbiol. Lett*. **145**, 113–116(1996).

[83] Arakawa, K., Cao, Z., Suzuki, N., and Kinashi, H. "Isolation, structural elucidation, and biosynthesis of 15-norlankamycin derivatives produced by a type-II thioesterase disruptant of *Streptomyces rochei.*" *Tetrahedron,* **67**, 5199–5205(2011).

[84] Yamauchi, Y., Nindita, Y., Hara, K., Umeshiro, A., Yabuuchi, Y., Suzuki, T., Kinashi, H., and Arakawa, K. "Quinoprotein dehydrogenase functions at the final oxidation step of lankacidin biosynthesis in *Streptomyces rochei* 7434AN4." *J. Biosci. Bioeng.,* **126**, 145-152(2018).

[85] Matsuno, K., Yamada, Y., Lee, C. K., and Nihira, T. "Identification by gene deletion analysis of barB as a negative regulator controlling an early process of virginiamycin biosynthesis in *Streptomyces virginiae*." *Arch. Microbiol*. **181**, 52–59(2004).

[86] Wang, W., Ji, J., Li, X., Wang, J., Li, S., Pan, G., Fan, K., and Yang, K. "Angucyclines as signals modulate the behaviors of *Streptomyces coelicolor*." *Proc. Natl. Acad. Sci. USA.*,**15**, 5688-5693(2014)

[87] Huang, J., Shi, J., Molle, V., Sohlberg, B., Weaver, D., Bibb, M.J., Karoonuthaisiri, N., Lih, C.J., Kao, C.M., Buttner, M.J., and Cohen, S.N. "Cross-regulation among disparate antibiotic biosynthetic pathways of *Streptomyces coelicolor*." *Mol. Microbiol.*, **58**, 1276-1287(2005)

[88] Cao, Z., Yoshida, R., Kinashi, H., and Arakawa, K. "Blockage of the early step of lankacidin biosynthesis caused a large production of pentamycin, citreodiol and epi-citreodiol in *Streptomyces rochei*." *J. Antibiot*., **68**, 328-33(2015)

[89] Kunitake, H., Hiramatsu, T., Kinashi, H., and Arakawa, K. "Isolation and Biosynthesis of an Azoxyalkene Compound Produced by a Multiple Gene Disruptant of *Streptomyces rochei*." *Chembiochem*,**16**, 2237-2243(2015)

[89] Fernández-Moreno, M.A., Caballero, J.L., Hopwood, D.A., and Malpartida. F. "The act cluster contains regulatory and antibiotic export genes, direct targets for translational control by the bldA tRNA gene of *Streptomyces*." *Cell*, **66**, 769-80(1991)

[90] Hiratsuka, T., Furihata, K., Ishikawa, J., Yamashita, H., Itoh, N., Seto, H., and Dairi, T. "An alternative menaquinone biosynthetic pathway operating in microorganisms." *Science*, **321**,1670-1673(2008)

[91] Mahanta, N., Fedoseyenko, D., Dairi, T., and Begley, T.P. "Menaquinone biosynthesis: formation of aminofutalosine requires a unique radical SAM enzyme." *J. Am. Chem. Soc.*, **135**,15318-21(2013)

[91] Fauzi, A. A. ”Integrative analysis of genome structure, secondary metabolites, and morphological differentiation in *Streptomyces* species”. Master Thesis, Hiroshima Univeristy, 2018.

[92] Nindita, Y., Cao, Z., Yang, Y., Arakawa, K., Shiwa, Y., Yoshikawa, H., Tagami, M., Lezhava, A., and Kinashi, H. "The tap-tpg gene pair on the linear plasmid functions to maintain a linear topology of the chromosome in *Streptomyces rochei*." *Mol. Microbiol.,* **95**, 846-58(2015)

[93] Olano, C., Abdelfattah, M.S., Gullón, S., Braña, A.F., Rohr, J., Méndez, C., and Salas, J.A. "Glycosylated derivatives of steffimycin: insights into the role of the sugar moieties for the biological activity." *Chembiochem,* **9**, 624-633(2008).

[94] Rutledge, P.J., and Challis, G.L. "Discovery of microbial natural products by activation of silent biosynthetic gene clusters." *Nat. Rev. Microbiol.,* **13**, 509-523 (2015)

[95] Yamada, Y., "Butyrolactone Autoregulators, Inducers of Secondary Metabolites, in *Streptomyces"*, **9**, *Actinomycetologica*,57-65(1995).

[96] Thao, N. B., Kitani S., Nitta H., Tomioka T. and Nihira T. "Discovering potential *Streptomyces* hormone producers by using disruptants of essential biosynthetic genes as indicator strains." *J. Antibiot.*, **70**, 1004-1008 (2017).

[97] Misaki, Y., Takahashi, Y., Hara, K., Tatsuno, S., and Arakawa, K. " Three 4-monosubstituted butyrolactones from a regulatory gene mutant of Streptomyces rochei 7434AN4." J. Biosci. Bioeng., https://doi.org/10.1016/j.jbiosc.2022.01.006

Appendix

Figure S1. ^{1}H NMR of natural YM3163-A (**9ab**)

(500 MHz, $CDCl_3$)

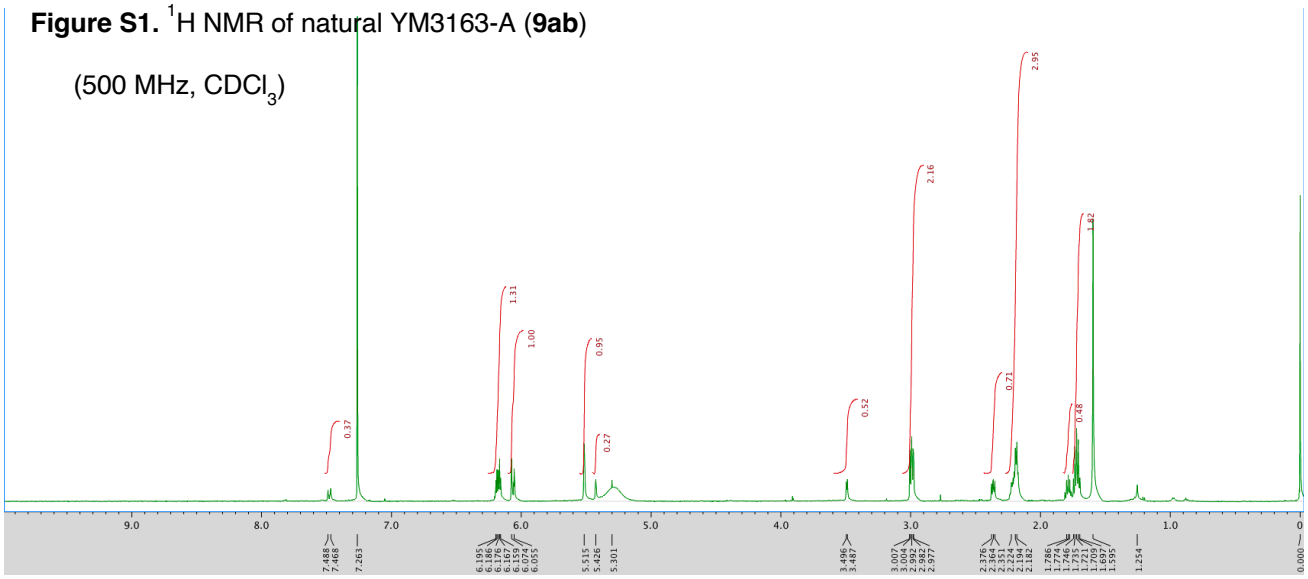

Figure S2. ^{13}C NMR of natural YM3163-A (**9ab**)

(125 MHz, $CDCl_3$)

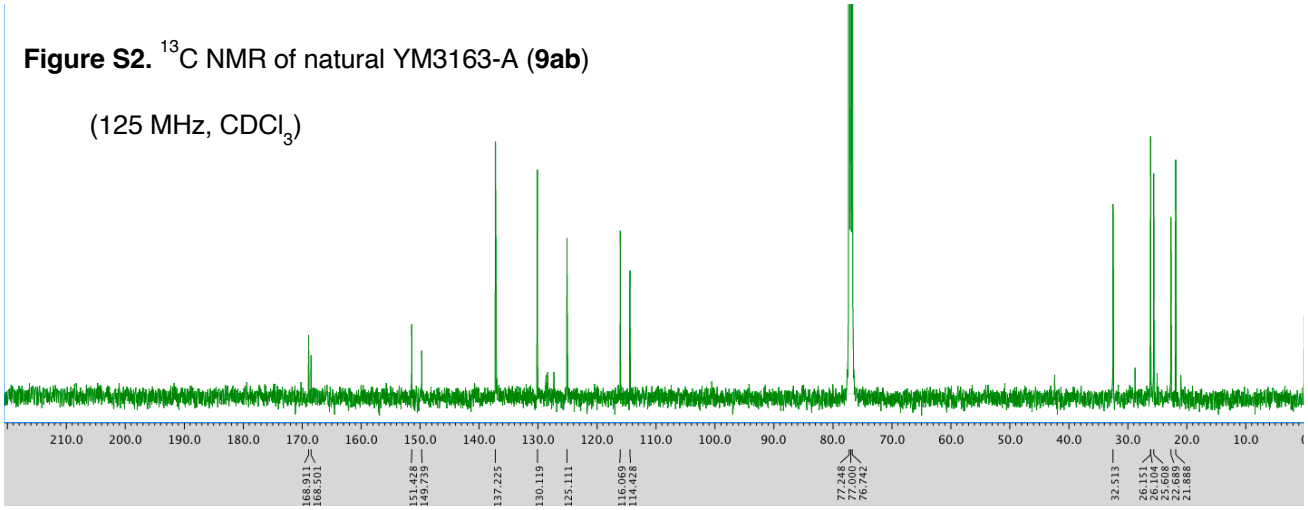

Figure S3. DEPT spectrum of natural YM3163-A (**9ab**)

(125 MHz, $CDCl_3$)

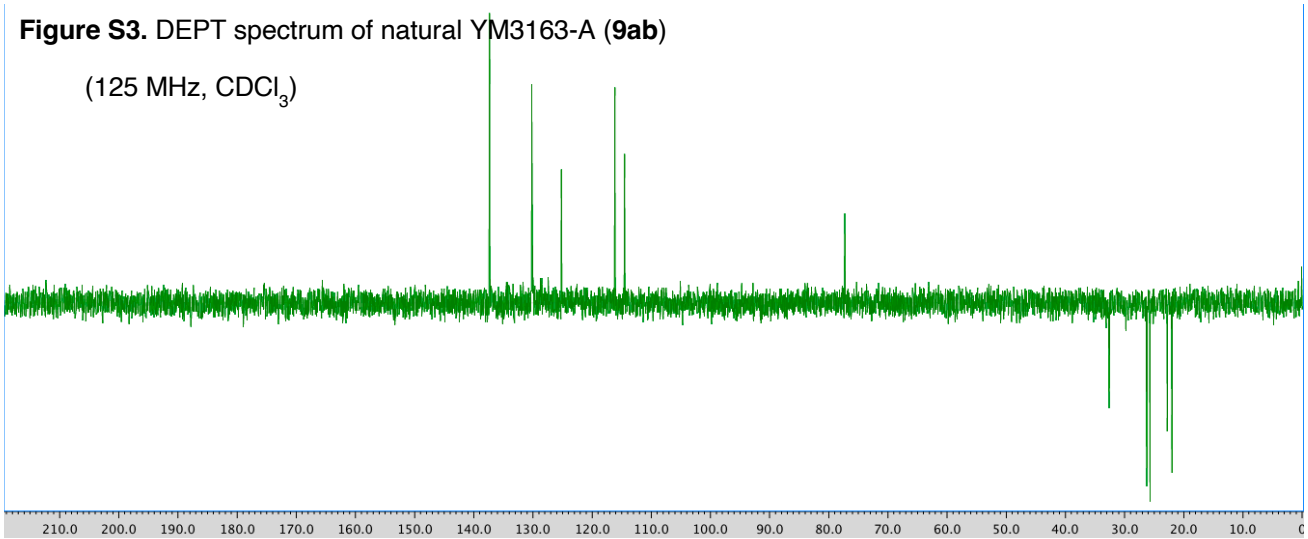

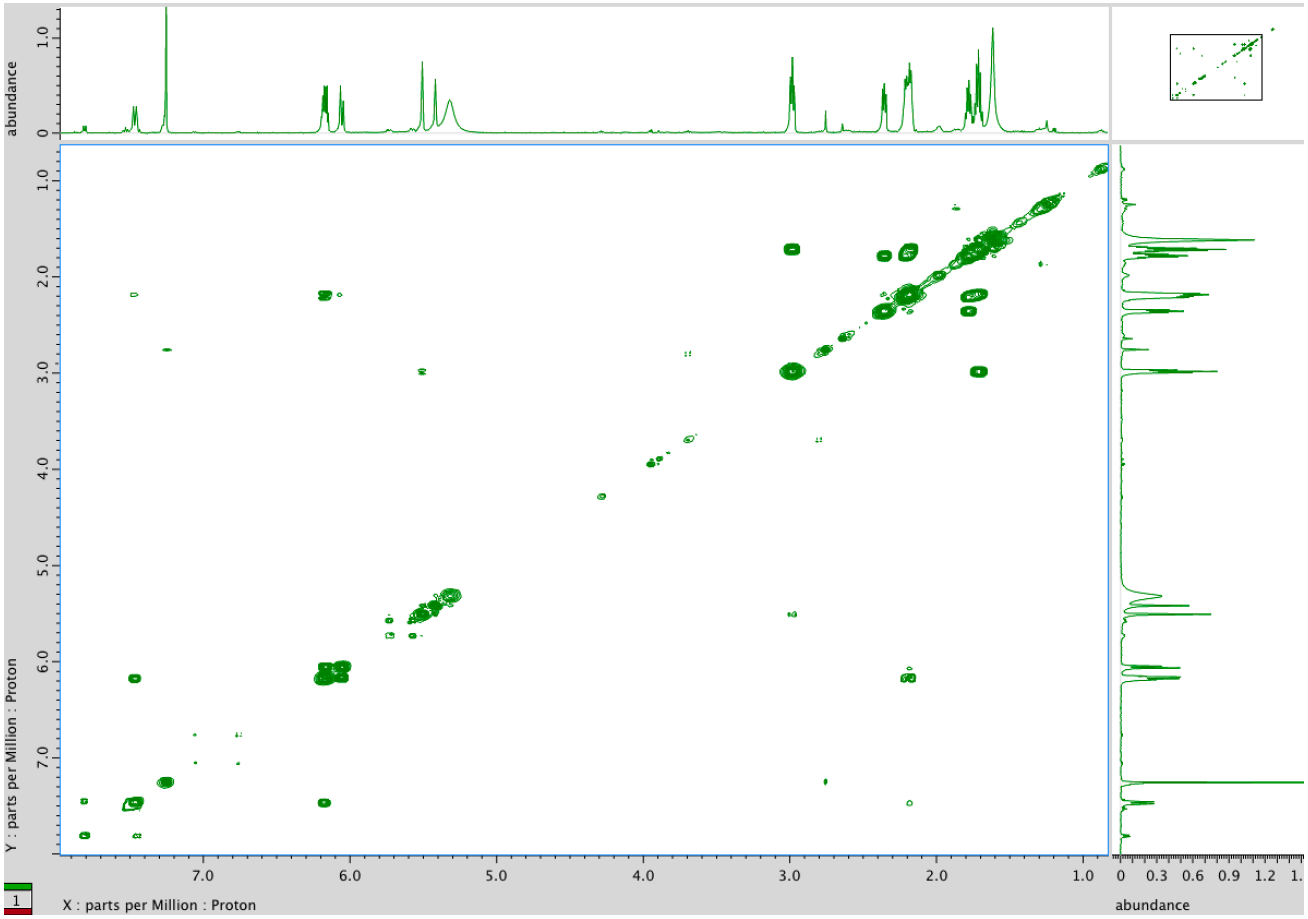

Figure S4. DQF-COSY spectrum of natural YM3163-A (**9ab**)

(500 MHz, $CDCl_3$)

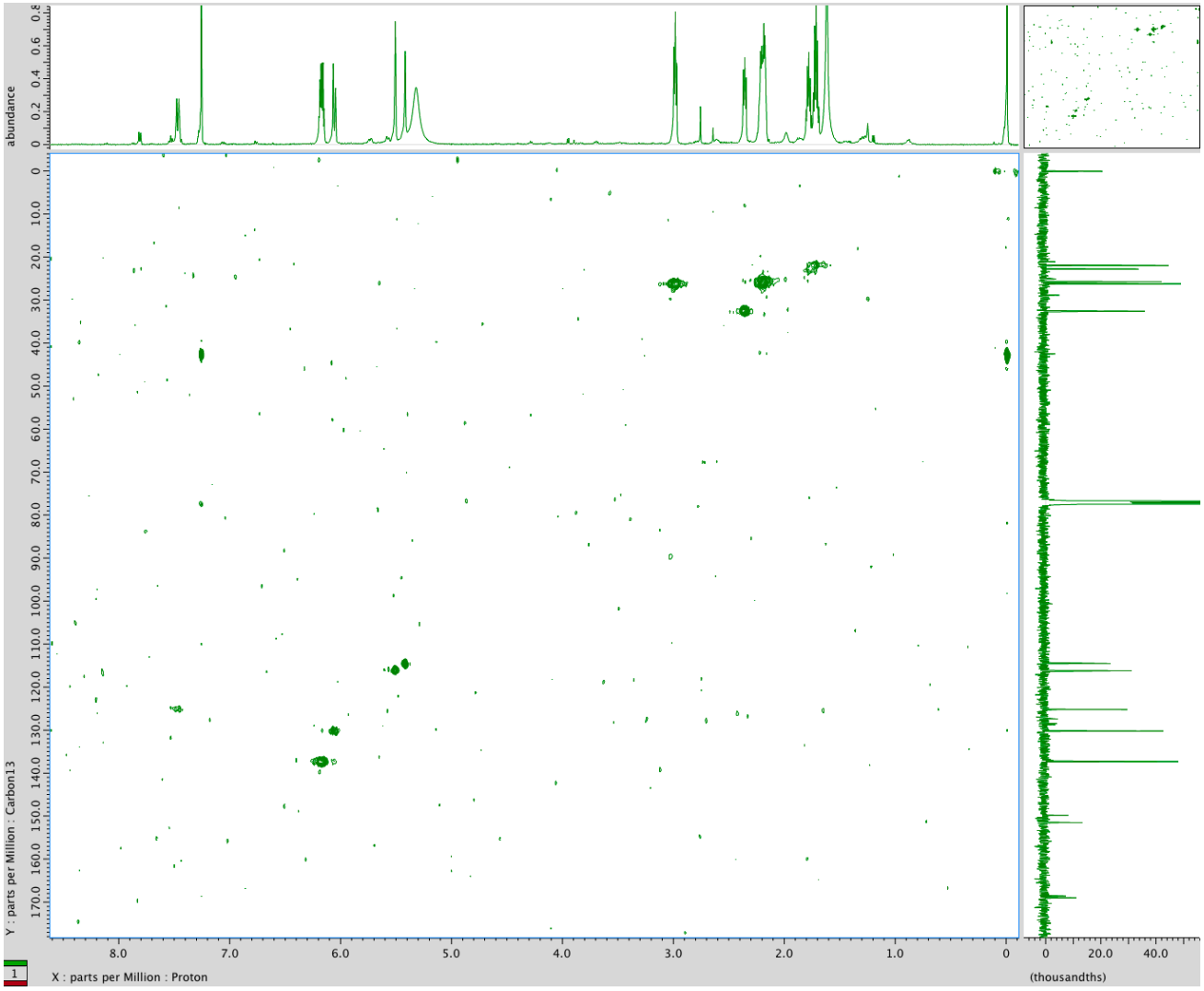

Figure S5. HMQC spectrum of natural YM3163-A (**9ab**)

(500 MHz, $CDCl_3$)

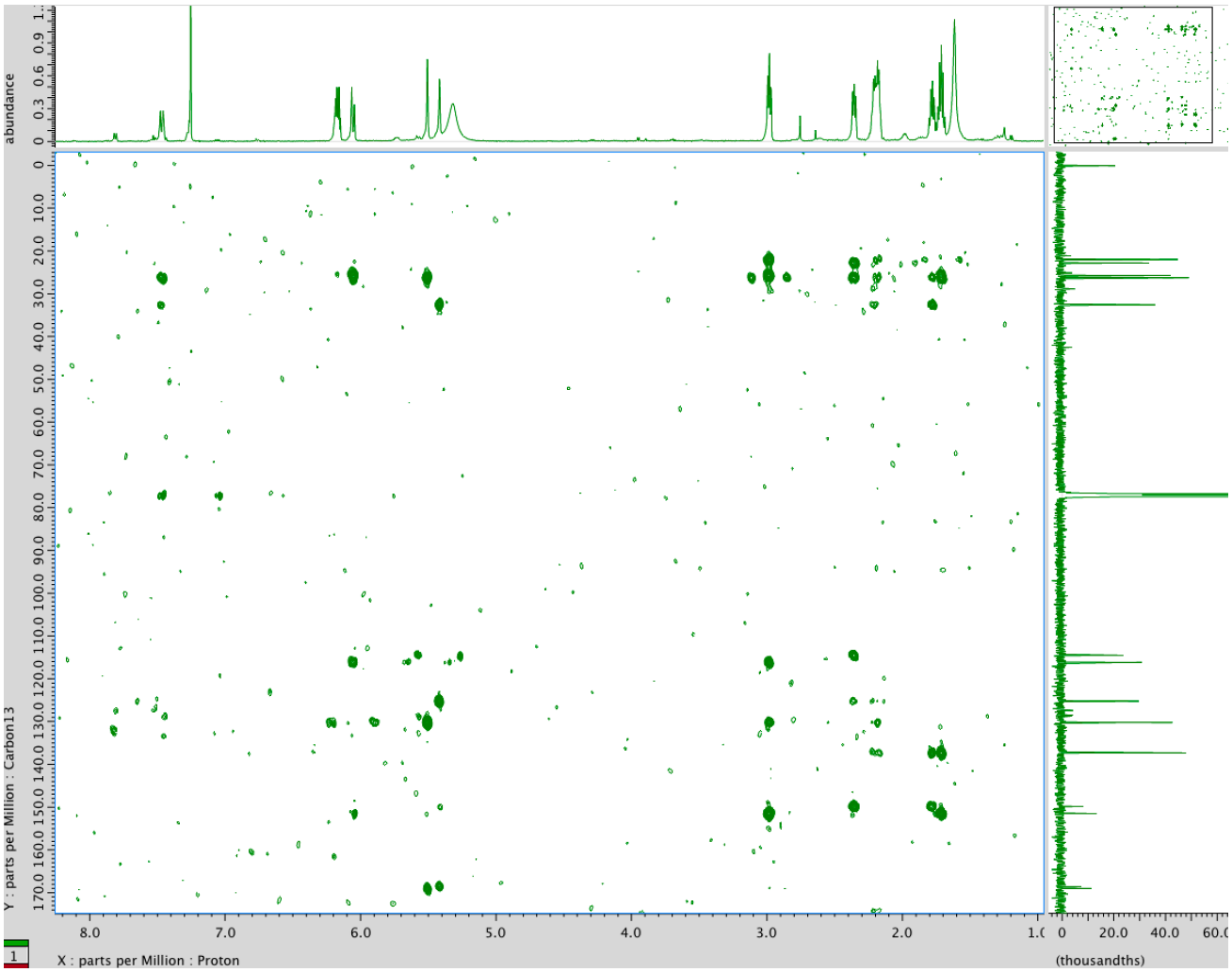

Figure S6. HMBC spectrum of natural YM3163-A (**9ab**)
(500 MHz, $CDCl_3$)

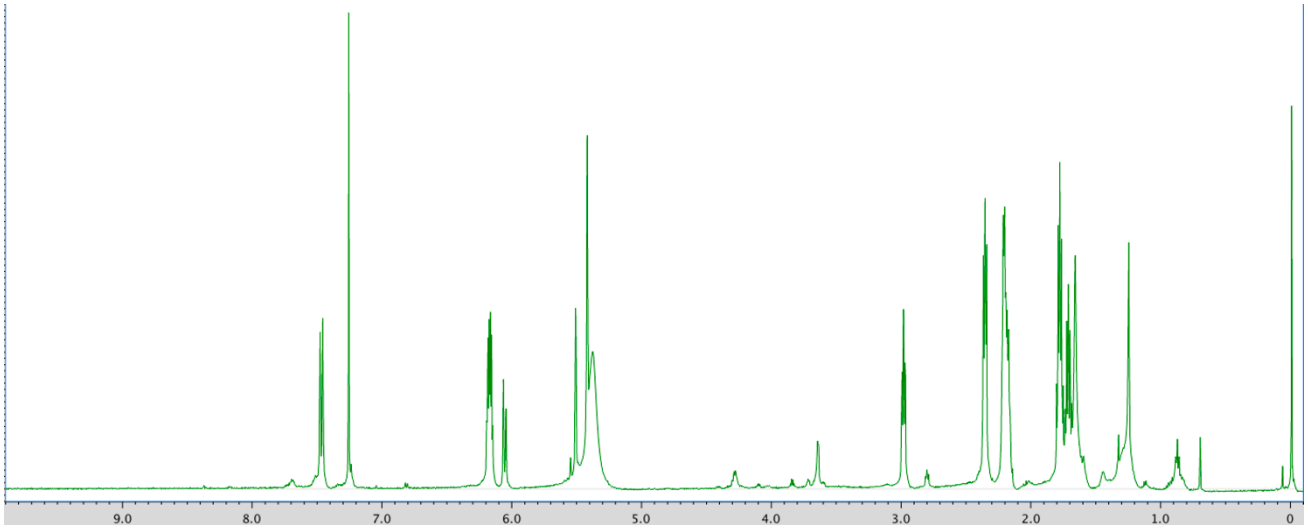

Figure S7. ^{1}H NMR of synthetic YM3163-A (**9ab**)
(500 MHz, $CDCl_3$)

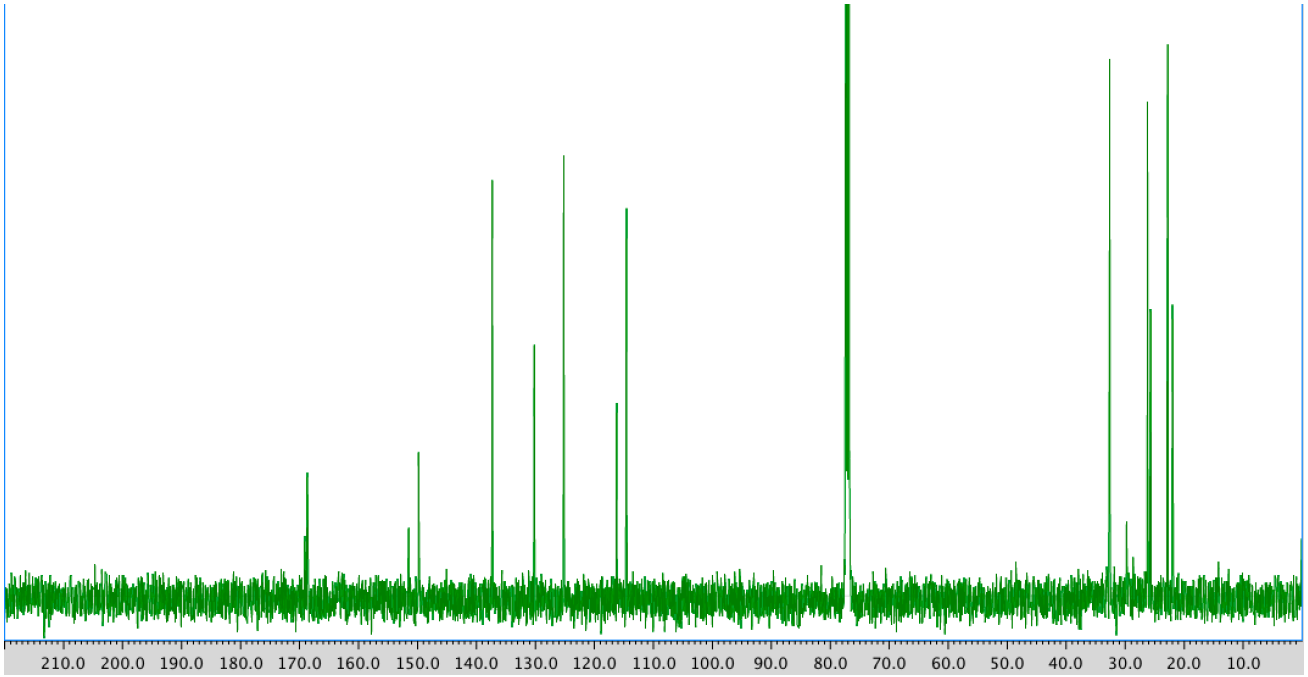

Figure S8. ^{13}C NMR of synthetic YM3163-A (**9ab**)

(125 MHz, $CDCl_3$)

参考論文

[1] **Y. Misaki**, S. Yamamoto, T. Suzuki, M. Iwakuni, H. Sasaki, Y. Takahashi, K. Inada, H. Kinashi, and K. Arakawa, "SrrB, a pseudo-receptor protein, acts as a negative regulator for lankacidin and lankamycin production in *Streptomyces rochei*", *Front. Microbiol.*, **11**:1089 (2020).

[2] **Y. Misaki**, Y. Nindita, K. Fujita, A. A. Fauzi, and K. Arakawa, "Overexpression of SRO_3163, a homolog of *Streptomyces* antibiotic regulatory protein, induces the production of novel cyclohexene-containing enamide in *Streptomyces rochei*", *Biosci. Biotechnol. Biochem.*, **86**(2):177-184 (2022).

関連論文

[1] Y. Nindita, Z. Cao, A. A. Fauzi, A. Teshima, **Y. Misaki**, R. Muslimin, Y. Yang, Y. Shiwa, H. Yoshikawa, M. Tagami, A. Lezhava, J. Ishikawa, M. Kuroda, T. Sekizuka, K. Inada, H. Kinashi, K. Arakawa, "The genome sequence of *Streptomyces rochei* 7434AN4, which carries a linear chromosome and three characteristic linear plasmids", *Sci. Rep*., **9**(1):10973 (2019).

[2] **Y. Misaki**, Y. Takahashi, K. Hara, S. Tatsuno and K. Arakawa, "Three 4-monosubstituted butyrolactones from a regulatory gene mutant of *Streptomyces rochei* 7434AN4", *J. Biosci. Bioeng.*, in press, DOI: 10.1016/j.jbiosc.2022.01.006